CHARACTERISATION AND ENGINEERING PROPERTIES OF NATURAL SOILS

volume 3

T.S. TAN
K.K. PHOON
D.W. HIGHT
S. LEROUEIL
editors

In-Situ Test Calibrations for Evaluating Soil Parameters

P.W. Mayne
Geosystems Engineering Group, Georgia Institute of Technology, Atlanta, GA, USA

ABSTRACT: The interpretation of in-situ geotechnical test data needs a unified approach so that soil parameters are evaluated in a consistent and complementary manner with laboratory results. A common thread in assessing in-situ tests is the focus on the geologic stress history, often expressed by the overconsolidation ratio (OCR). For clays, the OCR can be measured by consolidation tests on undisturbed samples, yet for sands is rather problematic to address. For 6 clays, a hybrid cavity expansion - critical state model is used to match responses measured CPT, CPTu, and DMT. Specifically, tip stress, sleeve friction, penetration porewater pressures, and flat dilatometer readings are fitted by parametric input of OCR, void ratio, friction angle, rigidity index, and compressibility parameters. The undrained shear strength (s_u) of clays is best handled via critical-state concepts. Discussions are included for pressuremeter, vane, and T-bar tests. For sands, select empirical methods derived from laboratory chamber testing on reconstituted clean quartz and siliceous sands are reviewed, specifically for effective friction angle ϕ', OCR, and K_0. In a novel look, a special set of undisturbed (frozen) sand samples from 15 locations in Japan, Canada, Italy, Norway, and China is used to check interrelationships for the following in-situ penetration tests: SPT, CPT, and V_s. Stiffness of all soils begins with the small-strain shear modulus ($G_0 = G_{max} = \rho_T V_s^2$) that can be used together with strength (s_u or ϕ') to evaluate stiffness over a range of strains. Supplementary testing by PMT and/or DMT can provide intermediate stiffnesses for tuning of modulus reduction schemes, as well as independent assessments of K_0 and OCR.

1 INTRODUCTION

1.1 *Natural Geomaterials*

Geomaterials encompass an extremely wide range of natural soils, rocks, and intermediate earthly substances, as well as artificial fills, mine tailings, and slurries (see Figure 1). Grain sizes of these materials vary tremendously from nano-particles in the very small angstroms domain and colloidal range (<0.5 microns), to clay particle sizes (< 2 microns), silts (< 75 microns) to coarse-grained soils (> 0.075 mm) including sands to gravels, as well as much larger cobbles (150 to 300 mm) and boulders (> 300 mm) to fractured rocks and massive intact rock formations (1 m to 1 km). These geomaterials are generally very old (thousands to millions of years old) with the youngest generally represented by Holocene age formations that have been placed only within the last several thousand years (< 10,000 years).

Natural geomaterials have been formed by an assortment of geologic processes including water sediment (marine, lacustrine, estuarine, alluvial, deltaic, fluvial), ice (glacial), wind (aeolian), disintegration (residual), mass wasting (colluvial), chemical (carbonates, calcarenites), biological (organic), and other mechanisms (e.g., meteoric). The varied minerologies (e.g., quartz, feldspar, mica, chlorite, illite, smectite, kaolinite, montmorillonite, hallosite, carbonates) can occur in unlimited combinations and permutations, thus forming infinite possible grain size distributions, as well variances in plasticity, particle shape, size, roundness, packing, porosity,

Figure 1. Illustrative examples of diversity in natural geomaterials found on planet Earth.

and fabric. These enumerable facets could be construed to defy any notion that characterization of these materials is at all possible.

After initial placement or forming, these materials are subjected to a wide range of environmental, geomorphological, and climatic changes including erosion, desiccation, ageing, wet-dry cycles, seasonal temperature fluctuations, and in some cases, special events such as glaciation, cyclic loading due to earthquakes, load fluctuations due to wave and tidal activities, and other activities. As a consequence, most soils are at least slightly to moderately overconsolidated to some degree. The significant fact that sea level has risen 30+ m in recent geologic times (thus associated groundwater tables), is sufficient alone in causing appreciable preconsolidation in soils (Locat, et al. 2003).

1.2 *Site Investigations*

A proper characterization of natural geomaterials is paramount in all site investigations because the results will impact the solution with respect to safety, performance, and economy. For instance, if the site characterization program has collected poor quality undisturbed samples of clays & silts for laboratory consolidation and triaxial shear testing, the soil stiffness and strength will be underestimated, perhaps resulting in the requirement of driven pile foundations for the building structure whereas shallow footings could have adequately sufficed. In site investigations of clean sands that are most difficult to sample, the assumption of normally-consolidated conditions will inevitably lead to an underestimate in pile side friction or an overestimate in shallow footing settlements. Therefore, a knowledge of in-situ test methods and their interpretation is of great value to the practicing geotechnical engineer in order to place the best value in the applied solution in site development.

A number of different approaches are available for the assessment of ground conditions at a particular site. These might be grouped into three categories, in preferred order:

A. Geophysics for general mapping of the relative variances across the site.
B. In-situ tests for profiling vertical geostratigraphic changes and/or soil parameter evaluation.
C. Drilling and sampling to obtain high quality and representative materials for the laboratory.

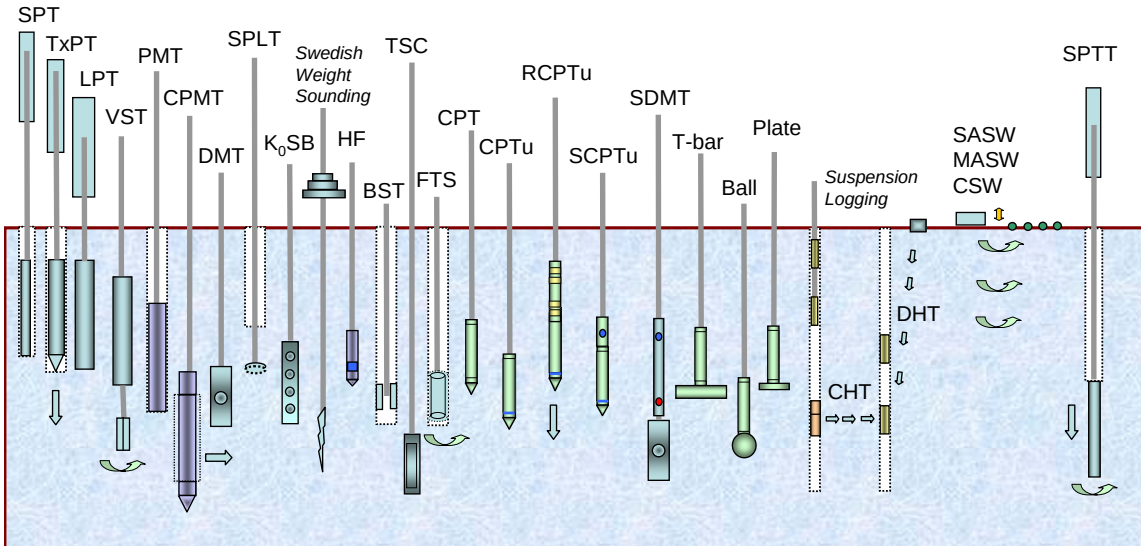

Figure 2. Selection of available in-situ geotechnical tests for determination of soil parameters

An integrated approach should be adopted for studying the ground whereby non-destructive geophysics are used first to guide the selection of expedient probe sounding locations, which in turn would aid in the choice & direction of the more expensive & laborious soil test borings to provide undisturbed samples for controlled laboratory testing by triaxial, simple shear, consolidation, and/or resonant column devices. A versatile and well-calibrated constitutive soil model would link these aspects together in a rational and consistent framework. A full discussion on the basic laboratory, field, & geophysical methods and their procedures is beyond the scope of this paper but may be found elsewhere (e.g., Mayne, Christopher, & DeJong, 2002).

A large number of in-situ devices and field tests are available to delineate the geostratigraphy and determine specific engineering parameters in the ground. As depicted by selected tests in Figure 2, these are quite numerous and include: standard penetration, cone penetration, dilatometers, pressuremeters, vanes, flat and stepped blades, hydro-fracture, borehole shear, torsional probes, and many other innovative designs. Robertson (1986) provides a detailed overview on many of the standardized and specialized devices that are primarily penetration type and/or direct-insertion type devices for testing the ground. Woods (1978) and Campanella (1994) give a review of applicable geophysical tests for determining mechanical wave properties. Wroth (1984, 1988), Jamiolkowski et al. (1985), and Lunne et al. (1994) provide summary papers concerning the use & interpretation of the more common standardized tests and recent updates have been made by Yu (2004), Mayne (2005), and Schnaid (2005). An optimization of site-specific site investigation is achieved with seismic piezocone testing (Campanella et al. 1986) together with intermittent dissipation testing (SCPTù), since five independent readings are obtained with depth in the same sounding (Mayne & Campanella 2005): q_t, f_s, u_b, t_{50}, and V_s. A similar procedure can be provided by the seismic dilatometer test (Mlynarek et al. 2006) with A-reading dissipations (SDMTà) to obtain: p_0, p_1, p_2, t_{flex}, and V_s.

1.3 *Conventional Approach for Clays*

In the conventional and classical methods of interpretation, the results of in-situ tests are commonly divided into two categories: (a) clays, whereby the undrained shear strength (s_u) is assessed; and (b) sands, whereby the relative density (D_R) and/or effective friction angle (ϕ') is evaluated. Yet, within the framework of critical state soil mechanics (CSSM), all soils in fact are frictional materials and their strength envelope can be best represented by their effective stress friction angle (ϕ'). For most soils, it can be taken that the effective cohesion intercept $c' \approx 0$ (unless true cementing or bonding is present). As these geologic materials are quite old and have

been lying uninterrupted for long eons of time, the drained strength, in most cases, is quite characteristic of their "normal" behavior. With the introduction of man's activities involving construction on the ground, however, short term conditions can result in what might be termed "undrained" loading, corresponding to shearing under constant volume. This undrained condition is critical for normally- to lightly-overconsolidated soils of low permeability (i.e., soft clays & silts) under relatively fast (geologically speaking) rates of loading. Notably, the undrained conditions are merely transient, and given time, excess porewater pressures will eventually dissipate to equilibrium conditions (i.e., hydrostatic porewater pressures, u_0).

For clays, one difficulty with the conventional interpretation methods involving in-situ tests is that a reference benchmark value of s_u is required in the calibration and/or verification of direct probe tests, such as the standard penetration test (SPT), cone penetration test (CPT), piezocone (CPTu), flat dilatometer test (DMT), and other devices (e.g., T-bar, ball penetrometer). The dilemma is depicted in Figure 3. The appropriate mode of undrained shearing is not always known at the time of interpretation and might include triaxial compression (CAUC, CK_0UE, CIUC), plane strain compression (PSC), simple shear (SS), torsional shear (TS), or one of the extension modes (CAUE, CIUE, PSE, CK_0UE). Moreover, multi-modes or non-standard modes may actually apply. In consideration of these possibilities, it is not at all clear how stress state, anisotropy, and direction of loading affects the interpretation of s_u from each of the field tests.

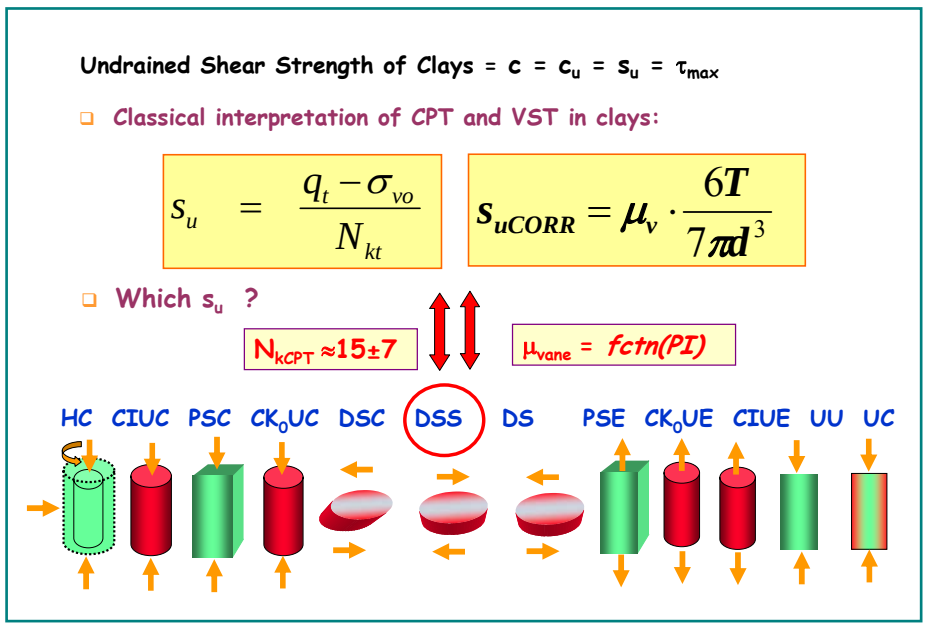

Figure 3. Dilemma in matching laboratory benchmark mode for undrained shear strength (s_u) with in-situ CPT and VST data. Note: Direct simple shear (DSS) is the likely reference for stability problems.

Another problem lies in the inconsistency amongst interpretative frameworks for in-situ tests. Specifically for clays, the vane shear test (VST) is analyzed using limit equilibrium methods, whilst the pressuremeter test (PMT) is assessed within cylindrical cavity expansion theory, and yet the bearing factor term for interpretation of the cone penetration test (CPT) might come from either strain path method or finite elements solutions. For a given parameter (i.e. s_u), the different theories alone will provide inconsistencies in interpretations amongst the various in-situ tests, within the same soil formation.

Each of the in-situ test types is conducted at a different rate of strain, thus affecting compatibility in the comparison of different tests. For example, at a rate of penetration of v = 20 mm/s, the CPT pseudo-strain rate could be considered to be v/d, where the diameter of a standard 10

cm^2 penetrometer is d = 35.7 mm. This pseudo-strain rate is 56 %/s, or about $2 \cdot 10^5$ %/hour. In comparison with a standard laboratory triaxial compression test performed at 1%/hour, this is over 5 orders of magnitude faster! For the aforementioned reasons of strength anisotropy, strain rate, boundary conditions, as well as other factors (e.g., progressive failure, drainage, fissuring), empirical factors have been included in the interpretation of undrained strengths from in-situ tests. Notably, the vane shear strength (s_{uv}) is often corrected using a factor (μ_v) obtained from the clay plasticity index (PI) to obtain the operational undrained shear strength for stability analysis: $s_{ucorr} = \mu_v \cdot s_{uv}$ (e.g., Chandler, 1988). Likely, this procedure provides a means of converting the vane data to a representative mode, such as direct simple shear (DSS). Yet, most commercial labs do not own nor operate DSS equipment. Consequently, practitioners will often compare the derived s_u values from the in-situ measurements with simpler tests that they can perform in-house, such as unconfined compression (UC), unconsolidated undrained (UU) triaxial, as well as very poor quality index values from the lowly pocket penetrometer and/or torvane devices. Occasionally, results from higher quality tests, such as consolidated triaxial compression tests (CIUC) will be available by the practicing engineer, but these provide values some 30% to 60% higher than the DSS mode. In terms of critical-state soil mechanics (CSSM), stress-induced anisotropy can be considered and shown to provide a reasonable hierarchy amongst the various lab testing modes in providing values of the normalized undrained shear strengths (s_u/σ_{vo}'). However, inherent anisotropy or fabric-induced features may not be well covered by simple constitutive soil models.

Using data from the British national experimental test site located at Bothkennar, Scotland, Figure 4 shows the various derived undrained shear strengths from laboratory triaxial compression, simple shear, and extension tests on undisturbed samples (Hight et al. 2003) together in comparison with direct measured values from self-boring pressuremeter (Powell & Shields, 1995) and field vane tests (Nash, et al. 1992). Quite a variation is seen for all depths. Also indicated is the backfigured operational value of s_u from a full-scale footing load test (B = 2.4 m) conducted at the site using a limit plasticity solution with a bearing factor $N_c^* = 7$, as reported by Jardine, et al. (1995).

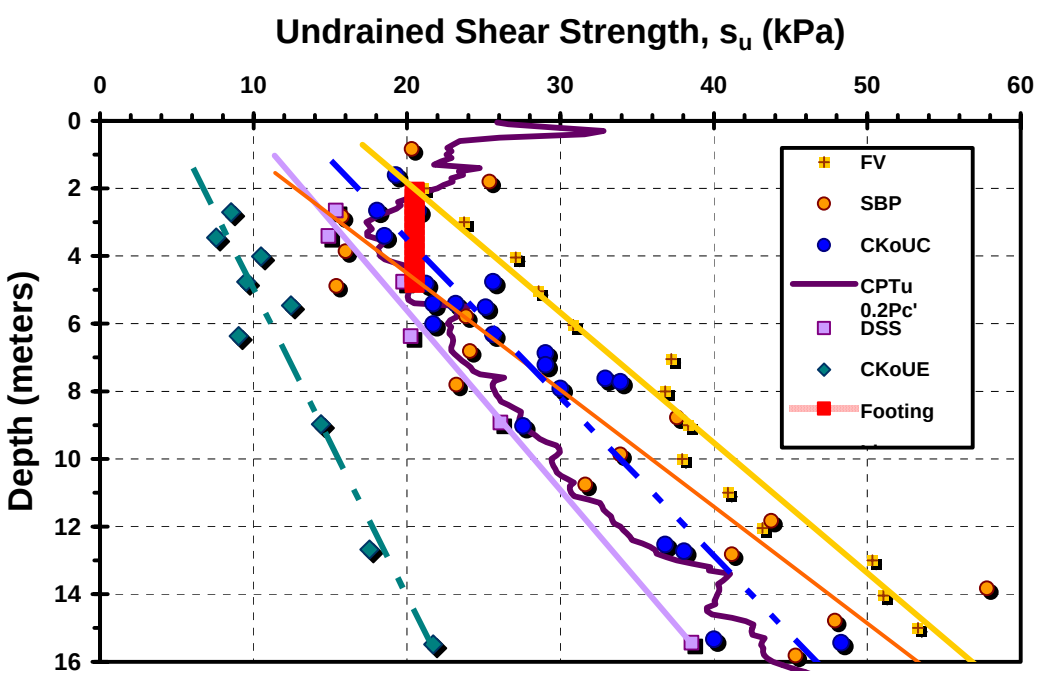

Figure 4. Different mode profiles of undrained strengths at Bothkennar clay site, UK.

1.4 *Conventional Approaches for Sands*

For sands, the major difficulty lies in the inability to collect true undisturbed samples from the field in order to establish a clear laboratory calibration value of strength or stiffness whatsoever. Therefore, primary efforts have resorted to collecting disturbed bulk samples of sands from the field and reconstituting the sand specimens at the "same density" in the laboratory. Presumably, the inplace density has been accurately assessed and the lab results give stress-strain-strength behavior that can be linked to the field tests. The reconstituted sands can either be formed into: (a) small triaxial- or direct shear-size specimens that are related back to field penetrometer readings, or (b) large diameter calibration chambers, mostly of the flexible-wall type, that allow the full probing by the penetrometers or in-situ tests. Dry to saturated sands under normally-consolidated to induced overconsolidated states have been prepared in this manner under different boundary conditions (Ghionna & Jamiolkowski 1991). After all is known beforehand about the chamber deposit of sand (particle shape & angularity, median particle size, percent fines, density, stress history), a miniature to full-size probe is inserted for the test performed (Figure 5). Laboratory calibration chamber tests (CCT) have included SPT, CPT, DMT, PMT, CPMT, and mechanical wave geophysics for compression or P-wave and shear or S-wave velocity measurements.

It is well-known that the CCT data suffer from their limited boundary sizes represented by the ratio D/d, where D = diameter of large sand sample and d = diameter of probe. Thus, the results need be corrected to far-field values (e.g., Salgado, et al. 1997; Jamiolkowski et al. 2001). Moreover, different preparation methods for placement of "sand deposits" have been used in CCT, including: compaction, air pluviation, water pluviation, moist tamping, vibration, and slurrying. For a given density of the sand, these in fact do not provide similar fabrics and thus the obtained probe results may differ significantly from field behavior (e.g., Hoeg et al. 2000; Jamiolkowski 2001). Finally, the supposed link in the relationships derived from the CCT correlations derives from the assumption that the in-situ tests can provide a direct measure of the relative density (D_R). In US practice, the notion of D_R only applies to cases of clean sands with percent fines PF ≤ 15%, In truth, the use of in-situ penetration measurements can provide only a rough index on the inplace packing arrangement such as void ratio, porosity, or relative density. Thus, other devices such as gamma logging, downhole nuclear gages (i.e., radio-isotope penetrometers), or time domain reflectometry (TDR) in direct push probes would serve better for assessing this initial state condition.

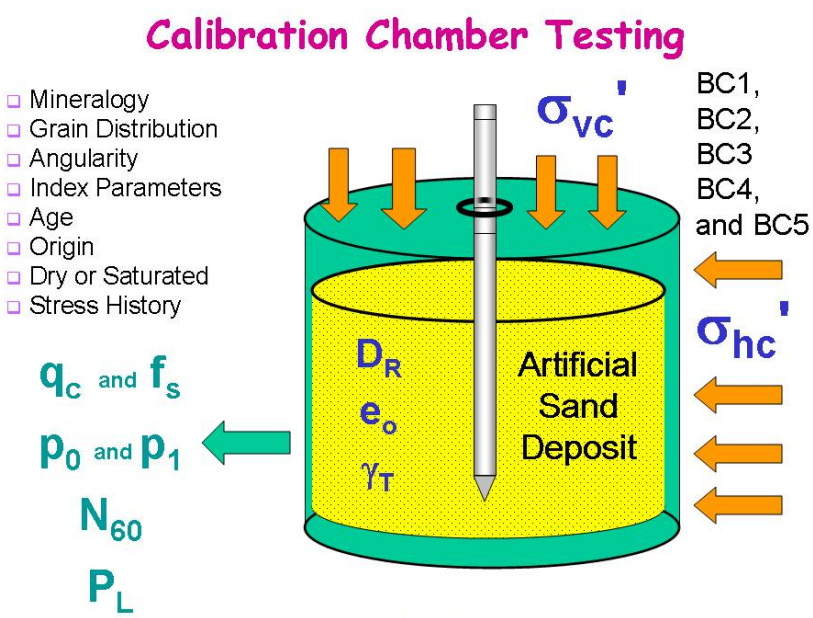

Figure 5. Calibration chamber testing setup for in-situ testing on reconstituted sands.

1.5 *Fitting & Calibration Approaches*

Herein, a couple of non-conventional approaches are presented for evaluating in-situ test results in clays and sands. The emphasis is initially on the CPT, CPTu, and DMT for clays, with dissipation response also considered; and SPT, CPT, and V_s testing in sands. The methods are not rigorous but utilized to show an important geotechnical need regarding a full set of complementary calibrations of in-situ tests within a soil medium.

For the clays, a known profile of stress history (i.e., OCR) is used to drive the fitting of in-situ penetration data in terms of simple closed-form expressions derived from hybrid cavity expansion–critical state models. Input parameters include the initial state (void ratio, e_0), effective friction angle (ϕ'), plastic volumetric strain potential ($\Lambda = 1 - C_s/C_c$), and rigidity index ($I_R = G/s_u$). Reasonably successful forward profiles of cone tip stress (q_t), penetration porewater pressures (u_1 and/or u_2), sleeve friction (f_s), dilatometer contact (p_0) and expansion pressures (p_1) are shown for three soft clay sites and two overconsolidated clays. Research needs include a generalized methodology for all types of in-situ tests that is internally consistent and then calibrated with well-researched test sites, as those reported in the 2003 and 2006 Singapore Workshops (Tan, et al. 2003).

For sands, a two phase study is given: (1) examination of selected existing relationships for stress history (K_0 and OCR) and friction angle (ϕ') at three documented sand sites; and (2) a specially-compiled triaxial database created from expensive undisturbed (primarily frozen) sand samples where in-situ standard penetration, piezocone penetration, and shear wave measurements were collected. These latter series document the measured void ratio (e_0), relative density (D_R), triaxial friction angle (ϕ'), and stiffness from stress-strain curves. The parameters can then be compared with their corresponding in-situ measurements of N-value, tip stress q_t, and downhole V_s values in terms of existing correlative trends, theoretical relationships, and/or to allow future calibration with soil constitutive models.

2 IN-SITU TESTS IN CLAYS

2.1 *Overview*

In this approach, simple analytical models will be matched to the measured in-situ field data based on its stress history profile. Soil input parameters are parametrically varied to provide the optimal fitting to all available tests. At this time, the author has experimented with a simple hybrid model based primarily on spherical cavity expansion and critical-state soil mechanics (CSSM) that can be applied to cone penetration, porewater pressures, and flat dilatometer tests in clays. Brief discussions are given subsequently on the topics of stress history, cavity expansion, and CSSM.

2.2 *Stress History*

The benchmark for the preconsolidation stress is that caused by mechanical processes, specifically the removal of overburden, as occurs by erosion, glaciation, and/or excavation (Chen & Mayne 1994; Locat et al. 2003). Yet, effects of overconsolidation that are caused by a rise in the groundwater table, desiccation, wet-dry cycles, freeze-thaw cycles, and/or quasi-preconsolidation due to secondary consolidation, creep, and/or ageing might also be ascertained from these approaches, at least on an approximate basis.

For clays, the preconsolidation stress ($\sigma_p' = \sigma_{vmax}' = P_c'$) can be uniquely determined as the yield point on conventional one-dimensional consolidation plots of void ratio vs. log effective stress (i.e., e-logσ_v' data). The normalized form is termed the overconsolidation ratio, OCR = (σ_p'/σ_{vo}'). Because of sample disturbance issues, the clear demarcation of σ_p' may be unclear or muddled, thus graphical "correction" schemes have been devised to better delineate its value (e.g., Grozic and Lunne 2004).

The OCR governs both the normalized undrained shear strength (s_u/σ_{vo}') and the lateral geostatic stress coefficient, $K_0 = (\sigma_{ho}'/\sigma_{vo}')$. The OCR has also been shown especially influential on laboratory-derived values of small-strain shear modulus ($G_0 = G_{max}$), Skempton's porewater parameter (A_f), and intermediate stiffness values of modulus and rigidity (E_u/s_u and E'/p_0'). For

natural sands, the effective preconsolidation occurs similarly by the same basic mechanisms. In calibration chamber tests involving sands, the prestressing is induced artificially as part of creating the "deposit", thus the OCR is known. In natural sands, however, it has been difficult to ascertain the OCR because of sampling problems and the very flat e-logσ_v' response of sands in one-dimensional compression tests.

In truth, the vertical preconsolidation stress is just one point of an infinite locus of memory on the three-dimensional yield surface (Leroueil & Hight, 2003). As such, it is possible to define additional points of yielding along specialized stress paths in the triaxial apparatus and define this complete yield surface. This yield surface is rotated and centered about the K_{0NC} compression line in MIT type q-p space and governed by the effective frictional characteristics of the soil (e.g., Diaz-Rodriguez, Leroueil, & Aleman, 1992). Thus, in sands, it is conceptually feasible to use the same penetration data (N_{60}, q_t, p_0) to define the centering of the yield surface, as well as the friction angle of the material, since the two are related. For clays, the in-situ data (VST, CPT, CPTu, SPT, DMT) relate to the effective preconsolidation stress, thus also to the yield surface. However, since these are relatively fast tests under undrained conditions ($\Delta V/V_0 = 0$), then additional data related to the generated excess porewater pressures are needed to define the effective frictional envelope (e.g., Senneset et al. 1989).

2.3 *Cavity Expansion Theory*

In cavity expansion, three possible geometric cases can arise during integration of the governing equations: (a) linearly, to create a wall; (b) radially, to form a cylinder; and (c) spherically, resulting in a ball. The use of cylindrical cavity expansion (CCE) theory for the reduction of pressuremeter test (PMT) data in clays has been well-appreciated for over 50 years (Gambin, et al. 2005). Assuming undrained conditions, four parameters can be individually assessed for each PMT including: lift-off pressure ($P_0 = \sigma_{ho}$), elastic shear modulus (G), undrained shear strength (s_u), and the limit pressure (P_L), such that:

$$P_L = \sigma_{ho} + s_u [\ln(I_R) + 1] \quad (1)$$

where $I_R = G/s_u$ = undrained rigidity index. Thus, all four parameters are interrelated via equation (1). Figure 6 shows a comparison of the graphically-interpreted limit pressure versus that calculated using (1) with data from 34 clays tested by self-boring pressuremeters (SBP), thus indicating the general validity of CCE.

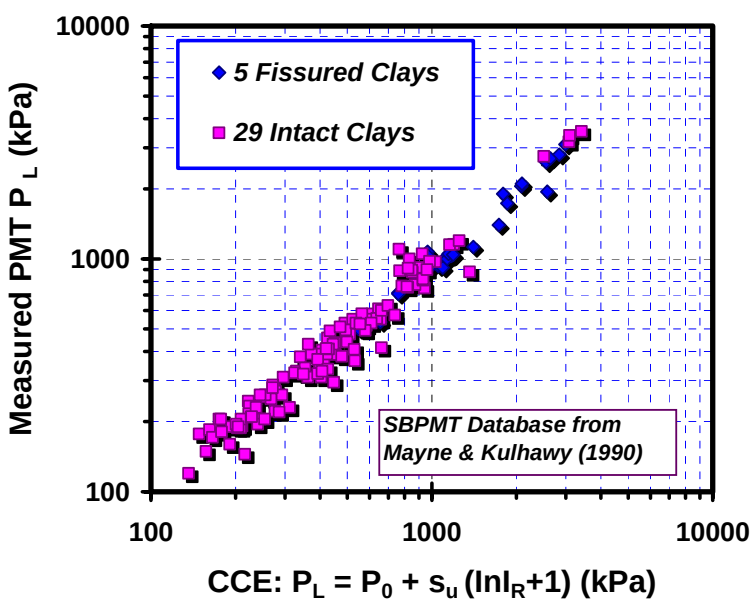

Figure 6. Measured vs. predicted limit pressure using SBPMT database in clays.

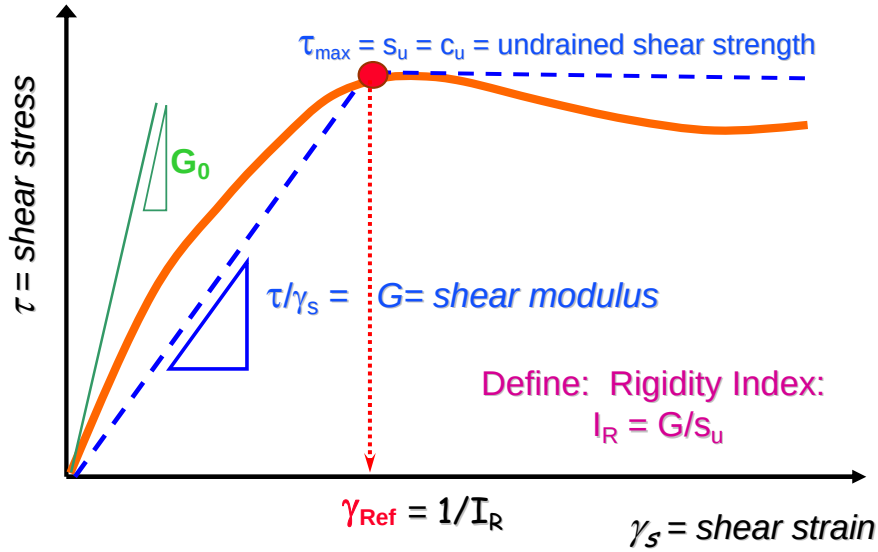

Figure 7. Shear stress vs. shear strain for soils and definitions of τ_{max}, G, γ_f, and I_R.

Details on the PMT interpretative procedures are given elsewhere (e.g., Wroth, 1984; Briaud, 1995; Ballivy 1995; Fahey & Carter, 1993; Clark & Gambin, 1998). Alternate approaches for cavity expansion interpretation include the derivation of a continuous stress-strain curve from the measured pressure vs. volume change field data (e.g., Gambin et al. 2005).

The cavity expansion approach has been also extended to drained loading conditions by consideration of volumetric strain changes (Vesic, 1972, 1977), or alternatively using dilatancy angle (Carter, et al. 1986). Additional work has been undertaken to evaluate the unloading cycles during full-displacement type pressuremeters, such as the cone pressuremeter test (CPMT), as detailed by Houlsby & Withers (1988) and Yu (2004).

A parameter of interest to all cavity expansion problems is the rigidity index, defined as the ratio of shear modulus to shear strength, $I_R = G/\tau_{max}$. The appropriate value of I_R is rather elusive since the shear modulus changes dramatically from an initial value ($G_0 = G_{max}$) to a secant value at peak strength, $G_{min} = \tau_{max}/\gamma_f$, where γ_f = strain at peak. The tangent G is zero at peak strength. Notably, in SBPMT, the value of G could be reported from the first-time loading (i.e., backbone curve), or else from an applied unload-reload cycle (G_{ur}) that is considerably stiffer than the former. For penetration tests, the value is likely closer to G_{min}. As illustrated by Figure 7, the rigidity index can also be considered as the reciprocal of the failure strain, or $I_R = 1/\gamma_f$.

2.4 *Critical-State Soil Mechanics*

Critical state soil mechanics (CSSM) is a valuable effective stress framework to interrelate concepts of frictional strength and consolidation (e.g., Schofield & Wroth, 1968). By specifying the initial state, CSSM can easily explain the differences between normally-consolidated (NC) and overconsolidated (OC) behavior, contractive vs. dilative response, undrained vs. drained strengths, positive vs. negative porewater pressure generation, as well as other behavioral facets such as partly drained to semi-undrained cases, cyclic behavior, creep, and strain rate (Leroueil & Hight 2003).

In the most simple version involving saturated soils, only three soil properties are considered (ϕ', C_c, C_s) in addition to the initial state (e_0, σ_{vo}', and OCR = σ_P'/σ_{vo}'). Essentially, CSSM is the link between the well-known compression curves from one-dimensional consolidation tests (termed e-logσ_v' space) and the Mohr's circles from triaxial or direct shear tests (represented by shear stress vs effective normal stress plots, or τ-σ_v' space). These two spaces are depicted in

Figure 8, along with a third diagram (e-σ_v' space) that really offers no new information, just a way to follow the compression results in arithmetic scale for σ_v' and tie to the τ-σ_v' space.

In its essence, the premise for CSSM is that all soil, regardless of starting point or drainage conditions, strives towards and eventually ends up on the critical state line (CSL). In the τ-σ_v' space, this line corresponds to the well-known strength envelope given by the Mohr-Coulomb criterion for c' = 0. Here, shear strength is represented by the maximum shear stress (τ_{max}) and is given by: $\tau = c' + \sigma' \tan\phi'$. In the e-log$\sigma_v$' space, the CSL represents a line parallel to the virgin compression line (VCL with slope C_c) for NC soils, yet offset to the left at stresses approximately half those of the VCL. All NC soils start on the VCL, while all OC soils begin from a preconsolidated condition along the recompression or swelling line (given by slope C_s). Regardless, all shearing results in peak stresses falling on the CSL. Figure 8 shows a summary of four basic stress paths corresponding to drained loading (no excess porewater pressures, or $\Delta u = 0$) and undrained loading (constant volume, or $\Delta V/V_0 = 0$) for both NC and OC initial states.

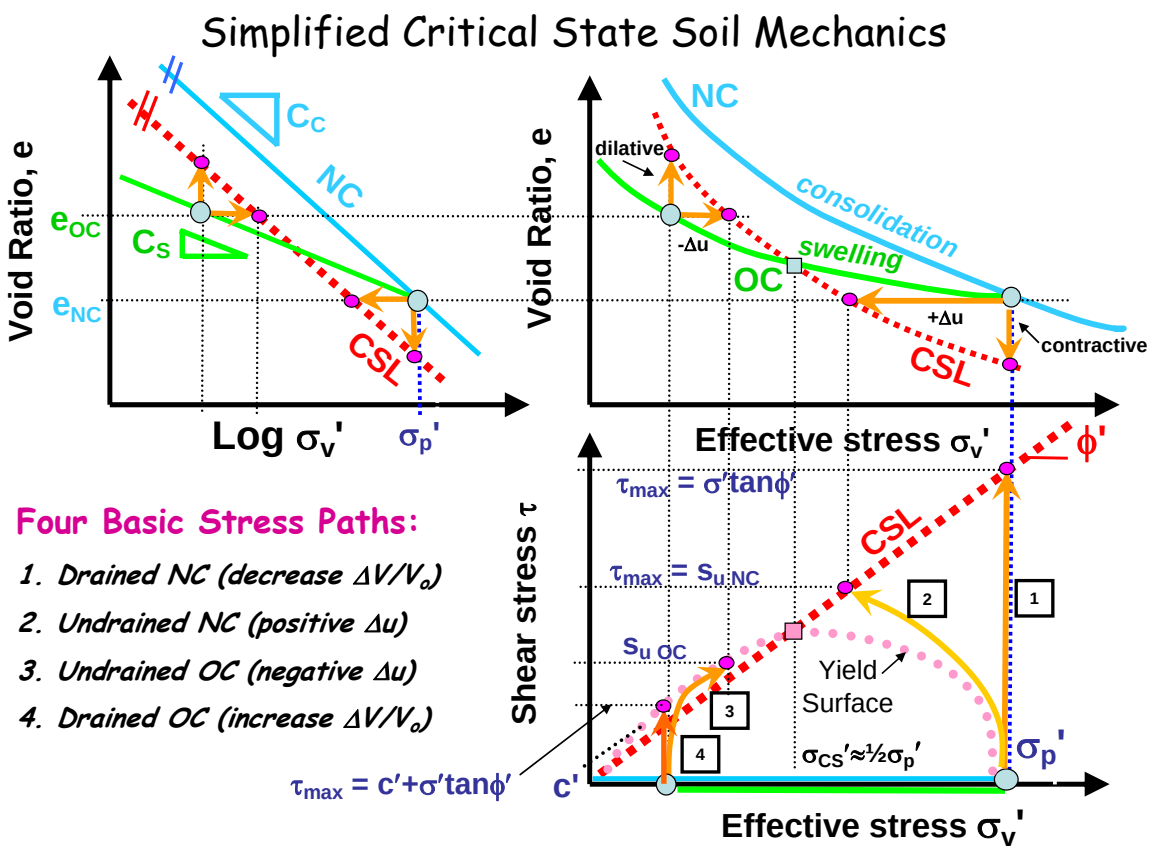

Figure 8. Simplified critical state soil mechanics, showing four common stress paths.

Surprisingly, geotechnical practice has still not adopted the framework of critical-state soil mechanics (CSSM), yet the supporting research and clear evidence have been available for over a half-century (e.g., Hvorslev, 1960). A review of geotechnical textbooks used in the USA, for example, reveals that the most popular and best-selling books do not discuss nor even mention CSSM, the exceptions being those by Budhu (2000) and Lancellotta (1995). Of course, there are several excellent books specific to CSSM (Schofield & Wroth, 1968; Wood, 1990), yet omitted in geotechnical education in USA, China, and many other countries.

With a lack of background in CSSM, many practitioners still cling to the incorrect notion of running strength tests on three specimens to produce a set of total stress "c and ϕ" parameters. For clays, the idea of "$\phi = 0$" analysis still prevails in practice, yet all soils (clays, silts, sands, gravels) are frictional materials. The observation of "$\phi = 0$" is really an illusion when porewater pressures are not monitored or not known, thus missing the CSL influence. As a consequence,

the term "cohesion" in often used ambiguously, in some instances referring to the *undrained shear strength* ($c = c_u = s_u$), yet in other circumstances, intending to mean the *effective cohesion intercept* (c'). The former is obtained as the peak shear stress in a stress path of constant volume. The latter is obtained by force-fitting a straight line (y = mx + b) to represent the Mohr-Coulomb strength criterion ($\tau = \sigma' \tan\phi' + c'$) from laboratory strength data.

As noted previously, the strength envelope is actually more complex and best described by a frictional envelope (ϕ') having a superimposed three-dimensional curved yield surface that is governed by the preconsolidation stress, σ_P' (Leroueil & Hight, 2003). The shape, size, features, and movement of the yield surface distinguishes one constitutive model from another (e.g., Lade 2005), yet this facet is not necessary in order to convey the overall simplicity and elegance of CSSM (e.g., Lancellotta, 1995). In Figure 8, the basic concept of a yield surface is shown in the τ-σ_v' space. It is the intersection of this yield surface with the frictional envelope which dictates the offset distance of the CSL to the left of the VCL.

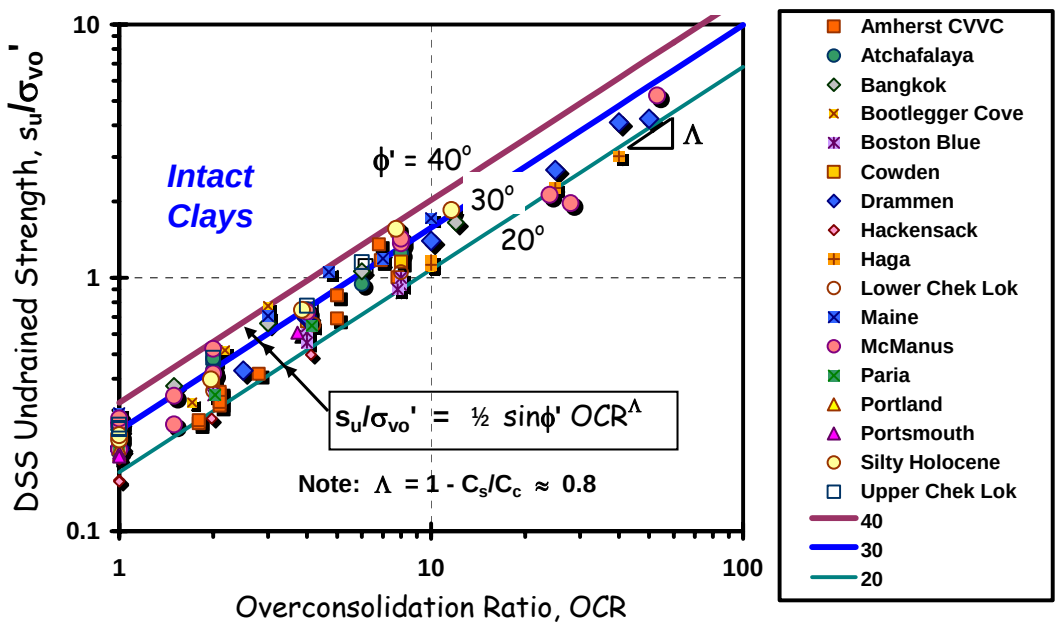

Figure 9. Experimental and CSSM variation of undrained DSS shear strengths with OCR.

2.5 *Undrained Shear Strength*

The undrained shear strength is best represented in normalized form (s_u/σ_{vo}') which is mode-dependent and reliant on initial stress state, strain rate, direction of loading, degree of fissuring, and other factors (Kulhawy & Mayne, 1990). The ratio s_u/σ_{vo}' can be evaluated using constitutive laws based on critical state soil mechanics (e.g., Wroth, 1984; Ohta et al. 1985; Whittle & Kavvadas, 1994), or alternatively using empirical approaches such as SHANSEP (Ladd, 1991). For general use, the author subscribes to a three-tiered hierarchy, based on the availability of site-specific data (Mayne, 2003). Since direct simple shear (DSS) provides an overall representative mode for stability and bearing capacity analyses, the preferred approach is via CSSM (Wroth, 1984), as illustrated by Figure 9 and expressed by:

$$\left(\frac{s_u}{\sigma_{vo}'}\right)_{DSS} = \frac{\sin\phi'}{2} \cdot OCR^{\Lambda} \quad \text{(2a)}$$

where ϕ' = effective friction angle, $\Lambda = 1 - C_s/C_c$ is the plastic volumetric strain ratio, and C_s and C_c are the swelling and virgin compression indices, respectively. For intact natural clays, the full

range of observed frictional characteristics vary from 18º < ϕ' < 43º (Diaz-Rodriguez, Leroueil, & Aleman, 1992). Clays of low to medium levels of sensitivity exhibit values between 0.7 < Λ < 0.8, whereas structured and sensitive soils show 0.9 < Λ < 1.

If the intrinsic property values are not known, a default form is taken as (Ladd, 1991):

$$\left(\frac{s_u}{\sigma'_{vo}}\right)_{DSS} = 0.22 \cdot OCR^{0.80} \quad \text{(2b)}$$

which is empirically-based on four decades of experimental lab testing by MIT on various clays worldwide. Interestingly, (2b) is also a subset of (2a) for the case where ϕ' = 27º and Λ = 0.80. Finally, if the material is lightly-overconsolidated with OCR < 2, the third tier estimate is simply (Trak, et al. 1980; Jamiolkowski, et al. 1985):

$$s_{uDSS} \approx 0.2\ \sigma_p' \quad \text{(2c)}$$

which is based in good part on corrected vane shear data from backcalculated failures of embankments, excavations, and footings on soft clays.

If more specific modes are needed, these can be assessed using constitutive relationships (e.g., Wroth, 1984; Ohta, et al. 1985; Kulhawy & Mayne 1990), or empirical trends based on plasticity index (e.g, Jamiolkowski et al. 1985; Ladd, 1991). For example, the triaxial compression mode (CIUC) that can be accommodated by most commercial laboratories is given by:

$$s_u / \sigma_{vo}'_{CIUC} = \left(\frac{M}{2}\right)\left(\frac{OCR}{2}\right)^{\Lambda} \quad (3)$$

where M = 6sinϕ'/(3-sinϕ') represents the frictional parameter in Cambridge q-p' space. Thus, CSSM offers a nice framework to organize laboratory strength data in terms of the stress history of the clay, as well as a means of predicting changes in strength should onsite construction require the addition of new fill loading, embankments, and/or excavation. For illustrative purposes, Fig. 10 shows a set of 15 CIUC triaxial tests and 5 DSS tests on Bootlegger Cove Clay from Anchorage, Alaska in terms of normalized undrained shear strengths vs. overconsolidation ratio (Mayne & Pearce, 2005). The data are well-represented by CSSM equations (2a) and (3) using the triaxial-determined friction angle ϕ' = 27.7º and compression parameters from standard consolidation tests (C_c = 0.24; C_s = 0.06; Λ = 1 - C_s/C_c = 0.75).

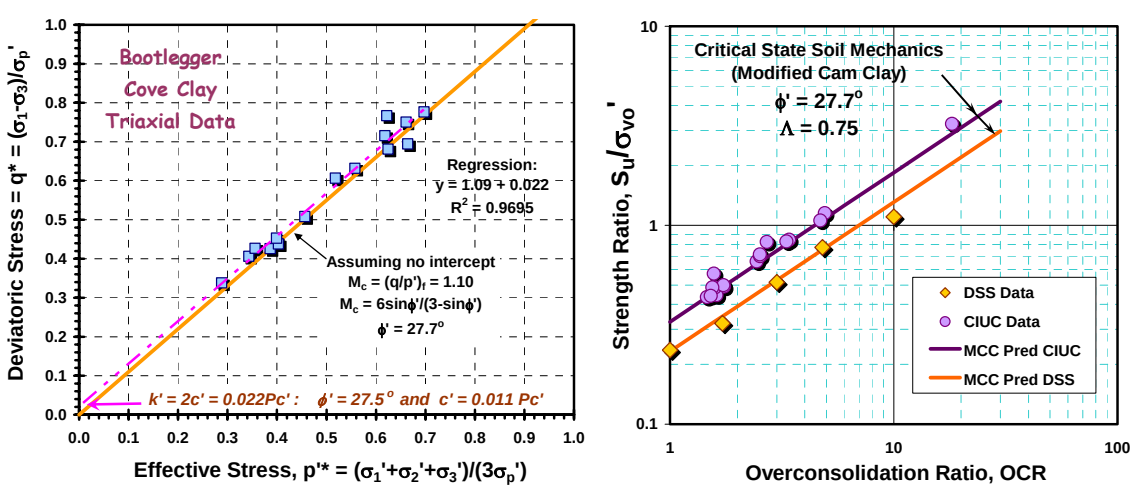

Figure 10. Measured and predicted s_u/σ_{vo}' vs. OCR for Bootlegger Cove Clay, Anchorage.

Note that for fissured clays (generally associated with high OCRs), the values from (2a), (2b), and (3) should be reduced by as much as one-half because of the macrofabric of existing fractures and cracking. For soils that are overconsolidated by mechanical unloading, a limiting OCR is reached in extension when the lateral stress coefficient (K_0) reaches the passive value (K_p). For simple virgin loading-unloading of "normal soils" that are not highly cemented nor structured, the K_0 value increases with OCR according to:

$$K_0 = (1-\sin\phi')\ OCR^{\sin\phi'} \tag{4}$$

If the passive condition is represented by the general condition, then K_0 cannot exceed:

$$\boldsymbol{K_p} = \frac{1+\sin\boldsymbol{\phi}'}{1-\sin\boldsymbol{\phi}'} + \frac{2\boldsymbol{c}'}{\boldsymbol{\sigma_{vo}}'}\sqrt{\frac{1+\sin\boldsymbol{\phi}'}{1-\sin\boldsymbol{\phi}'}} \tag{5}$$

Generally, the value of effective cohesion intercept $c' \approx 0$, although a small finite value can be sometimes justified as a projection from the portion of the yield surface extending above the frictional envelope. In these cases, $c' \approx 0.02\sigma_p'$ may be applicable (Mayne & Stewart, 1988; Mesri & Abdel-Ghaffar, 1993).

2.6 *Hybrid SCE-CSSM Model for Cone Penetration*

Cone penetration in clays can be modeled using a number of different theories (Yu & Mitchell, 1998), including limit plasticity (e.g., Konrad & Law, 1987), cavity expansion (Keaveny & Mitchell, 1986), and strain path methods (Whittle & Aubeny, 1993), as well as by finite elements (Houlsby & Teh 1988) and dislocation theory (Elsworth, 1998). Using a spherical cavity expansion solution (Vesic, 1977) with a CSSM representation of undrained loading for triaxial compression mode, Mayne (1991, 1993) showed that the cone tip stress could be expressed in closed-form by:

$$q_t = \sigma_{vo} + [(4/3)(\ln I_R + 1)+\pi/2 + 1]\cdot(M/2)(OCR/2)^{\Lambda}\ \sigma_{vo}' \tag{6}$$

Similarly, the penetration porewater pressure at the cone shoulder ($u_b = u_2$) can also be expressed in terms of these parameters:

$$u_2 = u_0 + (4/3)(\ln I_R)\cdot(M/2)(OCR/2)^{\Lambda}\ \sigma_{vo}' + [1 - (OCR/2)^{\Lambda}]\cdot\sigma_{vo}' \tag{7}$$

Porewater pressures measured by type 1 cones (designated u_1) depend upon the actual position of the filter element (apex, below or above midface), as shown by Chen & Mayne (1994). An additional component representing compression beneath the tip can be simulated by an elastic stress path, such that for a typical midface element (Mayne, Burns, & Chen 2002):

$$\Delta u_1 = \Delta u_2 + (1/s^*)\cdot M\cdot(OCR/2)^{\Lambda}\cdot\sigma_{vo}' \tag{8}$$

where s* is the slope of the total stress path in Cambridge q-p' space, averaging around $\Delta q/\Delta p' = 3/4$ for midface elements. A large database of 45 intact clays tested by paired type 1 and type 2 piezocones, or else by special multi-element penetrometers, shows good agreement for (5) in Fig. 11 using representative values of $M = 0.92$, $\Lambda = 0.80$, and $s^* = 0.75$. Data from five fissured clays are also shown for comparative purposes. The fissured clays are of particular interest in that positive recordings are observed at the tip/face (u_1), whereas readings at the shoulder (u_2) are negative (Mayne, et al. 1990). Nevertheless, (8) is seen to provide a reasonable transform from u_2 to u_1 for these fissured clays too.

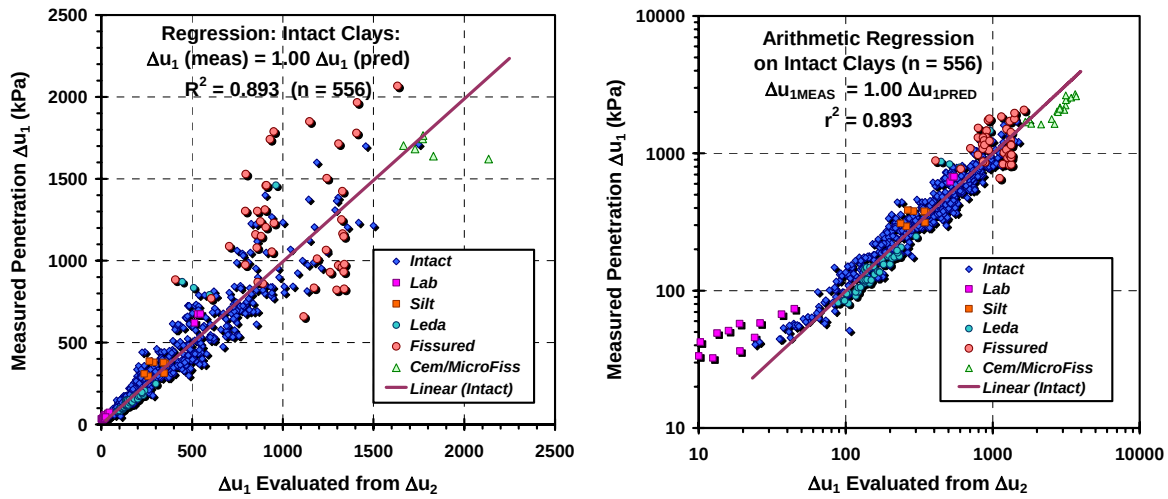

Figure 11. Measured midface u_1 porewater pressures from shoulder u_2 readings in (a) arithmetic and (b) log-log plots from 45 intact clays (data from 5 fissured clays also shown).

The sleeve friction in clays can be taken similar to a "Beta" method for calculating side friction of piles (e.g., Finno 1989). In this notion, the CPT sleeve resistance can be expressed by:

$$f_s = K_0 \tan\delta' \, \sigma_{vo}' \qquad (9)$$

where δ' is the interface friction between the steel penetrometer and the soil. Based on recent interface roughness research, a representative value can be taken as $\tan\delta'/\tan\phi' = 0.4$. Using this with (4) can provide a first-order evaluation of CPT f_s in clays.

To illustrate the forward use of stress history to drive the readings of cone tip, porewater pressures, and sleeve friction, Figure 12 shows the matched profiles obtained from the fitting of CPTu data for Sarapuí clay in Rio de Janeiro (data from Almeida & Marques, 2003) with parametric values: initial void ratio $e_0 = 3.0$, operational prestress = $\Delta\sigma_p' = 25$ kPa, $\phi' = 29^o$, $\Lambda = 0.7$, and operational rigidity index $I_R = 50$. The groundwater lies 0.2 m deep and the void ratio generates an average (light) unit weight for calculation of the total and effective overburden stresses. The overconsolidation has been caused by ageing (Almeida & Marques, 2003), yet it suffices to use an equivalent calculated OCR = $[\Delta\sigma_p'/\sigma_{vo}'+1]$. Then, equations (6) through (9) are adjusted to match the measured CPT readings with depth.

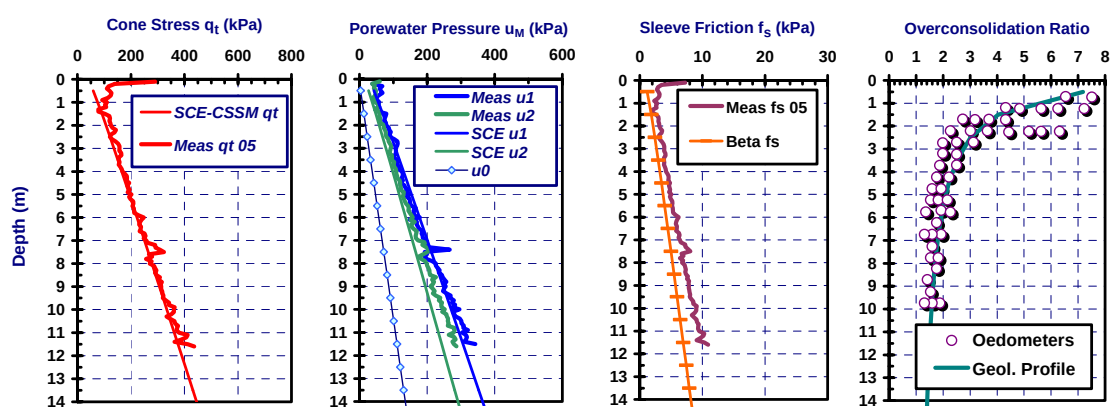

Figure 12. Generated and measured CPTu profiles in Sarapuí soft clay, Brazil.
(Data from Almeida & Marques, 2003).

2.7 *Hybrid SCE-CSSM Model for Dilatometer*

Although the flat dilatometer geometry does not directly lend itself to application by cavity expansion theory, the initial generated porewater pressure isochones are reasonably symmetric about the blade at early stages of penetration (Huang, et al. 1991). Prior studies have shown considerable similarity between the initial lift-off or contact pressure (p_0) measured by the flat dilatometer test (DMT) and the measured porewater pressures during cone penetration (Mayne & Bachus, 1989; Mayne 2006a). Also, similarities exist between the DMT p_0 and limit pressure (P_L) from companion series of pressuremeter tests (PMT) in the same clays (Clarke & Wroth, 1988). Using the latter as a guide, let us adopt (1) as applicable to the DMT using p_0 to represent the limiting pressure:

$$p_0 = \sigma_{ho} + s_u [\ln(I_R) + 1] \tag{10}$$

We can assume the same value of rigidity index applies to the DMT as to the CPT, as both invoke similarly large levels of straining during installation. The total horizontal stress can be calculated as $\sigma_{ho} = \sigma_{ho}' + u_o$, using the fact that $\sigma_{ho}' = K_0\, \sigma_{vo}'$.

For the expansion pressure measured by the DMT, a similar stress path concept (as used previously for the CPT u_1 reading) can be assumed whereby:

$$p_1 = p_0 + M\,(OCR/2)^{\Lambda}\, \sigma_{vo}' \tag{11}$$

While (11) is far from rigorous, it does in fact provide reasonable values for the DMT material index, $I_D = (p_1-p_0)/(p_0-u_0)$ that is useful in classifying soil types and consistency.

2.8 *Case Study Applications in Clays*

The simple representations for stress history ($\Delta\sigma_p'$, OCR) are used to generate full profiles of CPT q_t, f_s, u_1, and u_2, as well as DMT pressures p_0 and p_1 for three soft clays and two stiff overconsolidated soils. The soft clays include the UK national test site at Bothkennar (Hight, et al. 2003), the soft clay at Onsøy used by NGI (Lunne, et al. 2003), and a site very near the national geotechnical test site at Northwestern University (Finno, et al. 2000). For all these sites, a representative average void ratio and friction angle were known from lab tests on undisturbed samples taken from the site, as well as profiles of σ_p' from oedometer and/or consolidation tests. To check on the validity to stiffer clays, the method was also applied to two additional soils: (a) a sandy calcareous clay from Charleston, SC, known as the Cooper Marl (Camp, et al. 2002); and (b) stiff desiccated clay from Baton Rouge, Louisiana (Chen & Mayne, 1994). Table 1 summarizes the necessary input parameters that drive the complete analysis for each of the sites. For-

Table 1. List of clay sites with force-fitted CPTu and DMT calibrations and derived parameters

Site Name	**Location**	**z_w (m)**	**Void Ratio e_0**	**$\Delta\sigma_p'$ (kPa)**	**OCR State**	**ϕ'**	**Λ**	**Rigidity I_R**
Baton Rouge	Louisiana	5	0.92	850	4 to 15	28.5°	0.70	85
Bothkennar	Scotland	1	1.50	40	1 to 2	39.0°	0.90	85
Cooper Marl	S. Carolina	1	1.35	480	4 to 8	44.0°	0.90	750
Ford Center	Illinois	1	0.80	55	1 to 2	28.0°	0.80	300
Onsøy	Norway	0.5	1.75	30	1.2 to 3	32.0°	0.80	75
Sarapuí	Brazil	0.2	3.00	25	1 to 3	29.0°	0.70	50

Notes: z_w = depth to groundwater table; $\Delta\sigma_p'$ = prestress (also termed OCD by Locat, et al. 2003); OCR = overconsolidation ratio; ϕ' = effective stress friction angle; $\Lambda = 1 - C_s/C_c$ = plastic volumetric strain potential; C_s = swelling index; C_c = virgin compression index; and $I_R = G/s_u$ = operational rigidity index.

ward fitting of the SCE-CSSM algorithms for the in-situ tests in these six clays are presented in Figures 12 through 18. Brief descriptions of the clay sites, reference sources, and the calibrated fittings to in-situ test data are given below for each of the sites.

The *Bothkennar* clay site is located in Scotland and served as a major national test site for the British geotechnical community (Hight, et al. 2003). The entire June 1992 issue of Geotechnique is devoted to papers on the geology, geotechnical aspects, and lab and field testing in the soft Bothkennar clay (e.g. Nash, et al. 1992). The subsurface conditions consist of Holocene estuarine clays of 20-m thickness or more that have become lightly preconsolidated due to slight erosion ($\Delta\sigma_p'$ = 15 kPa) and groundwater fluctuations ($1 < z_w < 3.5$ m), plus additional structuration, including ageing since deposition some 8000 to 3000 years before present. Index testing shows plasticity characteristics changing with depth: $50 < w_n < 75\%$, $25 < w_p < 35\%$; and $55 < w_L < 85\%$. The Bothkennar clay has a rather high effective stress friction angle at peak of between 36º and 45º. Using representative values of ϕ' = 39º and I_R = 85, Figure 13 shows the forward fitting of the SCE-CSSM expressions for cone, piezocone, and flat dilatometer by adopting an equivalent prestress of $\Delta\sigma_p'$ = 40 kPa. Here, additional types of piezocone data from u_1 (midface) and u_2 (shoulder) elements were also available (Powell, et al. 1988; Jacobs & Coutts 1992).

The soft *Onsøy* clay in Norway has served as an experimental test site for NGI for almost 40 years (Lacasse & Lunne, 1982; Lunne, et al. 2003). The site consists of approximately 40 m of uniform marine clay of Holocene age. Primary mechanisms for apparent overconsolidation include groundwater fluctuations and ageing. Index parameters for the Onsøy clay include: $50 < w_n < 70\%$; $w_p \approx 30\%$; and $50 < w_L < 80\%$. Using representative values of ϕ' = 32º and I_R = 75, Figure 14 shows the good fitting observed for the SCE-CSSM expressions for cone, piezocone, and flat dilatometer by adopting an equivalent prestress of $\Delta\sigma_p'$ = 30 kPa.

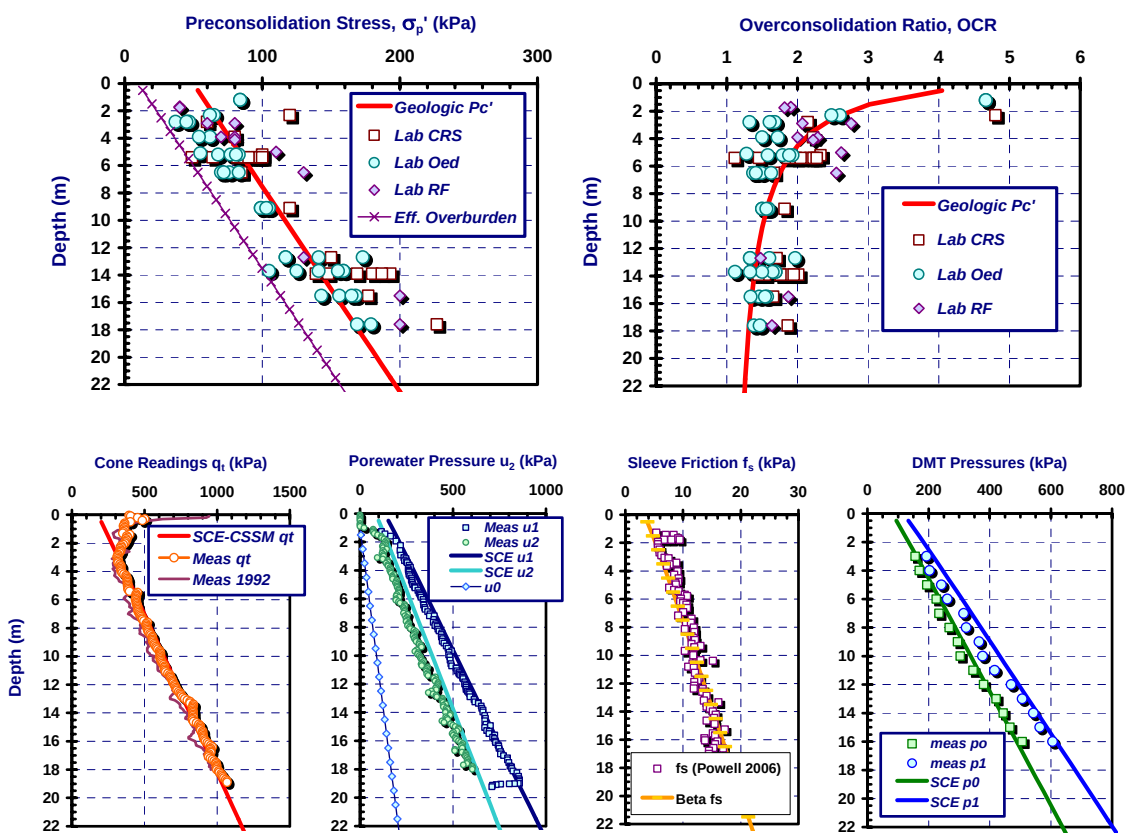

Fig. 13. Fitted OCR, CPT, CPTU, & DMT profiles for soft Bothkennar clay (data from Hight et al. 2003).

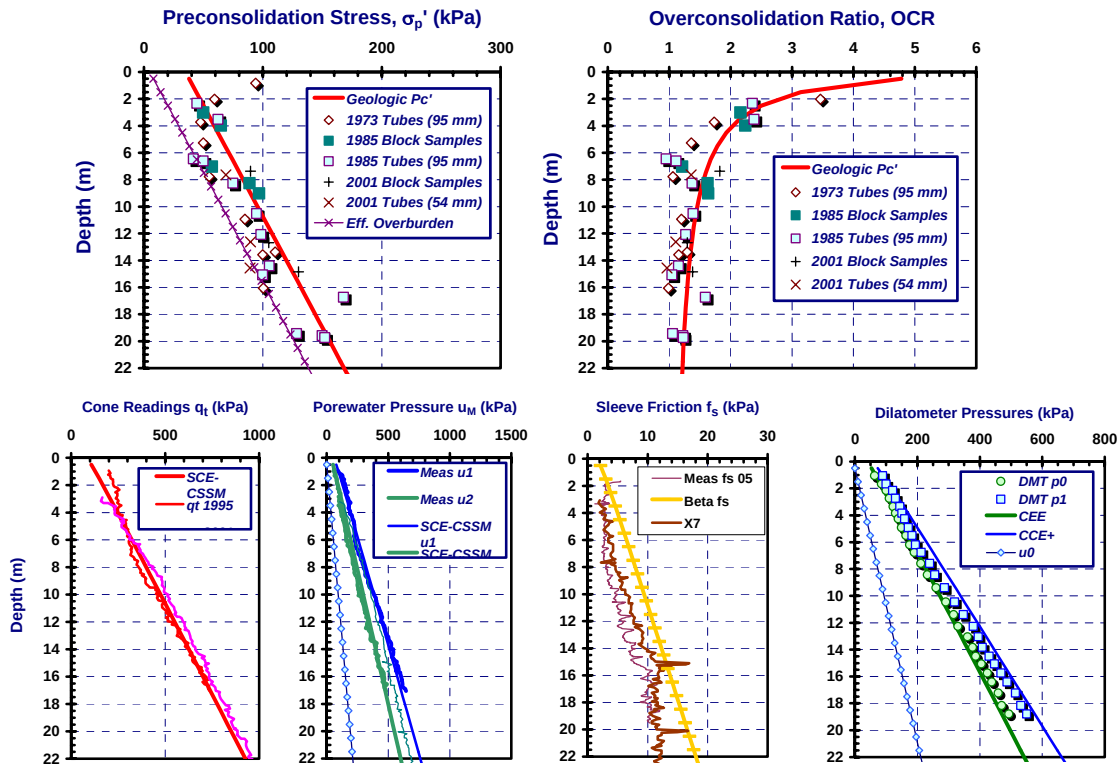

Fig. 14. Fitted OCR, CPT, CPTU, and DMT profiles for soft Onsøy clay (data from Lunne et al. 2003).

Soft freshwater clay deposits underlie the *Ford Design Center* (Blackburn, et al. 2005; Mayne 2006a) which is located near the national geotechnical experimentation site (NGES) on the campus of Northwestern University in Evanston, Illinois (Finno, 1989; Finno, et al. 2000). The author's CPT crew at Georgia Tech (GT) conducted CPTUs and DMTs at both the Ford site and nearby NGES in 2003 for the National Science Foundation (NSF). At both sites, an upper sand fill overlies soft clays that are lightly overconsolidated with 1.2 < OCRs < 2. Results from the 5 SCPTUs, one DMT, and a special frequent-interval downhole-type V_s probing (Mayne 2005) are presented in Figure 15. These soundings delineate the soft clays between 5 and 22 m depths. The forward fitting of CPT and DMT data are presented in Figure 16 using a prestress $\Delta\sigma_p' = 55$ kPa, representative $\phi' = 28^o$ (Finno 1989), and rather moderate high value of $I_R = 300$.

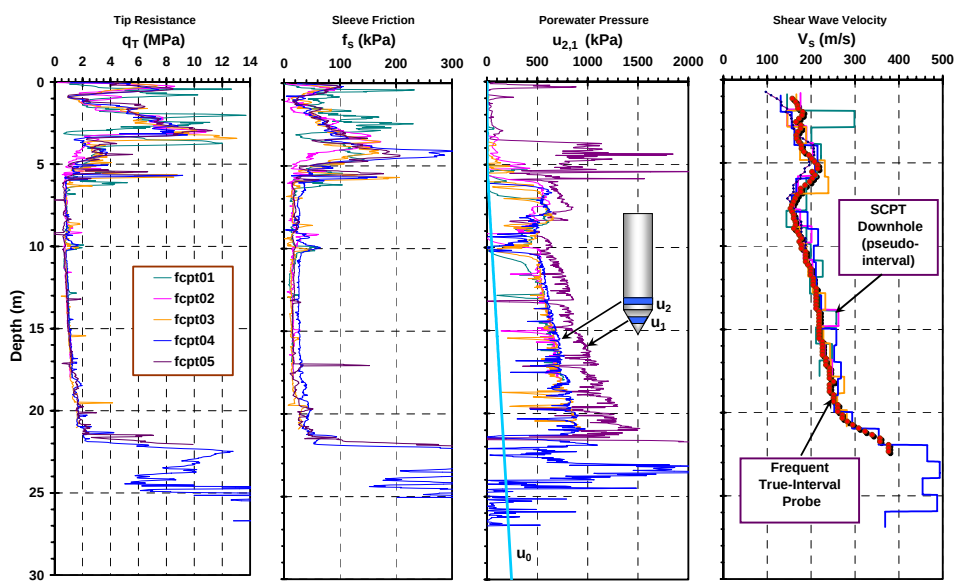

Figure 15. Summary of SCPTU soundings and frequent V_s profiles at Ford Center, Evanston, Illinois.

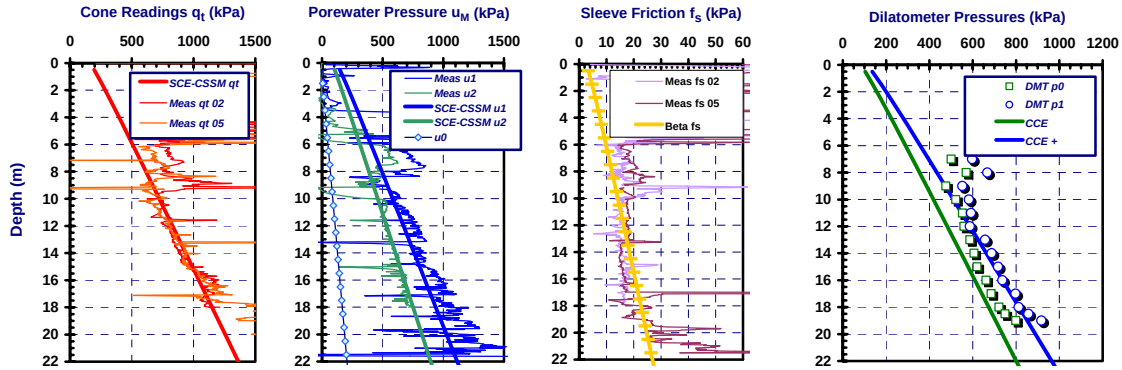

Figure 16. Fitted OCR, CPT, CPTU, and DMT profiles for soft clay at Ford Center, Illinois.

To illustrate the approach applicability for overconsolidated materials, two additional case studies from the author's files have been included here.

The stiff clays at the *Baton Rouge* site are Pleistocene age materials extending from 5 to over 40 meters thick (Chen & Mayne, 1994). In-situ test profiles are presented in Figure 17. These deltaic clays are fissured and desiccated. They are geologically & geographically related to the Beaumont clays of the Houston NGES (e.g., O'Neill, 2000). Mean values (± one S.D.) from lab index testing gave the water content w_n = 34 ± 12%; liquid limit w_L = 60 ± 20%, and plasticity index, PI = 33 ± 13%. Seven CPTs and one DMT sounding were performed using the cone truck at the Louisiana Transportation Research Center (LTRC) by the author under an NSF grant. The results of the piezocone type soundings were obtained using a Fugro triple-element penetrometer that showed good quality data at the midface (u_1) porewater pressure position, but

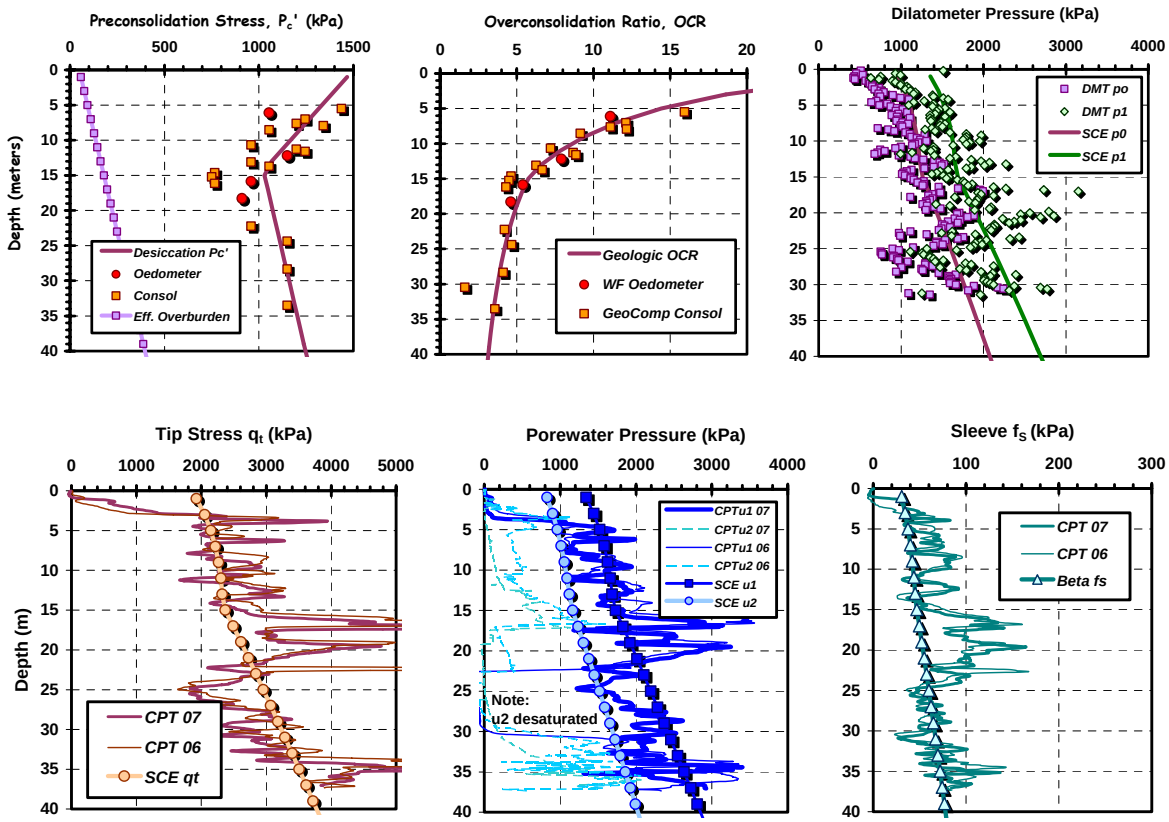

Figure 17. Fitted OCR, DMT, CPT and CPTU profiles for stiff clay in Baton Rouge, Louisiana.

irregular results at the shoulder (u_2) and behind sleeve (u_3) locations, probably due to use of water as the saturating fluid rather than the now-preferred glycerine (Mayne et al. 1995). The overconsolidation difference (OCD), as termed by Locat et al. (2003), is a quasi- prestress ($\Delta\sigma_p'$) that apparently varies with depth in the stiff Baton Rouge clays. Alternatively, a constant quasi-preconsolidation stress on the order of 1 MPa gives similar results (Chen & Mayne 1994). A series of 9 triaxial tests of the CIUC type determined c' = 0 and ϕ' = 28.5° for these materials. Using these values together with I_R = 85 gave the profiles of OCR, q_t, u_1, u_2, f_s, and DMT p_0 and p_1 for this site (Figure 16). It can be seen that the general magnitudes for CPTU and DMT readings are in line, yet the desaturated shoulder piezocone elements fall below the expected values, for reasons given above. Additional "squiggly lines" and variances in the measured in-situ profiles reflect other influences, including the macrofabric of fissures and a more complex stress history (as these are Pleistocene age materials), as well as variable sand fractions. Nevertheless, the fitted profiles are notably within the realm of measured resistances that are considerably higher than the four previously-shown soft clays at Bothkennar, Onsøy, Sarapuí, and Ford sites.

The stiff *Cooper Marl* lies beneath Charleston, South Carolina, and serves to support most of the large building, dock, and bridge structures in the region. This material appears as a sandy calcareous clay of Oligocene age, with a very high calcium carbonate content between 60 to 80% (Camp, et al. 2002). Representative mean values of index parameters include: w_n = 48%, w_L = 78%, and PI = 38%. Typical SPT-N values in this material are in the range of 12 to 16 bpf. A representative SCPTU is given in Mayne (2005). Separate sets of triaxial testing on undisturbed samples of the calcareous clay by various geotechnical firms for the newly-opened Arthur Ravenel Bridge in 2005 and 15-year old Mark Clark Bridge show consistently high effective stress friction angles 40° ≤ ϕ' ≤ 45° for the Cooper Marl. The material has been preconsolidated by erosion and groundwater changes, as well as added structuration due to the calcium carbonate chemistry. Using an OCD = 480 kPa, representative ϕ' = 44°, and very high I_R = 750, derived profiles of OCR, CPT, CPTU, and DMT resistances are given in Figure 18.

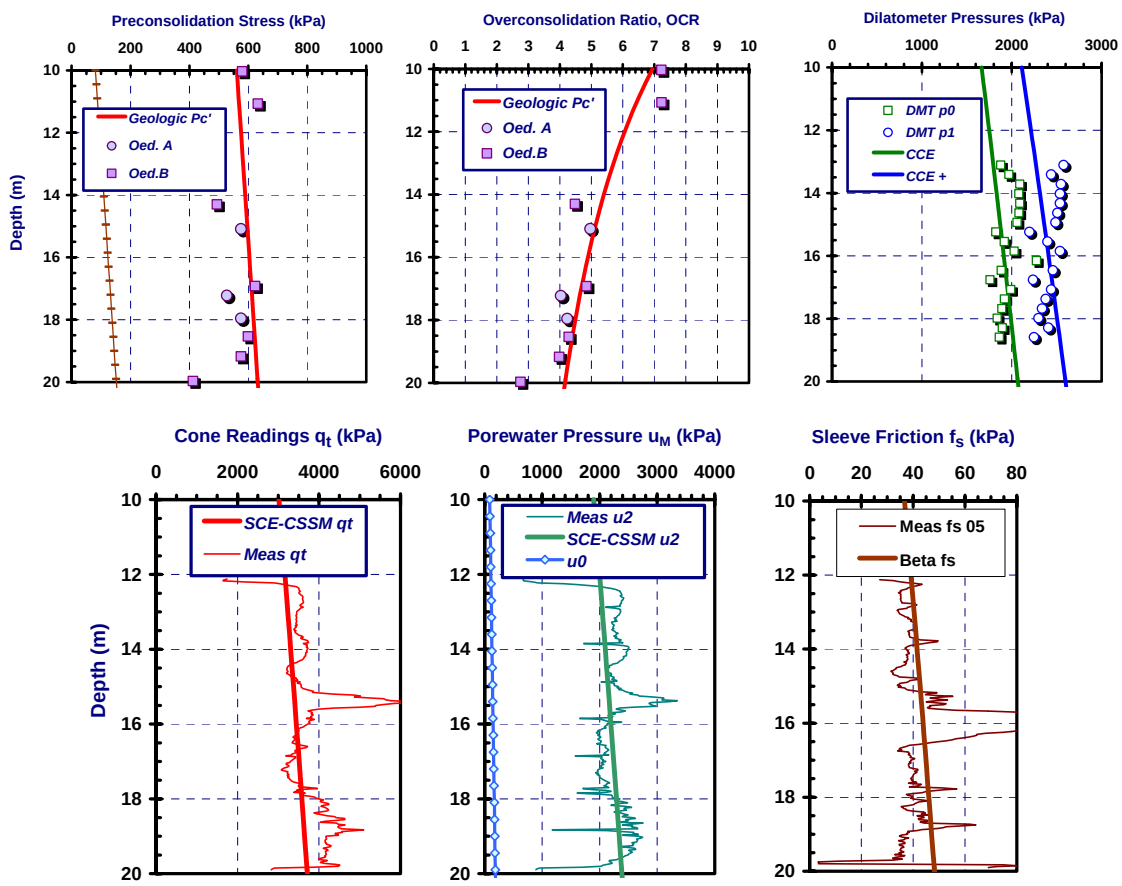

Figure 18. Fitted OCR, DMT, CPT, and CPTU profiles for stiff calcareous Cooper Marl, SC.

2.10 *First-Order OCRs from Piezocone and Dilatometer*

The aforementioned hybrid SCE-CSSM expressions can be used to help ascertain OCR and/or OCD profiles in clay deposits, requiring input values of effective friction angle, compressibility indices, and rigidity indices. A simplified approach utilizes representative values (e.g., $\phi' = 30^o$, $\Lambda = 0.80$, and $I_R = 100$) to obtain first-order expressions for cone and piezocone penetration in clays (Mayne 2005) that have also been validated by statistical regression analyses of databases in intact soft to firm to stiff clays (Kulhawy & Mayne 1990):

$$\sigma_p' \approx 0.33\ (q_t - \sigma_{vo}) \tag{12a}$$

$$\sigma_p' \approx 0.47\ (u_1 - u_o) \tag{12b}$$

$$\sigma_p' \approx 0.53\ (u_2 - u_o) \tag{12c}$$

$$\sigma_p' \approx 0.60\ (q_t - u_2) \tag{12d}$$

Independent studies by Demers & Leroueil (2002) confirmed the applicability of (12a) for 22 clay sites in eastern Canada.

Similarly, expressions for first-order DMT evaluations of preconsolidation stresses in intact clays have been developed (Mayne, 2001):

$$\sigma_p' \approx 0.51(p_0 - u_o) \tag{13}$$

For fissured clays, the above relationships underpredict the preconsolidation stresses because the additional macrofabric of cracks & fissures tends to open up during the advancement of the in-situ probe. In contrast, in the benchmark lab test that defines σ_p' (i.e., the one-dimensional consolidation test), the fissures continually close up during constrained compression. Thus, the coefficient terms for fissured geomaterials in the above expressions could be as much as double those shown for intact clays (Mayne & Bachus, 1989).

2.11 *Other In-Situ Tests in Clays*

It is also possible to infer σ_p' profiles in clays from other in-situ tests (SPT, VST, PMT, T-bar, and S-wave velocity). For the vane, the relationship depends upon the clay plasticity (Mayne & Mitchell, 1988), as shown in Figure 19.

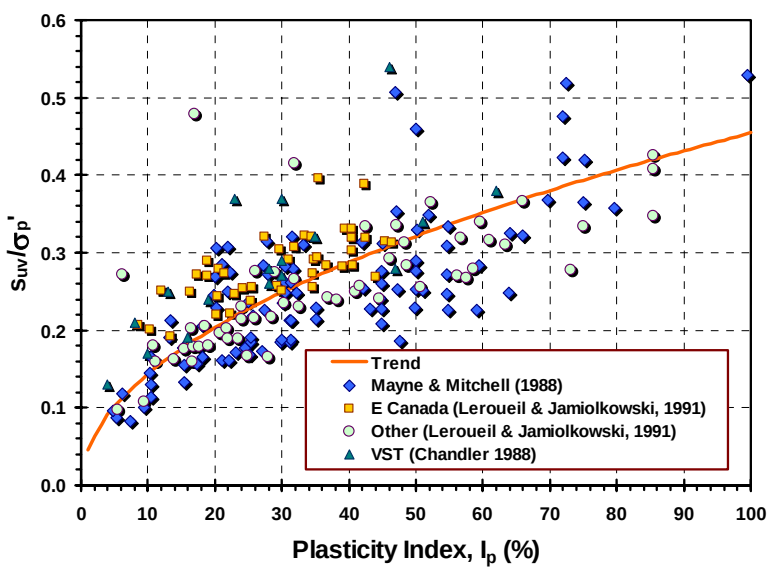

Figure 19. Evaluation of clay preconsolidation from vane strength and plasticity index.

The trend for the VST data is represented by:

$$\sigma_P' \approx \frac{22 \cdot s_{uv}}{\sqrt{PI}} \tag{14}$$

For the standard penetration test (SPT), the measured N-value should be corrected to an energy efficiency for the standard-of-practice (60% in the USA), designated N_{60} (e.g., Skempton 1986). In firm to stiff clays which are not highly sensitive nor structured, the approximation is (Kulhawy & Mayne, 1990):

$$\sigma_p' \approx 0.47\, N_{60} \cdot \sigma_{atm} \tag{15}$$

where σ_{atm} = 1 atmosphere = 1 bar = 100 kPa ≈ 1 tsf.

For the pressuremeter test, a cavity expansion formulation can be implemented to give (Mayne & Bachus, 1989):

$$\sigma_p' \approx 0.5 \cdot s_{uPMT} \cdot \ln(I_R) \tag{16}$$

where $I_R = G/s_{uPMT}$ is the operational value from the PMT. As seen in Figure 20, this is only to be used as a rough guide as the PMT is hardly utilized as an index test for profiling. Data are from self-boring type PMT collected by Mayne & Kulhawy (1990). For the PMT, the value of I_R is generally higher than that corresponding to the large strain I_R value appropriate for the penetration-type probes.

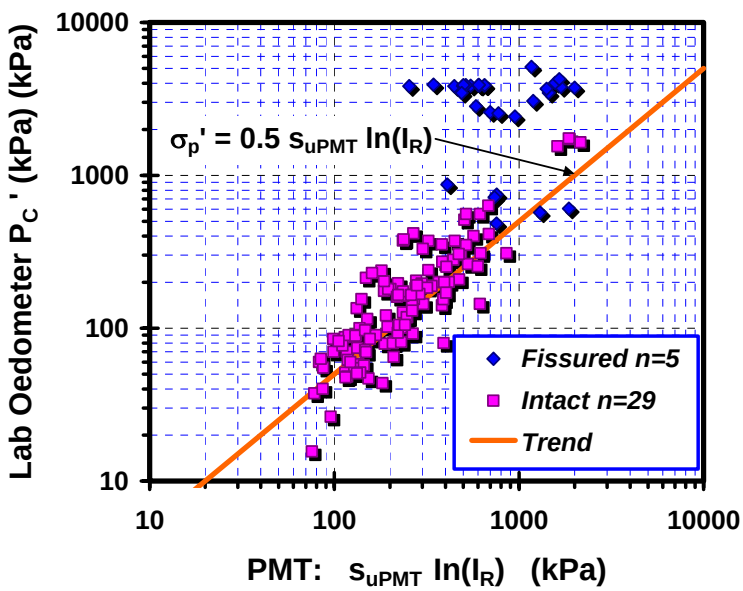

Figure 20. Trend between preconsolidation stress and PMT-calculated Δu in clays.

The relatively recent development of full-flow penetrometers have emerged to address the very soft clays found offshore at the murky mudline region (Watson et al. 1998). These offer 3 advantages over classical CPT. First, in lieu of a conventional conical point with 60-degree angle, the penetrometer can be fitted with a larger head-piece (ball, T-bar, or plate) at the front-end to increase resolution of the electronic load cell (i.e., generally 100-cm^2 area vs. standard 10-cm^2 with cone). On the second point, the correction of porewater pressures on unequal areas be-

comes less significant (q_{Tcorr}) because the measured force is much larger. Thirdly, since the soil is assumed to flow around the head, the tip stress is used directly (as compared with net resistance for the CPT: q_t-σ_{vo}), thus avoiding necessity and uncertainty in evaluation of the overburden stress at each depth. For very soft to soft clays and silts, a similar development in the direct assessment of σ_p' can be made by compilation of a database at sites with known stress history profiles. As such, T-bar penetration data from Onsøy, Norway (Lunne, et al. 2005), Gloucester, Ontario (Yafrate & DeJong 2005), Athalone, Ireland (Long & Gudjonsson 2004), Burswood, Australia (Chung, 2005), Amherst, Massachusetts (DeJong et al. 2004), and Louiseville, Quebec (Yafrate & DeJong, 2005) are collected in Figure 21 showing:

$$\sigma_p' \approx 0.357\ q_{TBar} \tag{17}$$

having a statistical coefficient of determination $r^2 = 0.846$ (n = 26).

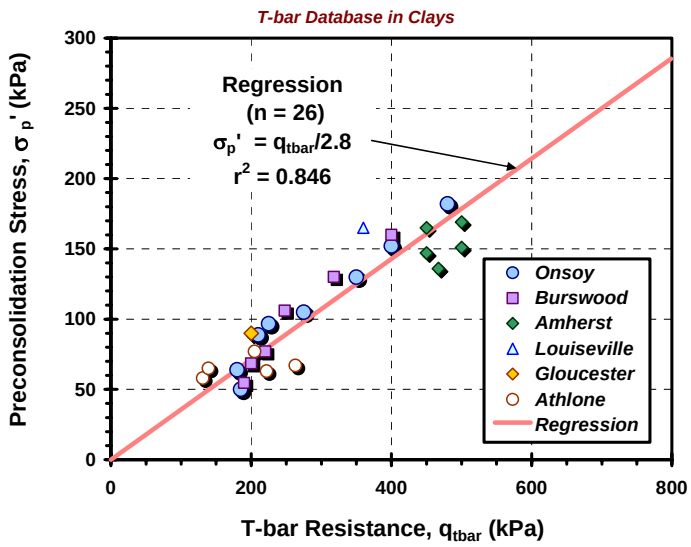

Figure 21. Trend between preconsolidation stress and T-bar resistance in very soft clays.

Finally, the results of shear wave velocity measurements (primarily downhole data) have been used to obtain a first-order evaluation of σ_p' in clays (Mayne, Robertson, & Lunne, 1998):

$$\sigma_p' \approx 0.107\ V_s^{\ 1.47} \tag{18}$$

where the preconsolidation stress is stated in units of kPa and shear wave velocity input in units of meters/sec (n = 262; $r^2 = 0.823$). This may prove valuable when using non-invasive types of geophysics in clay geologies, such as the surface wave measurements by SASW, CSW, and MASW.

For the above dataset, the coefficient of determination increased ($r^2 = 0.917$) if both net cone resistance and shear wave were included, giving:

$$\sigma_p' = (q_t\text{-}\sigma_{vo})^{0.702}\ (V_s/64)^{0.751} \tag{19}$$

thus optimized by use of the seismic piezocone, since both parameters are determined during the same sounding. In independent validations, Jamiolkowski & Pepe (2001) used (19) with success in Pancone clay at the Pisa tower site.

2.12 *Combinative In-Situ Data*

In the interpretation of in-situ tests, there is always uncertainty in the application of available empirical, analytical, and/or numerical methods to a particular clay formation. Thus, it behooves the site characterizer to use a combination of different readings and measurements taken at the site and compare their results for agreement and conformity. Else, convince the client to ante up more funds to conduct additional sampling and testing at the site. By using different test data together, the best estimate profile of stress history can be obtained.

An example of combining in-situ test data is shown below in Figure 22 for the offshore characterization of the lower two facies of the Bootlegger Cove Formation (BCF) at the Port of Anchorage expansion (Mayne & Pearce 2005). A jackup platform (SeaCore) was used for the drilling, sampling, and in-situ testing, since high-to-low tidal variations are 10 m twice a day. The results of cone tip stress, piezocone porewater pressures, vane shear, shear wave velocity, and lab oedometer tests can be collected together to assess the σ_p' profile in the clay. The preconsolidation stress then serves as a common denominator for all test data interpretation in the Bootlegger Cove clays. The approach here for the BCF clay shows the overconsolidated nature in consistent manner with an assumed simple erosional loss or OCD = 400 kPa. Actual inspection of Fig. 22 shows a more complex stress history, with perhaps sequential layers of different equivalent prestresses, such as OCD = 320 kPa from mudline level at 13 to 29 m, OCD = 460 kPa from 29 to 37 m, followed by OCD = 390 from 37 to 45 m. Below depths of 38 m, the Δu relationship shows a higher interpretation of σ_p' than the net cone resistance value, perhaps signifying a more sensitive facies in the lower part of the clay.

If classical "clay" methods of interpreting undrained shear strengths directly from the lab and field tests were applied instead, significant scatter plots would result, as s_u exhibits many faces and modes. In concept, σ_p' is uniquely defined as the yield point on the 1-D consolidation curve, corresponding to the top of the yield surface in 3-D q-p space. If one desires an undrained shear strength value, then application of (2) provides this in a consistent CSSM framework for a representative DSS mode (Trak et al. 1980; Jamiolkowski et al. 1985), else the user can buy into a constitutive soil model to provide other required modes (e.g., CAUC, PSE), such as discussed elsewhere (Ohta et al. 1985; Wroth & Houlsby 1985; Kulhawy & Mayne 1990; Whittle 1993), or by use of empirical methods based on clay plasticity (e.g., Ladd, 1991).

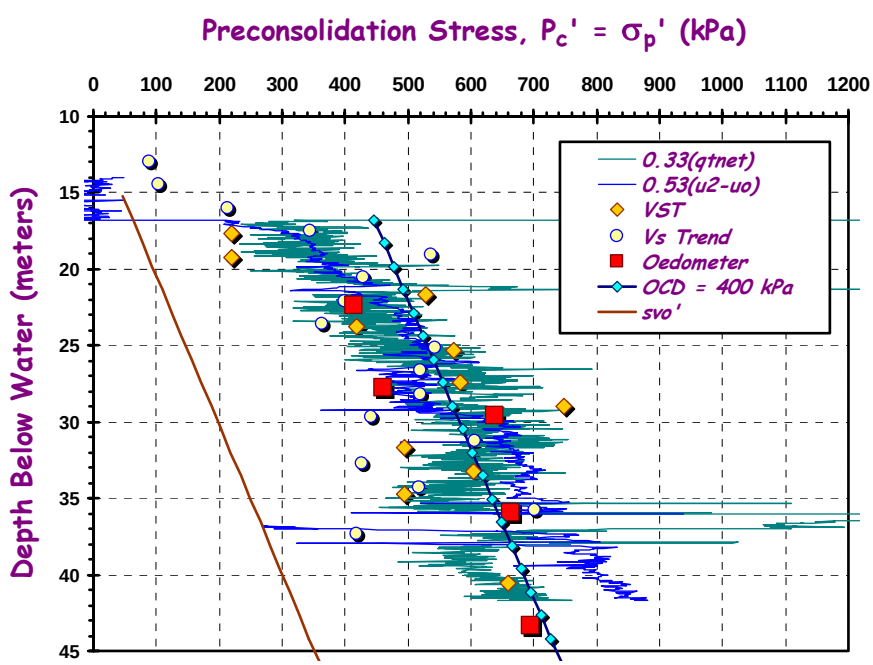

Figure 21. Combined in-situ and lab data for preconsolidation profile in Bootlegger Cove clay.

2.13 *Stress-Strain-Strength Representation for Clays*

The stress-strain-strength response of clays begins at the initial small-strain stiffness, represented by the maximum shear modulus: $G_0 = G_{max} = \rho_T V_s^2$. The equivalent elastic Young's modulus is also available from: $E = 2G(1+\nu)$, where $\nu' = 0.2$ applies for drained and $\nu_u = 0.5$ for undrained conditions.

The direct simple shear (DSS) gives the best suited mode for stress-strain-strength response for three reasons: (1) *shearing* is the primary mechanism involved in stability & deformation problems, as well as soil-structure interaction situations; (2) DSS data appear much less affected by sample disturbance than the more commonly-available triaxial compression modes (e.g., Lacasse, et al. 1985); and (3) the DSS stress-strain-strength curve is close to the overall average of compression, shear, and extension modes when strain compatibility considerations are made (Ladd, 1991). As such, from the DSS plots of shear stress vs. shear strain (τ vs. γ_s), as shown in Fig. 7, we may define the following: (a) the shear strength is the maximum shear stress (τ_{max}), (b) the slope is the shear modulus ($G = \tau/\gamma_s$), (c) the initial stiffness is given by the small-strain shear modulus $G_0 = G_{max}$; (d) the ratio of shear modulus to shear strength is the rigidity index ($I_R = G/\tau_{max}$); and (e) the strain at failure $\gamma_f = 1/I_R$. For drained loading, the shear strength is given simply by $\tau_{max} = c' + \sigma_{vo}' \tan\phi'$, with $c' = 0$ applicable in most cases. For saturated soils, the condition for undrained loading is given as $\tau_{max} = c_u = s_u$, termed the undrained shear strength (per equation 2). At the onset of loading in the field, the soil does not yet know which stress path will be pursued, as this depends upon the applied rate of loading relative to the permeability of the ground. Consequently, the initial stiffness in the field is G_{max} for any mode (since Δu will not develop until threshold strains are reached later).

A companion to the DSS is another pure shear mode given by the torsional shear (TS) test. This has an advantage in that the test can begin as a resonant column to directly determine the small-strain stiffness ($G_0 = G_{max}$), then proceed into the intermediate- and large-strain regions to evaluate shear moduli and shear strength. The G/G_{max} curves can be presented in terms of logarithm of shear strain (γ_s), as discussed by Jardine et al. (1986) and Atkinson (2000), or alternatively in terms of mobilized shear stress (τ/τ_{max}), as discussed by Tatsuoka & Shibuya (1992), Fahey & Carter (1993), and LoPresti et al. (1998). With the local strain measurements made on the midsection of triaxial specimens, similar curves of modulus reduction with mobilized deviator stress have been developed (e.g., Tatsuoka & Shibuya, 1992). In terms of fitting stress-strain data, G/G_{max} vs. mobilized stress level (τ/τ_{max}) plots are visually biased towards the intermediate- to large-strain regions of the soil response. In contrast, G/G_{max} vs. log γ_s curves tend to accentuate the small- to intermediate-strain range. The ratio (G/G_{max} or G/G_0) is a reduction factor to apply to the maximum shear modulus, depending on current loading conditions. The mobilized shear stress is analogous to the reciprocal of the factor of safety ($\tau/\tau_{max} = 1/FS$).

A selection of modulus reduction curves, represented by the ratio (G/G_{max}), has been collected from monotonic TS test performed on different materials (Mayne, 2005). The results are presented in Figure 23, where $G = \tau/\gamma$ = secant shear modulus. Additional monotonic static loading test data from special triaxial tests with internal local strain measurements are also included. Here, an assumed constant ν has been applied and the conversion: $E = 2G(1+\nu)$ to permit E/E_{max} vs. q/q_{max}. Undrained tests are shown by solid dots and drained tests are indicated by open symbols. In general, the clays were tested under undrained loading (except Pisa), and the sands were tested under drained shearing conditions (except Kentucky clayey sand). Similar curve trends are noted for both drainage conditions (undrained and drained) for both clays and sands.

Nonlinear representation of the stiffness has been a major focus of the recent series of conferences on the theme *Deformation Characteristics of Geomaterials*. A number of different mathematical expressions can be adopted to produce closed-form stress-strain-strength curves (e.g., LoPresti et al. 1998; Shibuya, et al. 2001; Santos & Correia, 2001; Tatsuoka et al. 2003; Jardine et al. 2005). For example, a simple hyperbola requires only two parameter constants for a nonlinear stress-strain representation, however, it can only fit one region of the strain range (small or intermediate or large), as discussed by Tatsuoka & Shibuya (1992). Thus other expressions have been sought. One example of the derived modulus reduction curves for a modified hyperbola (Fahey & Carter, 1993) is shown in Figure 24, with $f = 1$ and $0.2 < g < 0.4$ encompassing much of the TS and TX data shown previously. The stress-strain-strength curve can

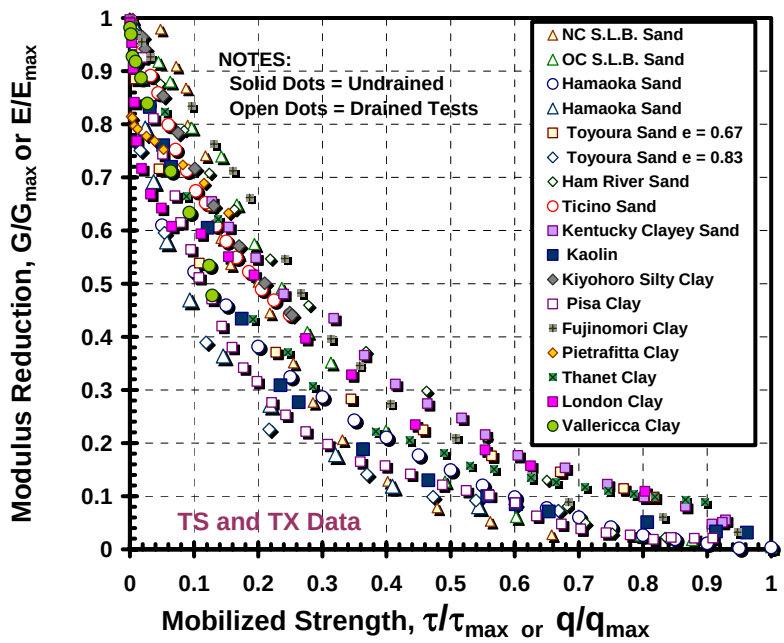

Figure 23. Modulus reduction from TS and TX data on clays and sands vs. mobilized strength.

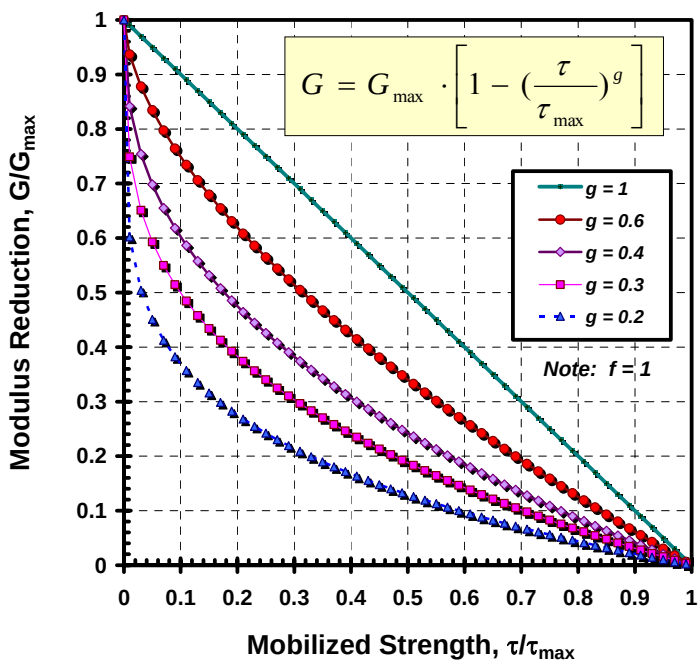

Figure 24. Modulus reduction vs. mobilized strength using modified hyperbola (after Fahey 1998).

be defined by the shear strength (τ_{max}), initial shear modulus ($G_0 = G_{max}$), and adopted exponent ($g \approx 0.3 \pm 0.1$ for "hourglass sands" and "vanilla clays"). Then the shear stress (τ) and secant shear modulus (G) can be determined at any load level ($\tau/\tau_{max} = 1/FS$):

$$\tau = G \cdot \gamma_s \tag{20}$$

$$G = G_{max} \cdot [\, 1 - (\tau/\tau_{max})^g] \tag{21}$$

Alternatively, a logarithmic function (Puzrin & Burland, 1996) can be employed with a simplified version relying on a normalized strain parameter (x_L) in the range: $20 < x_L < 50$ for the TS data set, where $x_L = G_{max}/G_{min}$, and $G_{min} = \tau_{max}/\gamma_f$. This has the advantage that all parameters have a recognized physical significance. Calibration fittings for soils using the log function are discussed by Elhakim & Mayne (2000).

An illustrative fitting for both approaches is presented for San Francisco Bay Mud, where field and lab data are reported by Pestana, et al. (2002). Results of SCPTu sounding at the California site are given in Figure 25. The cone tip stress, excess porewater pressures, and/or effective cone resistance can be used in (12) to obtain the estimated profile of σ_p' and OCR, which in turn, are utilized in (2) to evaluate the DSS mode for undrained shear strength. The stress-strain-strength curves obtained using s_{uDSS} = 21.8 kPa and G_0 = 10.3 MPa are shown in Fig. 26 for the modified hyperbola (g = 0.35) and log function (x_L = 35) with good agreement for both cases compared with measured DSS data on undisturbed samples taken from 7.3 m depth.

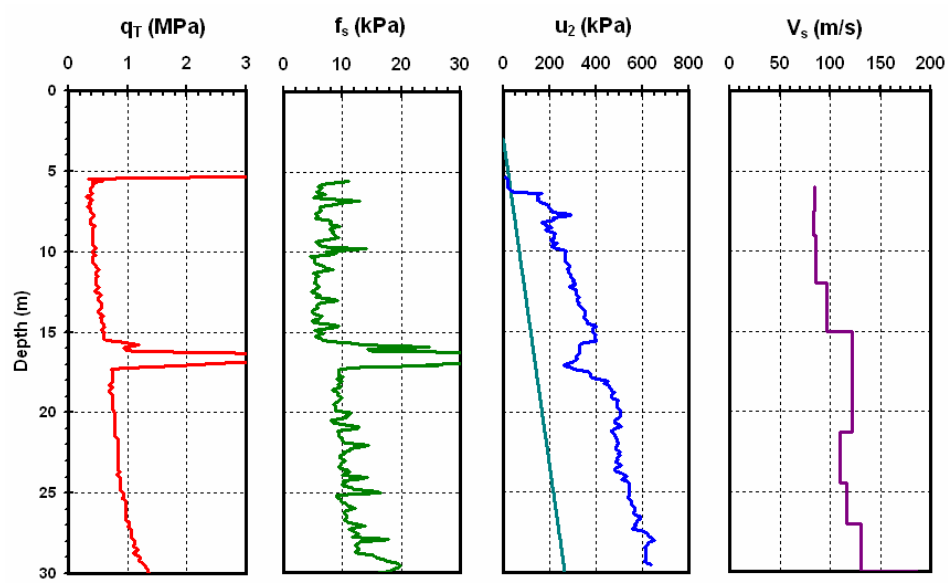

Figure 25. Results of SCPTU in San Francisco Bay Mud (data from Pestana et al. 2002)

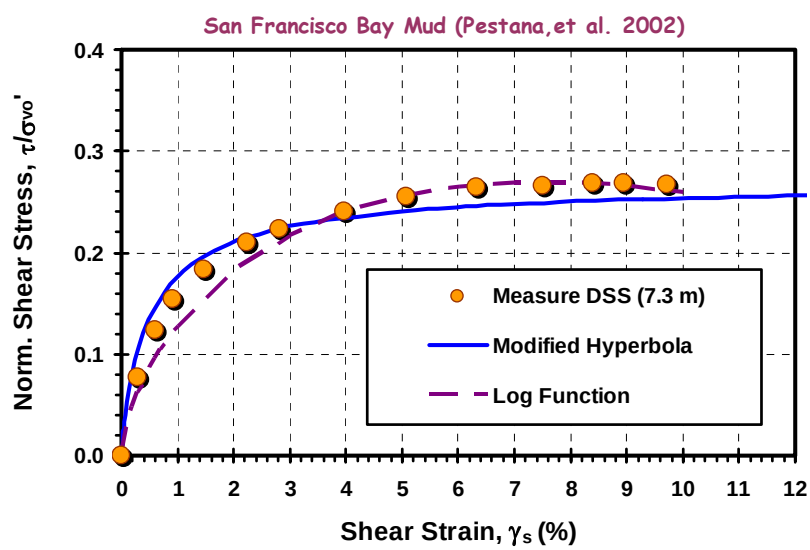

Figure 26. Measured and fitted DSS stress-strain-strength curves for San Francisco Bay Mud.

A unified constitutive model for sand and clay (Pestana & Whittle, 1999) provides theoretical relationships for G/G_{max} reduction with log shear strain that are found in good comparison with cyclic data from resonant column tests summarized by Vucetic & Dobry (1991). Careful studies by Shibuya, et al. (1997) and Yamashita, et al. (2001) have shown that differences in monotonic and cyclic reduction curves are predominantly explained by strain rate effects, thus the author suggests that monotonic curves be used as a basis for all other curves, that afterwards, can be adjusted for strain rate and/or uppers to form dynamic curves, as necessary.

In terms of in-situ testing, the use of mechanical wave geophysics (CHT, DHT, SASW, SL, SCPT, SDMT) is significant because the initial shear modulus can be defined. Since the SCPTu provides information on both the initial stiffness (G_{max}) at small-strains, as well as shear strength (τ_{max} from s_u and/or ϕ') at large-strains, the difficult question is how to determine stiffnesses at intermediate strain levels on a site-specific basis, without assuming values. One prospect is the cone pressuremeter (Schnaid & Houlsby, 1992; Ghionna, et al. 1995) with a geophone setup to produce a seismic piezocone pressuremeter (SCPMTu). Another approach would be the utilization of paired side-by-side in-situ tests, such as companion sets of SCPTu and DMT (Tanaka & Tanaka, 1998), or the commercially-available SDMT (e.g., Foti, et al. 2006).

2.14 *Strain Rate Effects*

Soils exhibit strain rate effects and these can be addressed by carefully-controlled lab tests (Tatsuoka, et al 1997; Shibuya et al. 1997). Commonly, the triaxial test has been utilized to investigate effects of strain rate effects on undrained stress-strain behavior, with stiffness and strength both increasing with rate of loading (e.g., Sheahan et al. 1996). Yet, considerable research has also shown that consolidation results (both e-logσ_v' curves and yield stress, σ_p') shift up with increasing strain rate, particularly in clays (Leroueil & Hight 2003). Consequently, the results of in-situ tests in the field are affected by strain rate. Of additional complication in the field is that drainage can occur during testing.

For vane shear tests, data were compiled by Peuchen & Mayne (2006) from 27 field sites and 7 lab series on clays. Two common means to show rate effects in soils include (1) time-to-failure, t_f, and (2) power function format (Soga & Mitchell, 1996). For the VST data, Figure 27 shows the effects of time-to-failure on normalized undrained shear strength (s_{uv}/s_{uv0}). These appear fairly consistent over a wide range of loading conditions, particularly from 0.01 minutes to

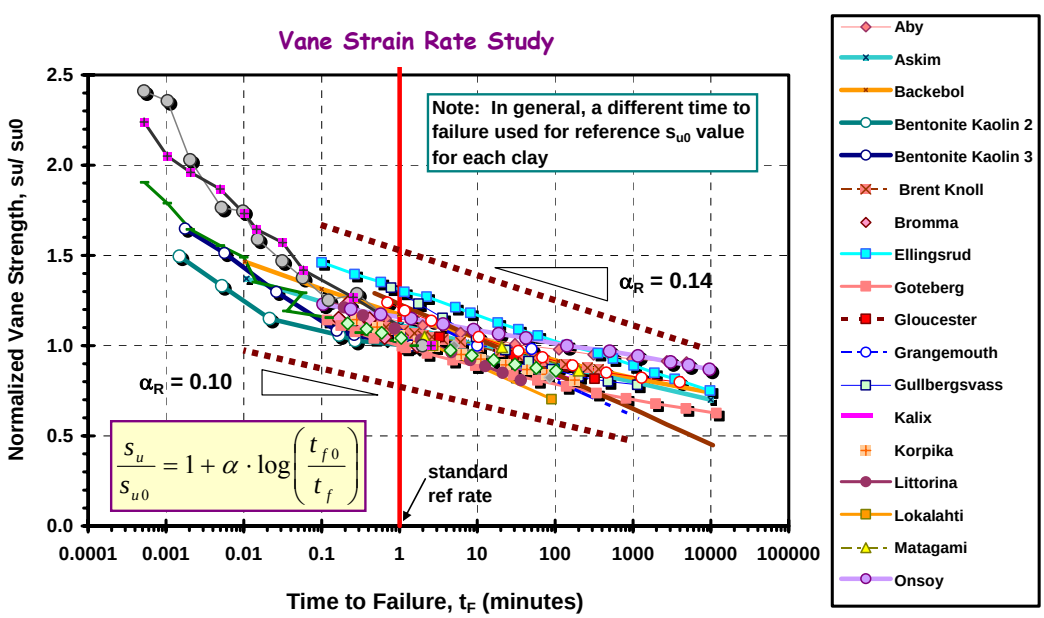

Figure 27. Variation of vane shear strengths with time-to-failure (Peuchen & Mayne 2006).

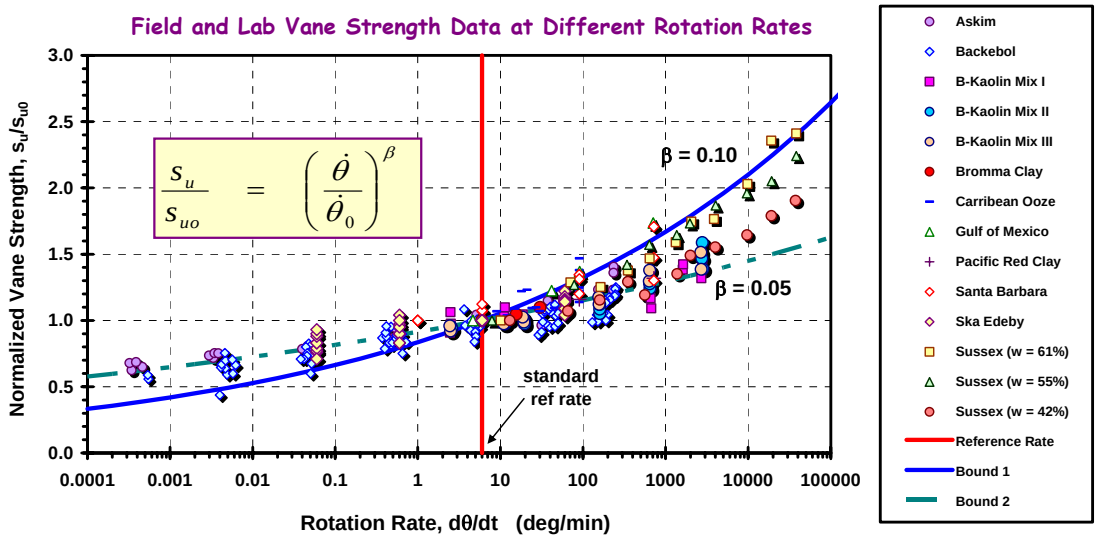

Figure 28. Trend of vane shear strength with increasing rate of rotation (Peuchen & Mayne 2006).

10,000 minutes. Here, the strain rate effect on undrained vane strength may be seen to increase on the order of 10 to 14% per log cycle which is comparable to that observed for laboratory test data (e.g., Kulhawy & Mayne, 1990; Leroueil & Hight, 2003). At very fast rates ($t_f < 0.01$ min), apparent dynamic effects may also occur, although those data are biased towards the small lab size equipment and use of remolded and synthetic clays.

Using the alternate plotting of normalized vane strength vs. rotation rate, the data are presented in Figure 28. The power law format shows that the exponent term is generally between 0.05 and 0.10, in agreement with lab triaxial and consolidation data (Soga & Mitchell, 1996).

For laboratory triaxial testing, truly undrained conditions can be maintained by locking off the drainage ports. In this case, as the shearing rates decrease to very slow values, the undrained shear strength will level off to a minimum value. Thus, in lieu of the semi-log function depicted in Figure 27 to represent strain rate effects on s_u, Randolph (2004) suggested an hyperbolic sine function that captures this facet.

In the field, if the rate of loading decreases significantly, then partial to full drainage can occur during in-situ testing, since there is no control on drainage. Lunne et al. (1997) present a table of CPT studies that look at rate effects and these can be consulted to further investigate rate effects concerning penetration testing. Randolph (2004) has proposed the addition of "twitch testing" to help evaluate strain rate and drainage effects, as discussed below in Section 2.16.

2.15 *Dissipation Testing*

In fine-grained soils, undrained loading is a transient case and represents but a particular stress path at constant volume ($\Delta V/V_0 = 0$) within an infinite number of possible stress paths in effective q-p' space. Given sufficient time, the temporary perturbation caused by in-situ testing will seek equilibrium and the dissipation of excess porewater pressures. The rate at which equilibrium is achieved is governed by the coefficient of permeability (k) of the medium, or alternatively by the coefficient of consolidation (c_{vh}):

$$c_{vh} = \frac{k \cdot D'}{\gamma_w} \tag{22}$$

where D' = constrained modulus and γ_w = unit weight of water. For most natural clays, the horizontal permeability is only 5 to 10% higher than the vertical value (Leroueil & Hight, 2003).

Since piezocone tests (CPTu) directly measure penetration porewater pressures, the practical emphasis is to utilize dissipation readings to evaluate c_{vh} in soils, although procedures have also

been developed for PMT (Fahey & Goh 1995; Clarke & Gambin 1998) and DMT (Robertson et al. 1998; Marchetti et al. 2001). The most popular CPTù method at present is the strain path method (SPM) solution of Houlsby & Teh (1988), although other available procedures are discussed by Jamiolkowski et al. (1985), Senneset et al. (1988, 1989), Danzinger et al. (1997), Burns & Mayne (1998, 2002), and others.

In terms of calibrating an approach, a fairly comprehensive study between lab c_v values and piezocone c_h values in clays and silts was reported by Robertson, et al. (1992). Assumptions were made between the ratio of horizontal to vertical permeability to address possible issues of anisotropy during interpretation. The study compared laboratory-determined results with the SPM solution (Teh & Houlsby 1991) using data from type 1 piezocones (22 sites) and type 2 piezocones (23 sites), as well as 8 sites where backcalculated field values of c_{vh} were obtained from full-scale loadings.

With the SPM approach in practice, it is common to use only the measured time to reach 50% consolidation, designated t_{50}. As such, if dissipation tests are carried out at select depth intervals during field testing, a fairly optimized data collection is achieved by the SCPTù since five measurements of soil behavior are captured in that single sounding: q_t, f_s, u_b, t_{50}, and V_s. The results of a (composite) SCPTù in the soft varved clays at the NGES in Amherst, Massachusetts are depicted in Figure 29. Here the results of a GT sounding are augmented with data from a separate series of dissipations conducted by DeGroot & Lutenegger (1994).

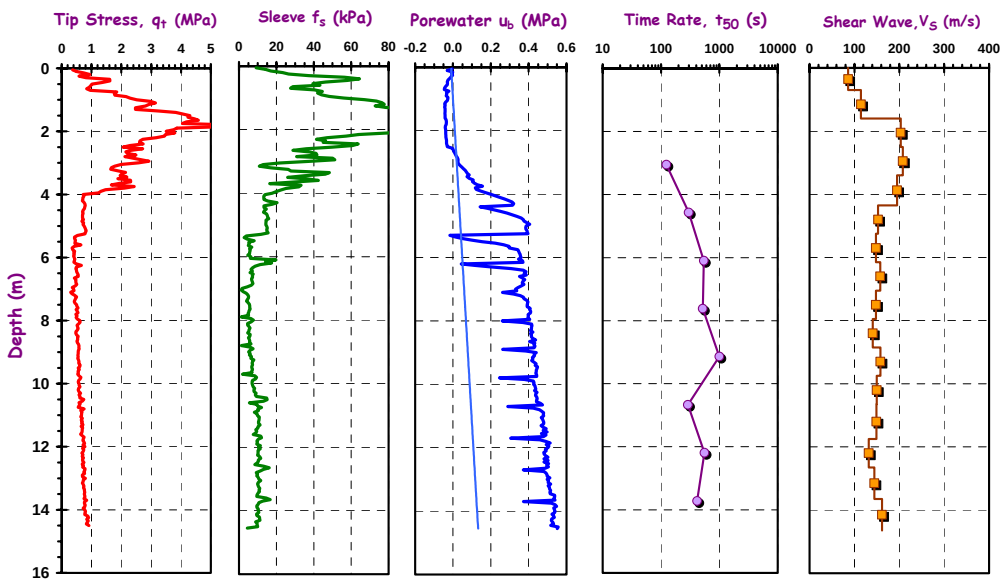

Figure 29. Seismic piezocone test with dissipations (SCPTù) at the Amherst soft clay test site.

In lieu of the focus on a single point corresponding to 50% degree of consolidation (U_{50}), other degrees of dissipation can be considered, or even better, an entire range of consolidation data points starting from penetration through the entire testing time. As such, Houlsby & Teh (1988) provided time factors for a range of porewater pressure dissipations. The degree of excess porewater pressure dissipation can be defined by: $U^* = \Delta u/\Delta u_i$, where Δu_i = initial value during penetration. The modified time factor T* is defined by:

$$T^* = \frac{c_{vh} \cdot t}{a^2 \cdot \sqrt{I_R}} \tag{23}$$

where t = corresponding measured time during dissipation and a = probe radius. The SPM solutions between U* and T* for midface u_1 and shoulder u_2 piezo-elements are shown in Figures 30 and 31, respectively. These can be conveniently represented using approximate algorithms as shown, thus offering a means to implement matching data on a spreadsheet.

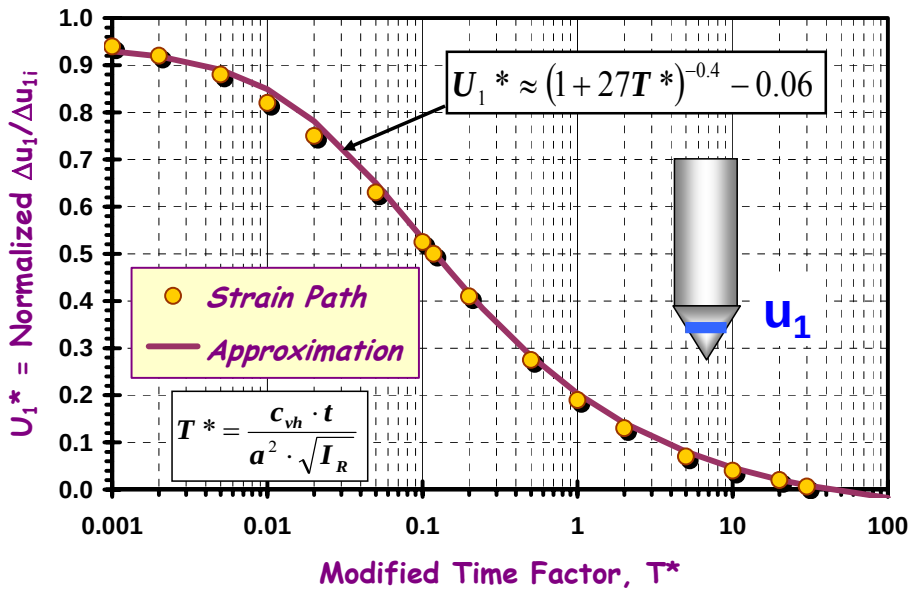

Fig. 30. Dissipation response for type 1 midface piezo-elements (SPM solution of Teh & Houlsby 1991).

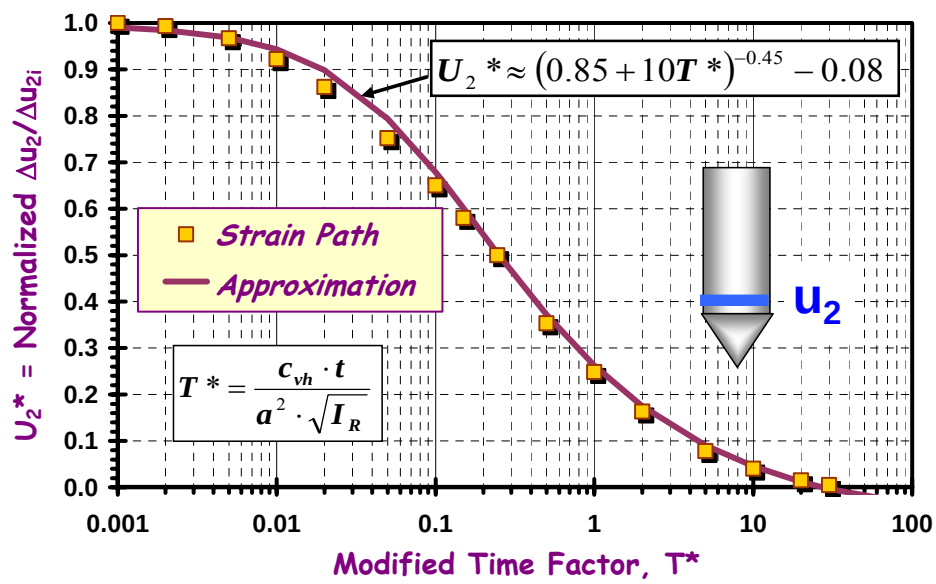

Fig. 31. Dissipation response for type 2 shoulder piezo-elements (SPM solution of Teh & Houlsby 1991).

To use the method, the following procedures are suggested:

a. Assume a range of values for T* starting from 10^{-5} to say 100. Note: Choose intermediate log values at the 1's, 2's, and 5's places.
b. Calculate the corresponding U* dissipations per the approximate expressions given in Figures 30 or 31, as appropriate.
c. Calculate the actual time by rearrangement of (23) to obtain: $t = T^* a^2 I_R^{0.5}/c_{vh}$. Plot U* vs. t.
d. Conduct parametric analyses by varying c_{vh} and/or I_R until a fitting with the measured data is achieved.

For the I_R value, a value may have already been attained from the fitting of penetration readings.

With the aforementioned procedure, the results of dissipation tests from the Bothkennar soft clay site have been forward fitted using the same corresponding value of rigidity index given in Table 1 (I_R = 85) and used in Figure 13. Different types of 10-cm^2 cones were used (a = 1.78 cm). The value of c_{vh} used to drive the analysis was chosen from full-scale footing load test performance reported by Jardine et al. (1995). Both short-term and long-term footing behavior was monitored and a backfigured c_{vh} = 8.5 m^2/year (0.0027 cm^2/s) was determined. Figure 32 presents the dissipation fitting for both type 1 and 2 piezo-dissipation data reported by Jacob & Coutts (1992) at a depth of 12 m at the site. Overall, there is good agreement between the SPM procedures and measured piezocone data.

A similar set of calculations have been carried out for the soft Sarapuí clay in Brazil. Data from 5-cm^2 quad-element piezocone dissipation tests have been reported by Danzinger et al. (1997) and Schnaid et al. (1997). The I_R = 50 from Table 1 has been used and a backfigured field value from embankment monitoring gave c_{vh} = 0.122/cm^2/min (Robertson, et al. 1992). The SPM predictions are shown for midface and shoulder elements in Figure 33, indicating some underpredictions in rate of decay. A better match is obtained with c_{vh} = 0.2/cm^2/min.

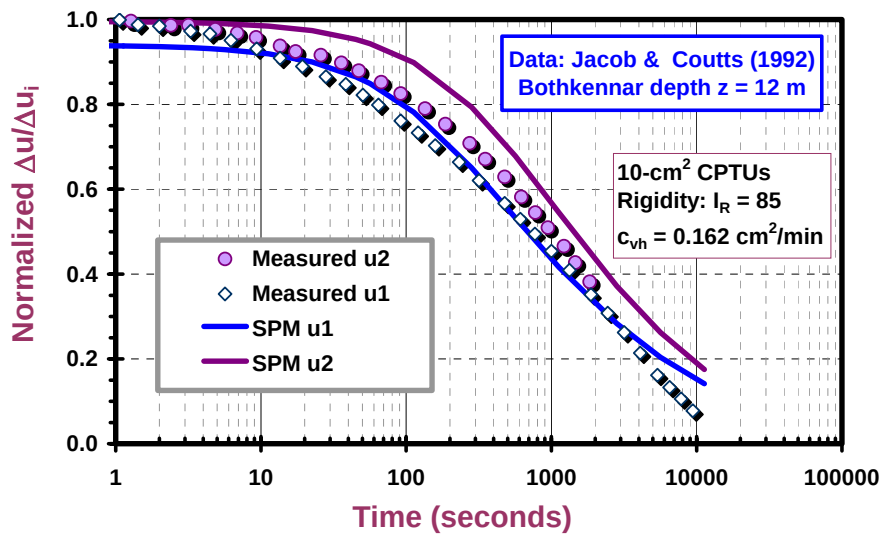

Figure 32. Forward SPM predictions and measured dissipations at Bothkennar site, UK.

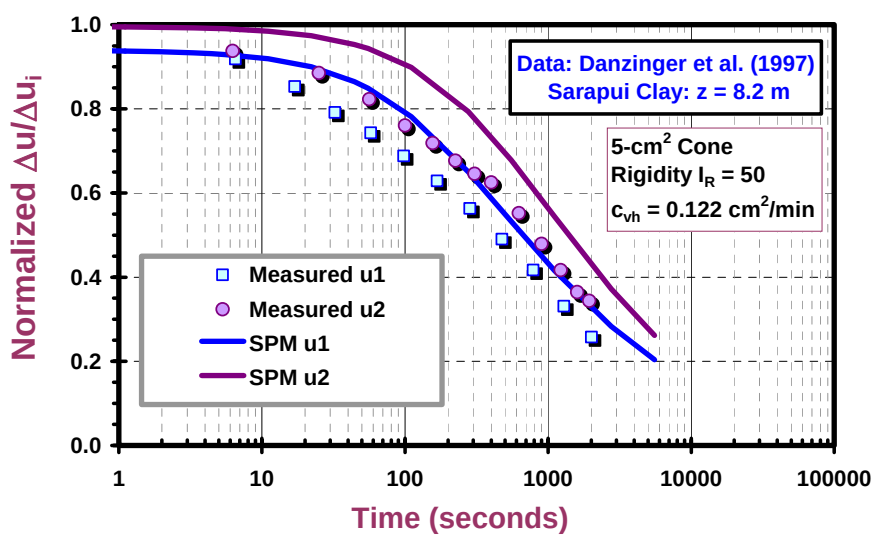

Figure 33. Forward SPM predictions and measured dissipations at Sarapuí site, Rio.

2.16 Partial Drainage Considerations

If in-situ tests in fine-grained soils are conducted slower than standard rates, a partially-drained or "semi-undrained" condition may prevail whereby dissipation occurs during the penetration or probing. This may actually be the common condition in silty soils because of the relative fast rates of in-situ testing relative to the moderate to high permeability of these materilas.

Randolph (2004) has suggested special series of "twitch tests" in clays whereby a variable rate of testing by the penetration probe provides data on both strain rate effects and partial drainage. His work has involved piezocones and full-flow probes, such as the T-bar. A dimensionless velocity term can be defined by:

$$V = v \cdot d / c_{vh} \tag{24}$$

where v = velocity and d = probe diameter. The dimensionless velocity V helps to quantify the regions that are governed by (a) undrained behavior (and strain rate), (b) semi-drained, and (c) fully-drained behavior. This would appear a valuable means to fit within the CSSM framework and allow a rational assessment of intermediate stress paths occurring between fully undrained and fully drained. The demarcation between the undrained region for VST response and partially-drained behavior can be seen for field test data from Canada and lab series on kaolinitic clay using a miniature vane in Figure 34 (Peuchen & Mayne 2006).

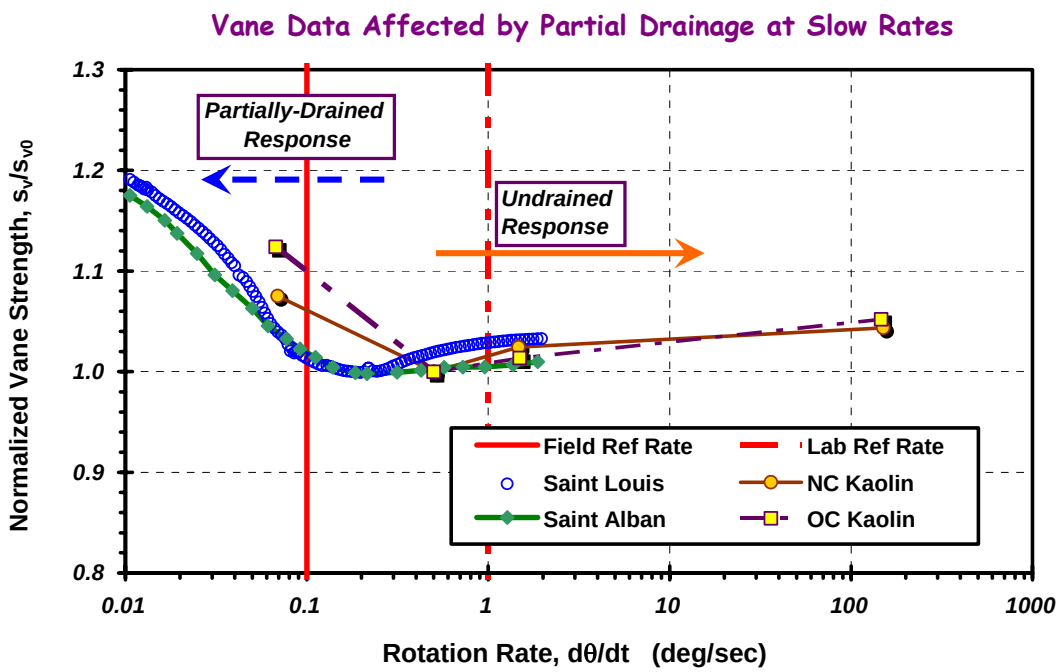

Figure 34. Threshold velocity on undrained vane response an onset of partial drainage.

In the above discussions of dissipation and partial drainage, monotonic decay of induced porewater pressures has been addressed. Yet, in many overconsolidated materials, a dilatory response can occur (e.g., Sully & Campanella, 1994; Burns & Mayne, 1998). Also, an incompatibility exists for the examples shown as the penetration and porewater data were represented by cavity expansion but the monotonic porewater decay addressed using strain path. What is needed is a consistent framework in SCE and/or SPM, else in finite elements, finite differences, and/or discrete elements.

3.0 IN-SITU TESTS IN SANDS

Available methods for evaluating the mechanical properties of sands have developed from an assortment of empirical-statistical, analytical, theoretical, and numerical simulation approaches. Their validity has mostly been established on the basis of reconstituted samples tested in the lab, on either small-size triaxial specimens (25 < D < 75 mm) or large calibration chamber tests (CCT with 0.9 < D < 2.5 m), or combination of both. The CCTs allow for the complete insertion of the in-situ device. However, the calibration chamber results must be corrected for the limited size chambers, since flexible-walled CCTs will under-register the measured penetration resistances compared to far-field conditions, whilst rigid-walled CCTs will over-register the readings.

Of recent vintage, special freezing methods have been developed to obtain field undisturbed samples of sands from the same medium as the in-situ testing locations (e.g., Hoffman et al. 1996). The expensive and time-consuming process requires a slow moving unidirectional freezing front. This is done so that the sand fabric and natural structure are not destroyed during the transformation of water to ice at T < 0°C that is accompanied by a volumetric increase of around 8.5%.

In this section, a review of CPT interpretative methods derived from corrected CCTs for clean quartz sands and siliceous sands (comparable parts of quartz & feldspar particles) is given, with a few well-chosen case study examples, followed by a short supplement of SPT-based methods. Then, a special dataset based on undisturbed sands is presented to evaluate select interpretative procedures. The emphasis in this paper is on CPT, SPT, and V_s methods, supplemented with DMT and PMT data where available.

3.1 *Cone Penetration in Clean Sands*

Using a large dataset of 702 CCTs conducted on 26 different clean quartz to siliceous sands with appropriate boundary size corrections applied to the measured CPT tip resistances, the derived relationship for obtaining the effective stress friction angle was (Kulhawy & Mayne 1990):

$$\phi' = 17.6^{o} + 11.0^{o} \log (q_{t1}) \tag{25}$$

where $q_{t1} = (q_{t1}/\sigma_{atm})/(\sigma_{vo}'/\sigma_{atm})^{0.5}$ is the stress-normalized cone tip stress and σ_{atm} = 1 bar = 100 kPa. The normalization to square root of effective overburden stress likely helps to account for sand compressibility and grain crushing effects, to some degree.

The effective lateral stress applied in chamber tests affects the cone tip stress, moreso than the effective vertical stress. Thus, the applied consolidation state used in the CCTs is given by both the lateral stress coefficient ($K_0 \approx K_c = \sigma_{hc}'/\sigma_{vc}'$) and overconsolidation ratio (OCR) that has been related to the measured q_t values via statistical analyses of the CCT data (Mayne 2005):

$$K_0 = 0.192\left(\frac{q_t}{\sigma_{atm}}\right)^{0.22}\left(\frac{\sigma_{vo}'}{\sigma_{atm}}\right)^{-0.31} OCR^{0.27} \tag{26}$$

The use of the above expression is rather limited, since the field evaluation of stress history of natural sands is often quite elusive. However, if an apriori relationship between K_0 and OCR can be established, the procedure can move forward. For instance, a methodology based on a combining of (4) with (26) is of the form (Mayne, 2001):

$$\boldsymbol{OCR} = \left[\frac{0.192\cdot(\boldsymbol{q_t}/\boldsymbol{\sigma_{atm}})^{0.22}}{(1-\sin\boldsymbol{\phi}')\cdot(\boldsymbol{\sigma_{vo}}'/\boldsymbol{\sigma_{atm}})^{0.31}}\right]^{\left(\frac{1}{\sin\boldsymbol{\phi}'-0.27}\right)} \tag{27}$$

where the apparent preconsolidation stress of the sand can be calculated from:

$$\sigma_p' = OCR \cdot \sigma_{vo}' \quad (28)$$

3.2 *CPT Case Study Examples*

Two case studies can be used to illustrate the evaluation of strength and stress history of natural sands: (1) nearly NC Po River Sand, Italy (Ghionna et al. 1995); and (2) OC glacial sand near Stockholm, Sweden (Dahlberg 1974). In both cases, the stress history is relatively well-known based on geologic setting and rather extensive lab & field testing which have been carried out.

The *Po River Sand* is a relatively thick deposit of clean to slightly silty sand that has been subjected to a great number of in-situ tests, including SPT, CPT, CPMT, PMT, SBP, DMT, and V_s (Jamiolkowski, et al. 1985; Bruzzi, et al. 1986; Ghionna et al. 1995). The sand is lightly overconsolidated due to groundwater fluctuations and ageing. Special sampling of occasional clay lenses of geologically-related materials were captured and tested in oedometers to quantify the stress history. Additional data on the stress state (i.e., K_0) was obtained from the independent pressuremeter testing (SBPMT). Figure 35 shows the application of the aforementioned relationships in evaluating the respective profiles of measured q_t and interpreted ϕ', OCR, and $\sigma_{ho}' = K_0 \cdot \sigma_{vo}'$ in Po River sand. Reasonable values of $1.5 < OCR < 2.5$ are obtained from the CPT data relative to the few oedometric results available. Results from self-boring type (SBP) and full-displacement type (CPMT) pressuremeter testing have been used to independently assess the effective ϕ' and K_0 conditions, where again the CPT values are seen to be in general accord.

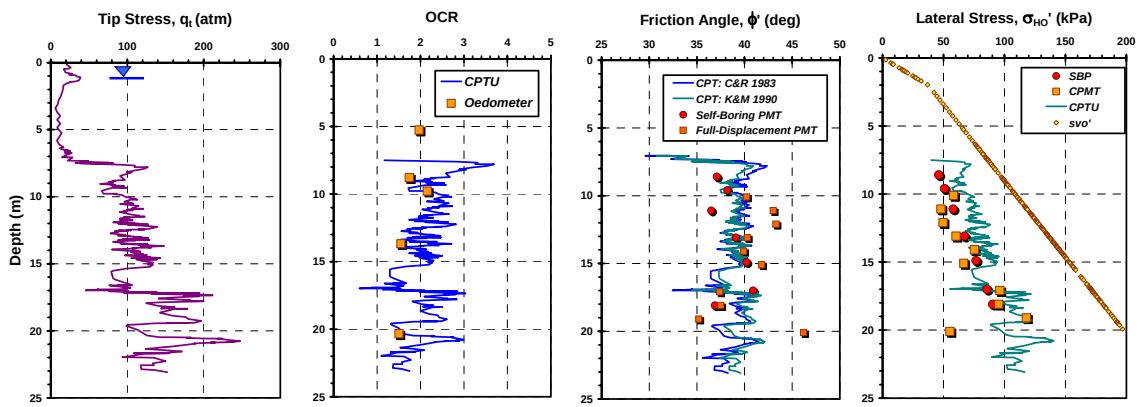

Figure 35. Profiles of CPT q_t, OCR, ϕ', and σ_{ho}' for Po River Sand (data from Ghionna et al. 1995).

For the *Stockholm Sand*, a Holocene deposit of clean glacial medium-coarse sand was quarried for use in construction, having an initial 24 m thickness overlying bedrock. After the upper 16 m was removed, series of in-situ testing (SPT, CPT, PMT, SPLT) were performed, in addition to special balloon density tests in trenches. Groundwater lies at the base of the sand just above bedrock. Index parameters of the sand include: mean grain size ($0.7 < D_{50} < 1.1$ mm); uniformity coefficient ($2.2 < UC < 3$), mean density $\rho_T = 1.67$ g/cc, and average $D_R \approx 60\%$. Results of the screw plate load tests (SPLT) were used by Dahlberg (1974) to interpret the preconsolidation stresses in the sand, very comparable to the known geologic values from mechanical overburden removal (OCD = $\Delta\sigma_v'$). Results of the lift-off pressures from PMTs gave corresponding K_0 values in the sand. Using results of 4 Borros electric CPTs at the site, Figure 45 shows the derived profiles of ϕ', OCR, and σ_p' in Stockholm sand. The CPT-interpreted ϕ' agrees well with triaxial tests on reconstituted samples. The stress history from CPT is consistent with the OCD and SPLT data, with additional support on K_0 given by PMT results.

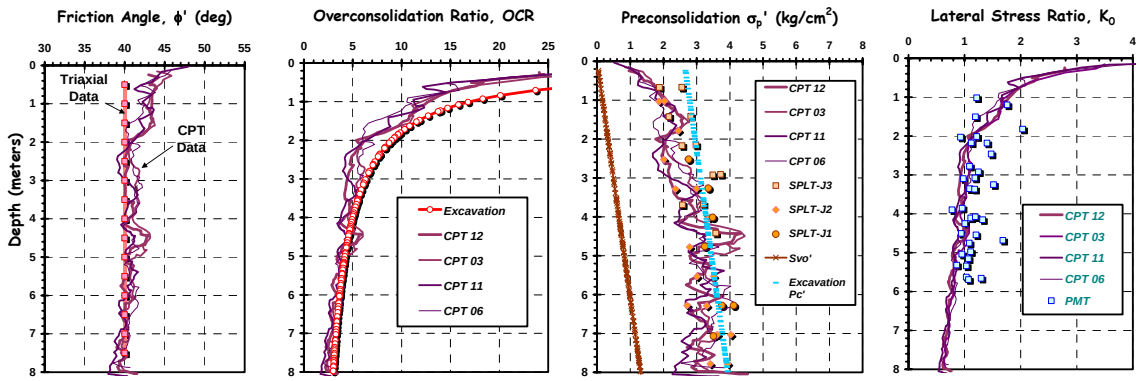

Figure 36. CPT-interpreted profiles of ϕ', OCR, and K_0 in Stockholm Sand (data from Dahlberg 1974).

3.3 *SPT Penetration in Clean Sands*

For the standard penetration test (SPT), empirical methods have been produced for assessing the strength and stress history of clean quartz to siliceous sands. Using results based on triaxial tests on frozen sand specimens, the effective stress friction angle can be obtained from the energy-corrected and stress-normalized N-value from the SPT (Hatanaka & Uchida 1996; Mayne et al. 2002):

$$\phi' = 20° + \sqrt{15.4 \cdot (N_1)_{60}} \tag{29}$$

where $(N_1)_{60} = N_{60}/(\sigma_{vo}'/\sigma_{atm})^{0.5}$.

The apparent preconsolidation stress in clean sands can be estimated from the relationship given in Figure 37. This can be combined with (15) in generalized form (Mayne, 1992):

$$\sigma_p' \approx 0.47\,(N_{60})^m \cdot \sigma_{atm} \tag{30}$$

where m = 0.6 for clean quartzitic sands, 0.8 for silty sands to sandy silts (e.g., Piedmont), and m = 1.0 for intact "vanilla" clays to clayey silts.

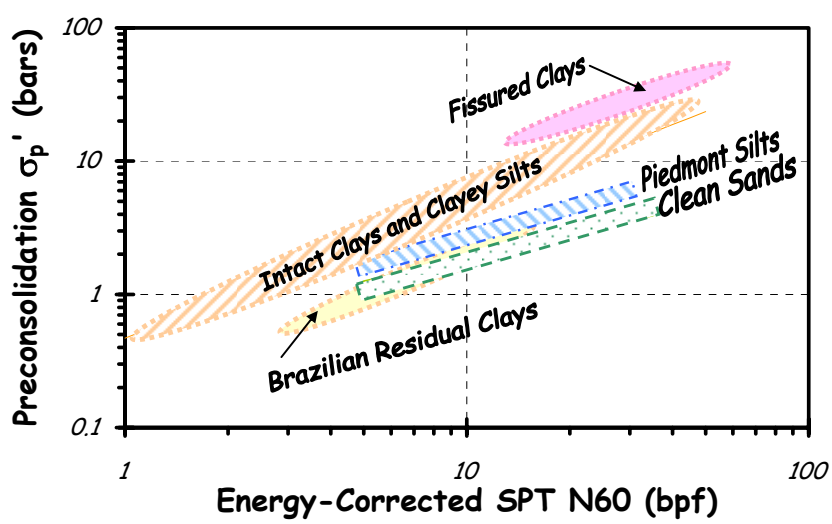

Figure 37. Apparent preconsolidation stress vs. N_{60} for soils (after Mayne 1992).

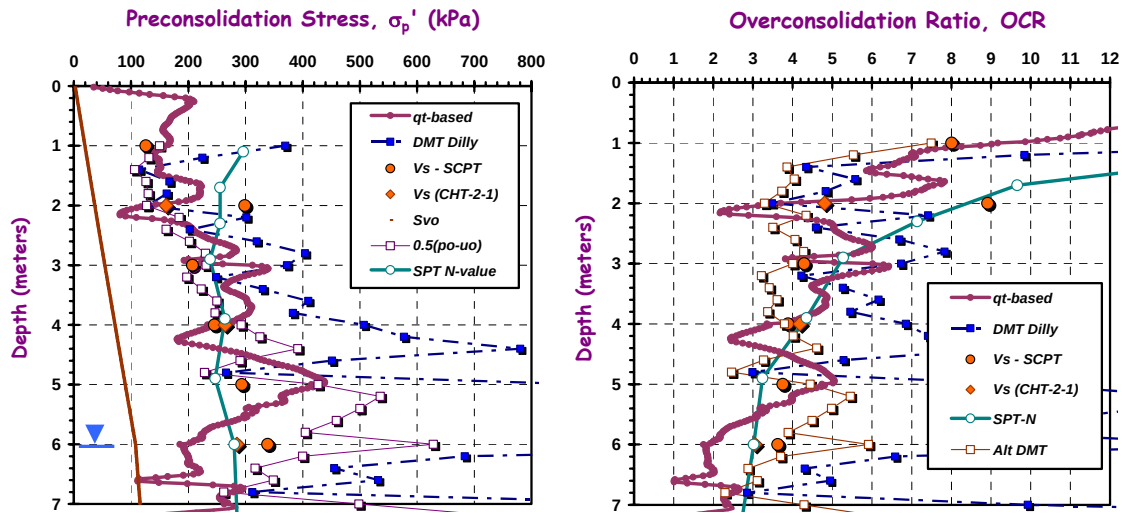

Figure 38. Combinative in-situ test interpretations of stress history at College Station sand site, Texas.

3.4 *Application Case Study to TAMU Sand*

A US national geotechnical experimentation site (NGES) has been established in Eocene age sand near Texas A&M University (Briaud 2000). Here the 10-m thick sand is relatively clean in the upper 4 or 5 meters, becoming slightly to somewhat more silty and clayey with depth. Extensive series on in-situ tests have been carried out at the site, including SPT (with and without energy measurements), CPTU, SCPT, DMT, PMT, and CHT, as well as full-scale load tests on pilings and footings (Briaud & Gibbens, 1994). The CPT evaluation gives an operational friction angle $\phi' = 39^o$ in the sands (Mayne 1994). The combined use of the SPT and CPT procedures for assessing profiles of preconsolidation stress and OCR at the NGES sand site located in College Station, Texas are shown in Figure 38. Both the SPT- and CPT-based profiles are in general agreement with each other. Also shown is an evaluation using shear wave velocity measurements from the site (both DHT by SCPT and CHT), based on a generalized approach (Mayne 2005):

$$\sigma_p' = 0.101 \cdot \sigma_{atm}^{0.102} \cdot G_{max}^{0.478} \cdot \sigma_{vo}'^{0.420} \tag{31}$$

Available DMT data from the site was input into the DILLY software program and these profiles are also presented, along with values from (13). Unfortunately, no real known OCR profile of this sand is documented, so that validity of these results cannot be checked. It is therefore apparent that significant research is needed in establishing the calibration and documentation of natural sand sites, particularly with respect to stress history considerations.

3.5 *CE and CSSM Frameworks for Sands*

Cavity expansion theory can be applied to cone penetration in sands since it represents an inverse problem of pile end bearing capacity (Vesić, 1972, 1977). Sand parameters include the effective friction angle (ϕ'), effective cohesion intercept (c'), rigidity index (I_R), and magnitude of induced volumetric strain ($\Delta V/V_0$). In lieu of the latter parameter, a formulation by Carter et al. (1986) develop a CE solution in terms of the dilatancy angle (ψ'). For the case of c' = 0 for these approaches, the normalized tip stress term is q_t/σ_{vo}' and therefore requires additional information in order to assess I_R and either ($\Delta V/V_0$) or ψ' (Mitchell & Keaveny, 1986; Yu 2004). Recently,

Mayne (2006) showed that the operational rigidity index, defined as $I_{RR} = 1/[(1/I_R) + (\Delta V/V_0)]$, may be related to the normalized shear modulus (G_0/σ_{vo}').

Critical-state concepts have been used to organize sand strength data together include the effects of state (relative density), confining stress level, mode, and dilatancy, as well as differences in mineralogy (Bolton, 1986). In this regard, the method is hindered somewhat because the penetration test data (i.e., SPT, CPT) are used solely to evaluate the inplace relative density (D_R) while values of the fitting parameters (Q, R, and baseline ϕ'_{cs}) are often assumed (Jamiolkowski, et al. 2001). The advantage is that the CSSM framework does allow variants and adjustments to sands of differing origins and constituencies. Using the Bolton CSSM relationship for peak ϕ' in sands, Salgado et al. (1997a, 1997b, 1998) developed a numerical code (*CONPOINT*) that utilizes cavity expansion theory and initial shear modulus to model cone penetration in sands. This has been extended now to address silty sands within a similar framework (Salgado et al. 2000; Lee et al. 2004).

Been & Jefferies (1985) present an alternate CSSM framework to represent sand behavior. They define the sand state parameter (Ψ) as the vertical difference in void ratio between the initial in-place condition and the critical state line (CSL), termed steady state line ($\Psi = e_0 - e_{cs}$). In this light, Been et al. (1986, 1987) were able to relate CPT resistances to describe sand response ranging from loose contractive to dense dilatant behavior, as well as undrained modes. Series of laboratory triaxial shear tests are needed to define λ (and κ), yet recent efforts by Cho et al. (2006) have related the parameters to simple index tests. The state parameter method has since been implemented into a modeling framework for CPT (Shuttle & Jefferies, 1998). Of particular interest herein, it is possible to show that Ψ is actually just another means to express stress history, and thus related to OCR. In fact, Been et al. (1988) show:

$$\log OCR_p = \log 2^{\Lambda} + \Psi/(\kappa - \lambda) \qquad (32)$$

where OCR_p = overconsolidation ratio in Cambridge q-p' space, $\Lambda = 1-\kappa/\lambda$, $\lambda = C_c/\ln(10)$ = compression index, and $\kappa \approx C_s/\ln(10)$ = swelling index, with latter two slopes defined in e-lnp' space (although some confusion here as original reference is defined in terms of log base 10). The state parameter method has since been implemented into a framework for CPT interpretation (Shuttle & Jefferies, 1998) that involves a CSSM constitutive soil model (*NorSand*) that appears to be quite versatile (Jefferies & Shuttle, 2005).

3.10 *Undisturbed Sand Database*

Conventional approaches to cross-linking of lab-determined engineering parameters and in-situ field tests have relied upon reconstituted samples, specimens, and chamber deposits. For reconstitution, a number of preparation methods are available, including: vibration, compaction, air and water pluviation, moist tamping, and slurrying. The primary assumption is that if the sand is replaced at the same initial density and void ratio in the laboratory, then this will give comparable behavior to the same natural sand that exists in the field. This approach is depicted in Figure 39. It is further assumed that our present practices of assessing the inplace relative density (D_R), unit weight (γ_T), and/or void ratio (e_0) of that sand from in-situ test methods (SPT, CPT, DMT) is relatively reliable. Neither of these assumptions is well-supported, as shown by recent comparisons from triaxial tests on the same sand tested in undisturbed states as well as artificially prepared sand samples by different reconstitutive measures (e.g., Hoeg, et al. 2000; Vaid & Sivathayalan 2000; Jamiolkowski 2001). Available methods to assess D_R from in-situ tests do not appear especially reliable, particularly using penetration type tests including SPT and CPT (e.g., Wride et al. 2000) and DMT (e.g., Jamiolkowski, et al. 2001).

To further check on the validity of these major assumptions, a new elite database on undisturbed clean quartz and siliceous sands was created. A total of 13 sands that were sampled using special techniques (primarily expensive freezing technology) was collected (Mayne 2006b).

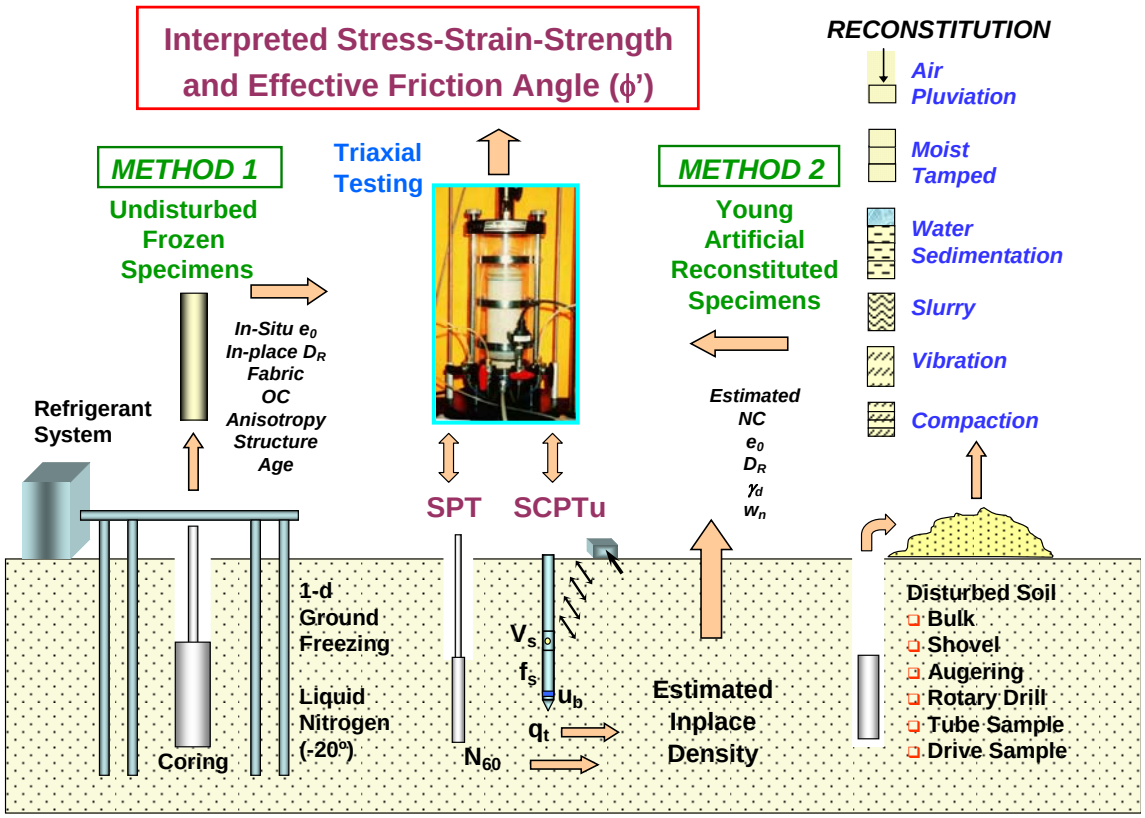

Fig. 39. Procedures depicting undisturbed vs. reconstituted methods for calibrating in-situ tests in sands.

The sands are located in Canada (6 sands), Japan (4 sands), Norway (1 site), China (1 site), and Italy (1 site), as listed in Tables 2 and 3 with pertinent index parameters and reference sources of the data. Notably, all four of the Japanese sands (Mimura 2003), two Canadian sands (Robertson et al. 2000), and the Holmen, Norway (Lunne et al. 2003) were discussed at the Singapore workshop. In general, the sands can be considered as clean to slightly dirty sands of quartz, feldspar, and/or other rock mineralogy, excepting two of the Canadian sands derived from mining operations that had more unusual constituents of clay and other mineralogies.

In terms of grain size distributions, the materials include 10 fine sands, 4 medium sands, and one coarse sand (Italy). The sands from Canada were dirty having fines contents: $5 < FC < 15\%$, whereas the other sands were all relatively clean with $FC < 4\%$. Mean values of index parameters (with plus and minus one standard deviation) of these sands indicated: specific gravity ($G_s = 2.66 \pm 0.03$), fines content ($FC = 4.36 \pm 4.49$), particle size ($D_{50} = 0.35 \pm 0.23$ mm)[1], and uniformity coefficient ($UC = D_{60}/D_{10} = 2.80 \pm 1.19$). The mean grain size statistics would be better represented by a log normal function.

At all sites, results from SPT and CPT were available, as well as downhole V_s measurements (except the China site). A summary of mean values of the normalized SPT $(N_1)_{60}$, normalized CPT results (Q, F, R_f, q_{t1}, and $\Delta u/\sigma_{vo}'$), and normalized shear wave velocity (V_{s1}) is presented in Table 4, where $(N_1)_{60} = N_{60}/(\sigma_{vo}'/\sigma_{atm})^{0.5}$, $Q = (q_t-\sigma_{vo})/\sigma_{vo}'$, $F = f_s/(q_t-\sigma_{vo})$, $R_f = f_s/q_t$ (%), $q_{t1} = q_t/(\sigma_{vo}'\cdot\sigma_{atm})^{0.5}$, and $V_{s1} = V_s/(\sigma_{vo}'/\sigma_{atm})^{0.25}$.

An initial check on the data is made by cross-linking the in-situ measurements using prior-available relationships. Figure 40 shows a plot of cone resistance versus the energy-corrected N-values for the sands. A common assumption is that the direct ratio of cone tip resistance (bars) to N-value (bpf) is in the range of $4 \leq q_t/N_{60} \leq 5$ for such materials (e.g., Schmertmann, 1978).

[1] Note: Coarse sand from Italy with $D_{50} = 2$ mm not included. If included, then $D_{50} = 0.46 \pm 0.48$ mm.

Table 2. List of undisturbed sands, reference sources of data, origin, and sample type.

Sand Name	Country Location	Reference Source	Type Sand	Sampling Method
Edo River	Japan	Yamashita et al. (2003); Mimura (2003)	Natural Alluvial	Frozen
Gioia Tauro	Italy	Ghionna & Porcino (2003, 2006) Porcino & Ghionna (2004)	Natural Coarse Sand	Frozen
Highmont Dam	Canada	Wride & Robertson (1999); Robertson et al. (2000)	Tailings	Frozen
Holmen	Norway	Lunne, et al. (1986); Lunne, Long, & Forsberg (2003)	Natural Alluvial	Tube (Frozen)
J-pit	Canada	Robertson, Wride, et al. (2000); Wride & Robertson (1999)	Hydraulic Fill	Frozen
Kidd	Canada	Robertson, Wride, et al. (2000) Wride & Robertson (1999)	Natural Alluvial	Frozen
Kowloon	China	Lee, Shen, Leung, Mitchell (1999)	Hydraulic Fill	Mazier Tube
LL Dam	Canada	Robertson, Wride, et al. (2000)	Tailings	Frozen
Massey	Canada	Robertson, Wride, et al. (2000)	Natural Alluvial	Frozen
Mildred Lake	Canada	Robertson, Wride, et al. (2000); Wride & Robertson (1999)	Hydraulic Fill	Frozen
Natori River	Japan	Matsuo & Tsutsumi (1998); Mimura (2003)	Natural Alluvial	Frozen
Tone River	Japan	Matsuo & Tsutsumi (1998) Mimura (2003)	Natural Alluvial	Frozen
Yodo R. (8)	Japan	Mimura (2003)	Natural Alluvial	Frozen
Yodo R.(10)	Japan	Mimura (2003)	Natural Alluvial	Frozen
Yodo R.(12)	Japan	Mimura (2003)	Natural Alluvial	Frozen

Table 3. Undisturbed sands, mean depths, index parameters, and overburden stress levels.

Sand Name	Depth z (m)	GWL (m)	PF (%)	D_{50} (mm)	G_s	e_o	e_{max}	e_{min}	D_R (%)	σ_{vo}' (atm)
Edo	3.85	2.1	0.42	0.29	2.68	1.043	1.227	0.812	44.3	0.51
Gioia Tauro	3	1.5	0.66	2	2.69	0.589	0.690	0.450	42.0	0.42
Highmont	10	4	10	0.25	2.66	0.825	1.015	0.507	37.4	1.38
Holmen	10	1	2	0.55	2.71	0.724	0.840	0.460	30.5	1.10
J-pit	5	0.5	15	0.17	2.62	0.762	0.986	0.461	42.7	0.55
Kidd	14.5	1.5	<5	0.2	2.72	0.981	1.100	0.700	29.8	1.60
Kowloon	11.8	9	1	0.72	2.63	0.492	0.634	0.328	46.5	1.80
LL Dam	8	2.1	8	0.2	2.66	0.849	1.055	0.544	40.3	1.00
Massey	10.5	1.5	<5	0.2	2.68	0.970	1.100	0.700	32.5	1.20
Mildred L.	32	21	10	0.16	2.66	0.768	0.958	0.522	43.6	5.16
Natori	8.25	2.1	0.23	0.22	2.65	0.857	1.167	0.765	77.2	0.87
Tone	7.3	1.4	3.78	0.18	2.68	0.947	1.330	0.775	69.1	0.84
Yodo	8.1	2.1	1.9	0.32	2.64	0.820	1.054	0.665	60.2	1.02
Yodo	10.9	2.1	0.27	0.82	2.63	0.720	0.883	0.569	51.9	1.23
Yodo	12.7	2.1	2.1	0.62	2.63	0.790	0.921	0.567	37.0	1.43

Table 4. Undisturbed sands, triaxial friction angles, and in-situ SPT, CPT, and DHT data.

Sand	Triaxial Type	ϕ' (deg)	SPT $(N_1)_{60}$	Q	F	R_f (%)	q_{t1}	$\Delta u/\sigma_{vo}'$	V_{s1} (m/s)
Edo River	CIDC	39.7	22	156	0.73	0.72	111	-0.08	164
Gioia Tauro	CIDC, CIUC, CTX	41.5*	30	279	0.26	0.26	174	-0.26	221
Highmon t	CIUC, CKoUC	41.5	5	35	0.38	0.38	44	0.11	141
Holmen	CKoUC, CKoDC	33.2	1	29	0.42	0.40	28	-0.33	157
J-pit	CIUC, CKoUC	32.7	3	31	0.87	0.75	20	0.19	127
Kidd	CIUC, CKoUC	37.3	13	52	0.37	0.36	68	-0.02	177
Kowloon	CIUC	38.1	21	55	1.84	1.80	74	0.07	NA
LL Dam	CIUC, CKoUC	39.1	5	39	0.41	0.39	39	0.01	153
Massey	CIUC, CKoUC	36.7	10	49	0.40	0.38	53	-0.09	168
Mildred Lake	CIUC, CKoUC	39.6	18	32	0.73	0.70	74	0.02	156
Natori R.	CIDC	40.9	50	226	0.30	0.30	207	-0.48	218
Tone R.	CIDC	41.7	32	154	0.24	0.24	147	-0.46	203
Yodo(8)	CIDC	42.4	27	194	0.95	0.94	176	-0.05	197
Yodo(10)	CIDC	38.4	35	103	1.03	1.01	102	-0.19	213
Yodo(12)	CIDC	39.1	31	96	0.89	0.88	106	-0.19	195
	*Note: Results above for final q/p' from CTX series; monotonic tests give 37.8°. NA = not available								

For the 15 datapoints considered, the ratio averages q_t/N_{60} = 4.38, thus within the expected range. The specific ratio q_t/N_{60} has been shown to partially depend upon the mean grain size of the soil (D_{50}), as well as the percent fines content, FC (e.g., Robertson & Campanella 1983; Kulhawy & Mayne 1990). However, it appears this ratio decreases with low N-values and that a better overall match would be attained using either an intercept, such as $q_t/(N_{60} + n^*)$ with a value n* = 6 bpf, else fitting of a power function format such that $q_{t1} = \alpha^* [(N_1)_{60}]^{\beta^*}$, as suggested by Suzuki, et al. (1998). The minor improved coefficients of determination (r^2) shown in Figure 41 lend support to this notion. Alternatively, the procedures for stress normalization of SPT and/or CPT data may be involved in the observed trends (e.g., Boulanger & Idriss 2004; Moss, et al. 2006).

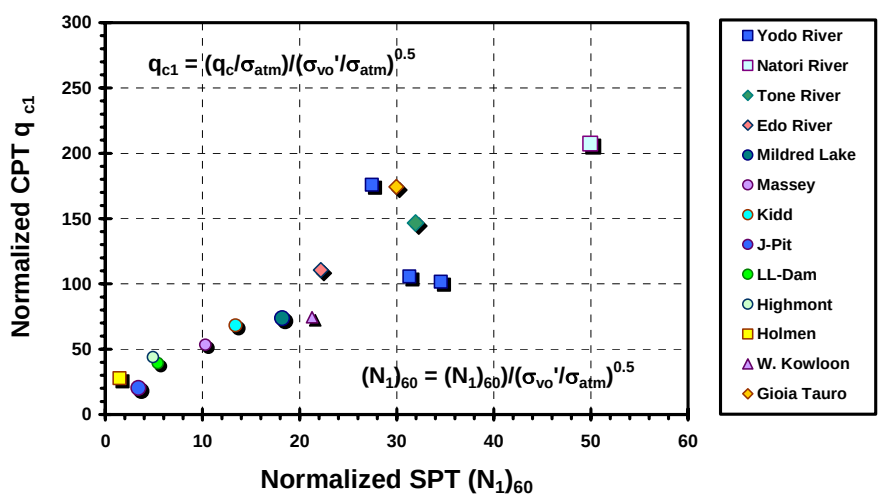

Figure 40. Trend between CPT and SPT data for undisturbed sand database.

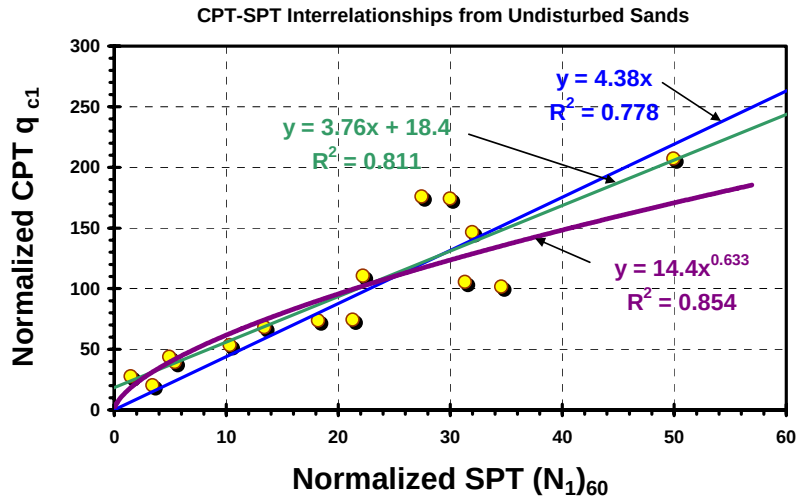

Figure 40. Regression relationships between CPT and SPT for undisturbed sand database.

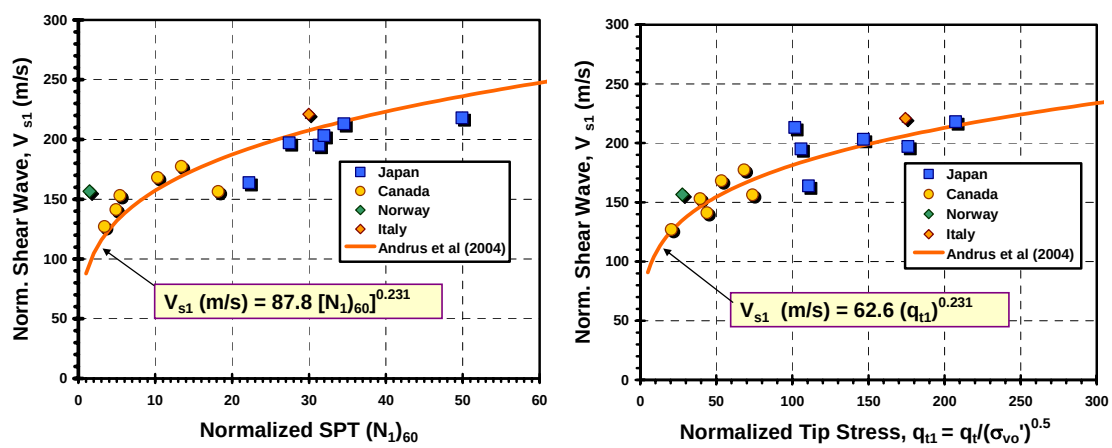

Figure 41. Normalized shear wave velocity vs. (a) SPT $(N_1)_{60}$ and (b) CPT q_{t1} for undisturbed sands.

Andrus & Stokoe (2000) present a relationship between the normalized shear wave velocity, $V_{s1} = V_s/(\sigma_{vo}'/\sigma_{atm})^{0.25}$, and the energy-corrected & stress-normalized N-value, $(N_1)_{60}$. The data from the undisturbed sands appear to conform fairly well with this correlation, as shown by Figure 41a. Similarly, Andrus et al. (2004) developed a similar interrelationship between V_{s1} and normalized cone tip stress (q_{t1}), as supported by the dataset from the undisturbed sands (reference Figure 41b). Thus, the compiled in-situ data from SPT, CPT, and V_s appear internally consistent.

All of the undisturbed sands were tested under consolidated triaxial compression tests to determine their respective effective stress friction angles (ϕ'). The measured values are reported in Table 4. This permits an opportunity to check on the validity of selected relationships in evaluating sand strength from available in-situ test data (Mayne 2006b). Using the aforementioned expression between ϕ' and $(N_1)_{60}$ developed by Hatanaka & Uchida (1996), only a fair agreement is noted for the new dataset in comparison with their frozen sand samples from additional Japanese test sites (Figure 42). The trend is much flatter for the new data and suggests a relative insensitivity of $(N_1)_{60}$ in accurately estimating effective ϕ' in sands. The friction angles of loose to firm sands at low to medium N-values are significantly underpredicted by the expression. Perhaps, the repeated dynamic nature of the SPT at low N-values is more indicative of an "undrained" type cyclic loading.

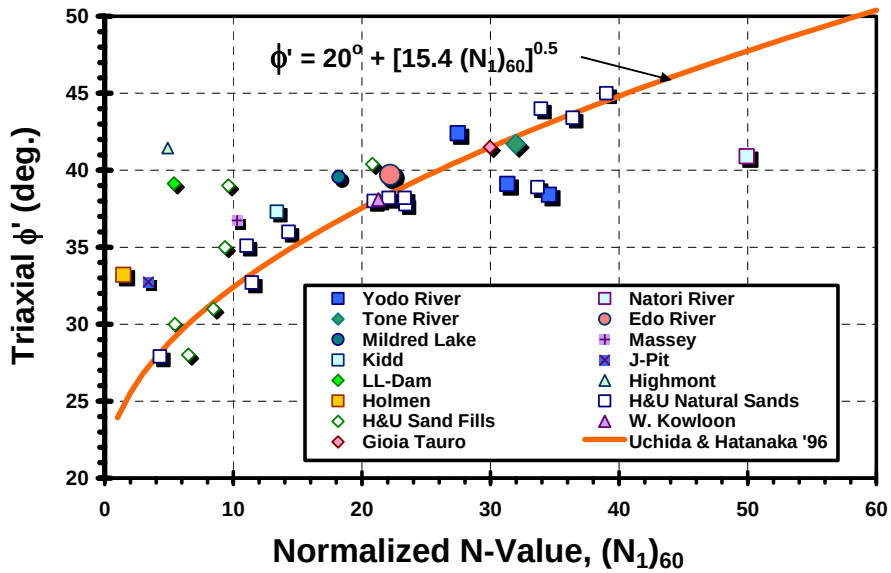

Figure 42. Effective friction angle of undisturbed sands vs. normalized SPT resistance in comparison with Hatanaka & Uchida (1996) relationship.

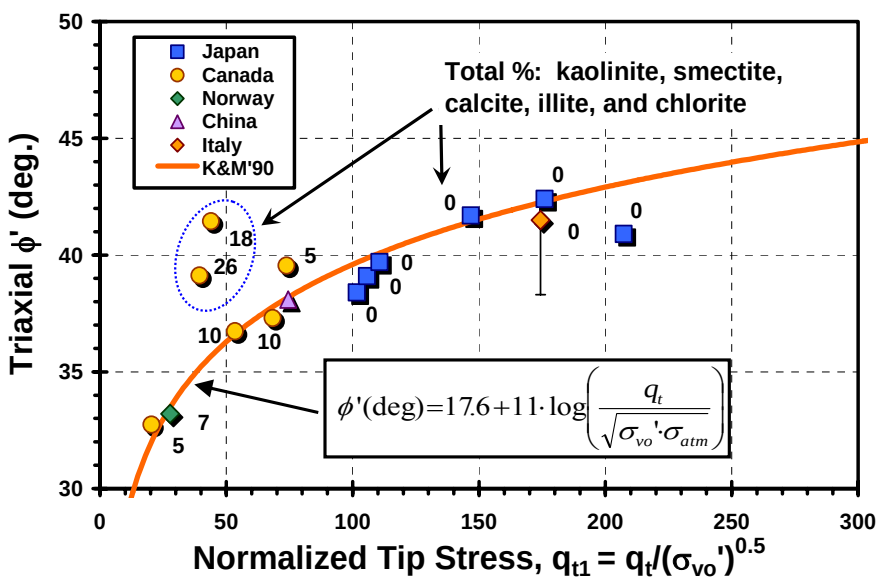

Figure 43. Effective triaxial friction angle of undisturbed sands vs. normalized cone tip stress.

The relationship between the triaxial-measured ϕ' of undisturbed sands and normalized cone tip resistance is presented in Figure 43. Here, the CPT proves to be an excellent predictor in representing the drained strength of the sands. The two outliers from LL and Highmont Dams are sands with some unusual mineralogies beyond the normal quartzitic & feldspathic types, exhibiting higher percentages of clay and other minerals (as noted). In fact, if the mica content were also included, LL Dam would have 50% and Highmont would show composition of 20% of minerals other than quartz & feldspar.

Another interesting comparison is the between the apparent OCRs as suggested from the SPT and CPT data, shown in Figure 44. The agreement from these two separate approaches is quite remarkable for all fifteen sand datapoints. Both the SPT and CPT indicate values of OCR < 1 for three sands (Holmen, Highmont, and Mildred Lake), with values up to as high as OCR = 7 for Gioia Tauro sand. Sands with OCRs < 1 imply unstable structure and perhaps this could

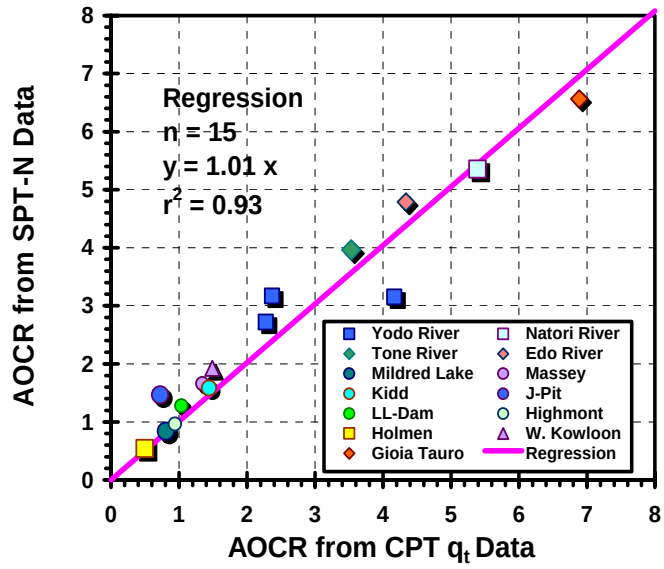

Figure 44. Apparent OCRs of undisturbed sands from SPT and CPT inferences.

be used as an indicator of liquefaction potential. The CPT data also infers that the sands at J-pit and LL dam have OCRs ≤ 1 (although SPT results indicate OCR > 1). This is of interest as both LL and Highmont were noted earlier to have some unusual mineralogy, as compared with the other eleven sands. Also, the J-pit site was selected for the full-scale attempt at liquefaction for the CANLEX experiments, yet did not liquefy (Robertson, et al. 2000a,b).

3.15 *Stress-Strain-Strength Response of Sands*

The stress-strain-strength response of sands can be handled similarly to the aforementioned approach, using a variety of nonlinear expressions or algorithms to represent modulus reduction (G/G_{max}), or alternatively using constitutive soil models. In the generalized modified hyperbola version by Fahey & Carter (1993), two parameters (f and g) are used to obtain the secant modulus reduction factors (Fahey, 1998) by one of the following:

$$G/G_{max} = 1 - f\,(\tau/\tau_{max})^g \qquad (33a)$$

$$E/E_{max} = 1 - f\,(q/q_{max})^g \qquad (33b)$$

For the above, no changes in ν' are made during loading, however, could be implemented as needed (e.g., Fahey & Carter, 1993). Poisson's ratio data on 6 sands presented by Lehane & Cosgove (2000) show relatively constant ν' during loading up to about 0.1% strains, afterwards indicating increases in ν'. The expressions of (33) have been used effectively to represent stress-strain-strength curves in simple & torsion shear and triaxial modes for different soil types, including: clays (e.g., Elhakim & Mayne, 2003; Mayne et al. 2003), silts (Mayne et al. 1999), clean sands (Fahey 1998; Lehane & Fahey, 2002), and silty sands (Lee, et al. 2004). For uncemented soils that are not highly structured, adoptive values of $f = 1$ and $g = 0.3 \pm 0.1$ have been suggested for initial guestimates (Mayne 2005).

The drained strength of sands depends on the particular mode of loading application. For direct simple shear (DSS), the shear strength may be stated simply by: $\tau_{max} = \sigma_{vo}'\cdot\tan\phi'$; while for isotropic triaxial drained compression tests (CIDC), the peak deviator stress is obtained from: $q_{max} = (\sigma_1 - \sigma_3)_{max} = 2\,\sigma_o'\cdot \sin\phi'/(1 - \sin\phi')$. For torsional shear tests (TS) and anisotropically-consolidated triaxial tests (CADC), consideration of the initial K_0 state can be made by stress path analyses. For CADC, this gives: $q_{max} = (\sigma_1 - \sigma_3)_{max} = 2\,K_0\,\sigma_{vo}'\cdot[1/(1/\sin\phi'-1)]$.

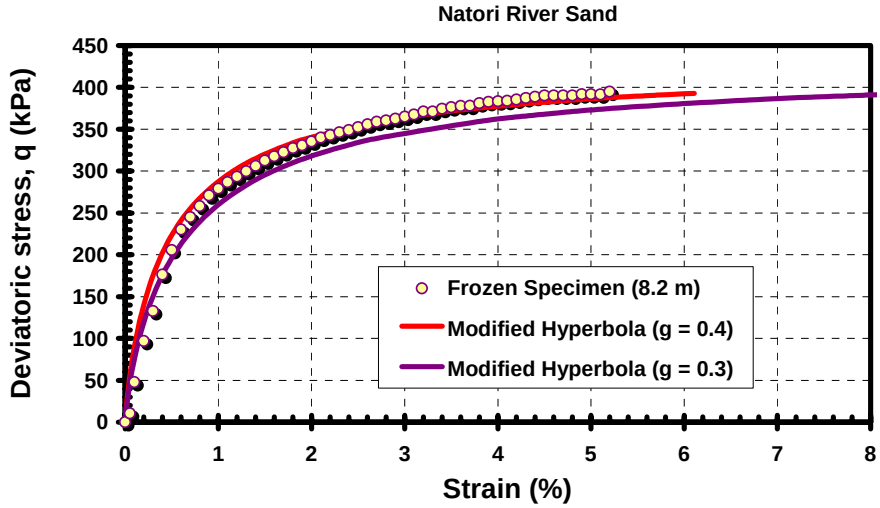

Figure 45. Triaxial stress-strain curve from undisturbed sand represented by modified hyperbola fitting (data from Mimura 2003).

The use of the modified hyperbola for representing stress-strain-strength curves of sand is illustrated in Fig. 45 for Natori River sand reported by Mimura (2003). Here, f = 1 and an exponent value g = 0.3 to 0.4 gives an overall good fitting.

While the aforementioned fitting technique was shown to be simple and reasonable for a given sand, it cannot effectively address complex stress paths and behavior, because of its empirical basis. The use of a constitutive soil model would therefore be beneficial since it may be capable of handling additional facets of soil behavior, including: drained and undrained loading, variable stress paths, volumetric strain predictions & dilatancy, cyclic response, and post-peak softening. Summaries of some available models are given by Duncan (1994) and Lade (2005).

Some constitutive models of interest include the rather versatile *NorSand* (Jefferies, 1993; Jefferies & Shuttle, 2005) which requires only 8 soil parameters and has been calibrated with several sands and clays. Also, the more sophisticated *MIT-S-1 model* (Pestana & Whittle, 1999) can produce a variety of stress paths, modes, and varied responses for both sands and clays. Consequently, future research should be directed towards the calibration of laboratory and in-situ tests within the framework of constitutive soil models as these will allow versatility. The initiation of this database on undisturbed sands will help begin the important calibration of parameters as needed for these constitutive soil models.

4.0 IN-SITU TESTING OF INTERMEDIATE and NONTEXTBOOK GEOMATERIALS

In nature, there are enumerable types of soils with varying components, packing arrangements, and origins. Yet, in the "ivory tower" of academe, it is usual to group soil behavior into two broad categories (as has been covered herein): *sands* (drained behavior) and *clays* (undrained behavior). Thus, anything outside of the "hourglass sands" and "vanilla clay" categories could be termed *nontextbook geomaterials*.

Within the CSSM context, all soils (clays, silts, sands, gravels) can exhibit drained to semi-drained to partially-undrained to fully-undrained conditions, given the particular circumstances. Mixed soils with varying percent fines, weathering, high structure, fabric, unusual mineralogical components, and particles have been encountered in geotechnical practice and do not fit within the empirical domain of existing correlations and procedures of analysis. As such, a consensus version of CSSM framework for unsaturated structured soils based in micromechanics would be desired to account for many additional facets of soil behavior (e.g. Cho & Santamarina, 2001; Leroueil & Hight, 2003) and is really beyond the scope & capabilities of this paper.

A number of recent papers have addressed the concerns and significance of in-situ test interpretation in nontextbook geomaterials. Such geomaterials are widespread and diverse, including:

calcareous soils, carbonate sands, partially-saturated soils, diatomaceous clays, weathered residuum, lateritic soils, loess, mine tailings, and gaseous sediments. For these issues, the reader is directed towards the efforts reported in such references as Lunne et al. (1995; 1997), Hight & Leroueil (2003), Schnaid et al. (2004), and Schnaid (2005), as well as the many individual papers found in the 2003 and 2006 Singapore Workshop proceedings.

4.1 *Global Correlations*

Of interest to the post-processing of in-situ data is the development of generalized correlations, as these may find use in the assessment of geotechnical parameters for all types of "well-behaved" soils. Soil behavioral charts have been produced that utilize in-situ readings and indirectly assess soil type. For instance, the DMT readings p_0 and p_1 give the material index ID that determines type of soil. Two readings from CPT (q_t and f_s) can be used to give approximate soil types in low sensitivity and noncemented geomaterials (e.g. Schmertmann 1978), else in CPTU, two readings could focus on q_t and B_q (Senneset et al. 1988). In fact, all three readings from CPTU (q_t, f_s, and Δu) can be used for soil behavioral identification (e.g., Robertson 1990).

These comparison of intra-measurements can be utilized to find "unusual" or anomalous soils that would classify as problematic geomaterials. For instance, Fahey (1998) and Schnaid et al. (2004) plot the ratio G_0/q_t which decreases with q_{t1} for unaged quartz and siliceous sandy soils. This baseline is then used to distinguish cemented or structured soils, as these tend to fall above this curve. Thus a cross-comparison of multiple readings taken during the same sounding helps to identify the soil type. With the seismic piezocone, four parameters are obtained (Q, F, B_q, $G_0./q_t$) to allow a better means to notice or define prospective nontextbook soils.

From a global database on soils (n = 731), the saturated unit weight (γ_{sat}) of "well-behaved" soils can be guestimated from the stress-normalized shear wave velocity (V_{s1}) within about ± 1 kN/m^3, as suggested by Figure 46. The figure also includes the 14 undisturbed sands from Tables 2 to 4. Unit weights from 10 to 26 kN/m^3 are associated with normalized shear wave velocities from 30 to 800 m/s. As V_{s1} is dependent upon the current effective overburden stress, the procedure should be used in a depth-stepwise fashion, starting from the ground surface and proceeding downward. It can be expected that cemented soils and carbonate sands would lie somewhat to the right of the mean relationships shown, as the bonding would promote a more open porous structure (and low unit weight), yet a fast velocity in the matrix.

For dry soils above the water table and no capillarity effects, a similar relationship can be derived from lab resonant column test data. Figure 47 shows the reprocessed RCT data from four

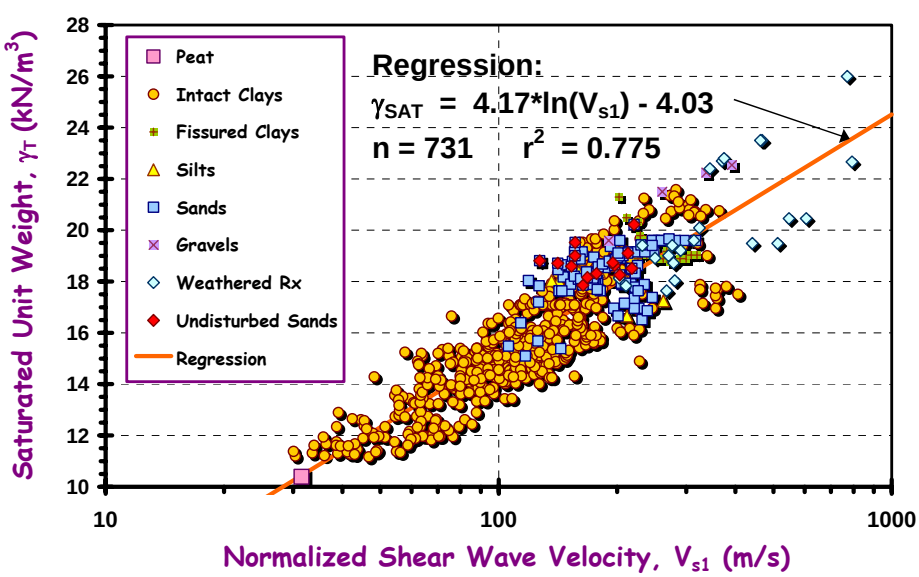

Figure 46. Saturated unit weight evaluation from stress-normalized V_{s1} in non-cemented soils.

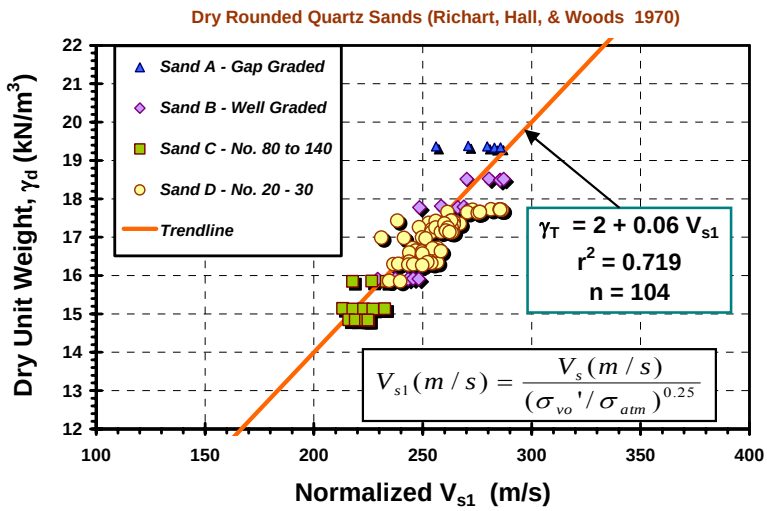

Figure 47. Trend of dry unit weight of sands in terms of stress-normalized shear wave velocity.

series of reconstituted quartz sands tests (Richart et al. 1970) in terms of dry unit weight vs. V_{s1}. Dry unit weights from 14 to 20 kN/m^3 are associated with normalized V_{s1} from 220 to 280 m/s.

The real difficulty with this indirect approach comes with partially-saturated soils in the field. Here, use of measured shear wave velocities in the vadoze zone above the groundwater table is complicated because of capillarity effects. As the soil is desaturated, the shear wave velocity increases by two-fold to five-fold, the extent depending upon the grain size distribution of the soil (Cho & Santamarina, 2001). Thus, a measure of the degree of saturation may be necessary. Towards this purpose, Jamiolkowski (2001) has suggested that in-situ compression wave measurements (V_p) can aid in evaluating the degree of saturation.

With many well-documented geotechnical experimental test sites now established (such as those cases reported in the 2003 and 2006 Singapore Workshops), it is now feasible to seek comparisons across diverse soil types and formations, looking for more global (and presumably, more reliable) correlations that can serve as baselines in cross-checking site-specific data and generalized interpretation of soil engineering parameters. The author has made some initial steps towards this purpose using compiled SCPTU data from a variety of clays, silts, and sands, including many reported in the first Singapore proceedings (Tan et. al. 2003). In addition to intact clays, the selection considers fissured clays, organic clays, and silts. A collection of cross-comparisons from the CPTs from these sites is shown in terms of cone tip resistance vs. friction resistance in Figure 48. The undisturbed sands from Tables 2 to 4 are also included.

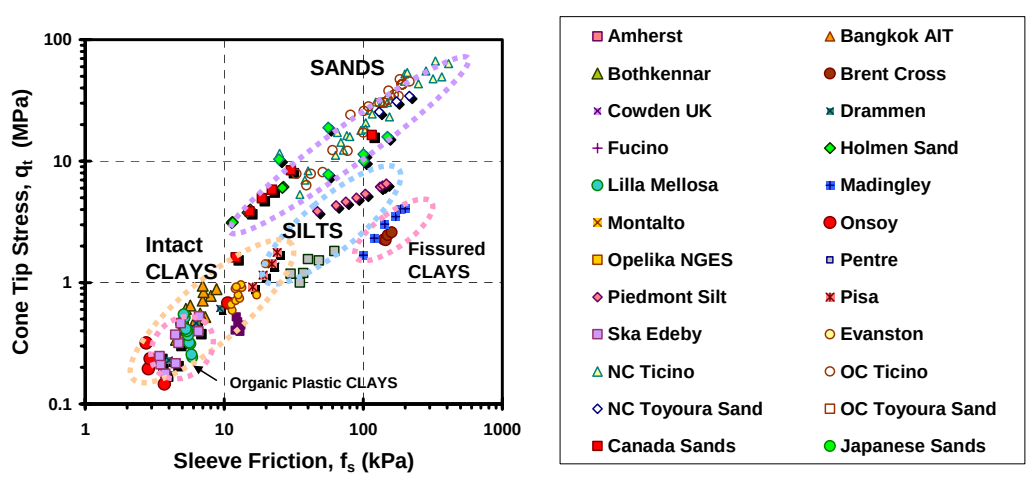

Figure 48. Combinative SCPTU database with q_t vs. f_s summary for varied clays, silts, and sands.

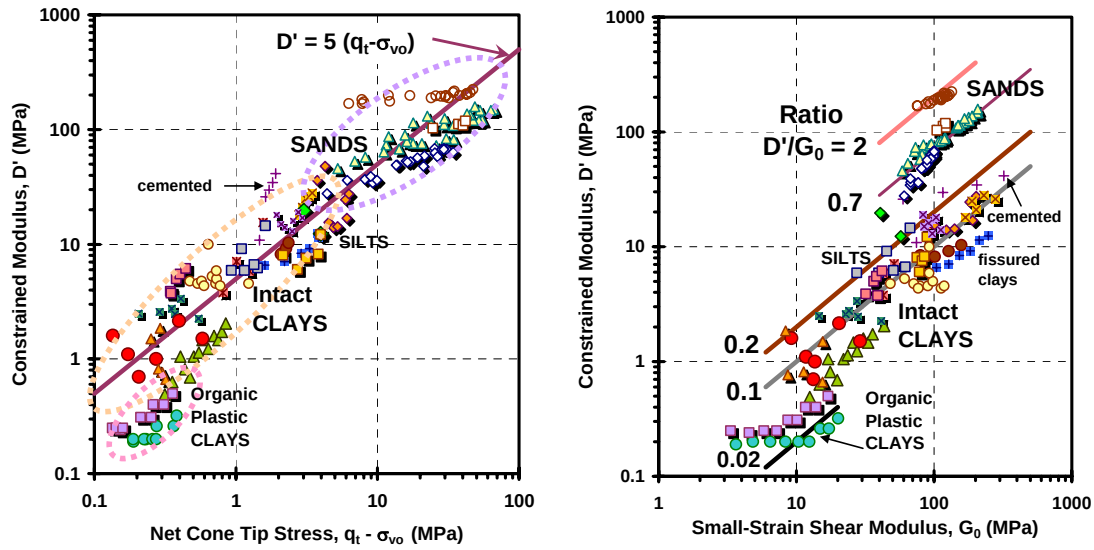

Figure 49. Combinative soil SCPTU database relationships between oedometric modulus (D') and (a) net cone tip resistance and (b) small-strain shear modulus

For foundation settlement analyses, a representative constrained modulus of the supporting soil medium is usually sought. The one-dimensional consolidation test (or oedometer) provides the constrained modulus ($D' = \Delta\sigma'/\Delta\varepsilon$), although in some cases, the modulus values can be back-calculated from field performance data from embankment loadings or footings. In practice, it has been usual to further correlate the modulus D' to a penetration resistance, as in-situ penetration tests are the most common type employed in routine site investigations. From the global plotting of diverse geomaterials, Figure 49a shows that a relationship for "well-behaved" soils might take the form (Schmertmann 1978):

$$D' \approx \alpha_C' \cdot (q_t - \sigma_{vo}) \tag{34}$$

with a representative value of $\alpha_C' \approx 5$ for soft to firm "vanilla clays" and NC "hourglass sands". However, for organic plastic clays of Sweden, a considerably lower $\alpha_C' \approx 1$ to 2 may be appropriate. For cemented Fucino clay, a value $\alpha_C' \approx 10$ to 20 may be assigned.

An alternate correlation can be sought between D' and small-strain shear modulus (G_0), as presented in Figure 49b. In this case, a similar adopted format could be:

$$D' \approx \alpha_G' \cdot G_0 \tag{35}$$

with assigned values of α_G' ranging from 0.02 for the organic plastic clays up to 2 for overconsolidated quartz sands. Additional studies with multiple regression, artificial neural networks, and numerical modeling may help guide the development of more universally-applied global relationships.

During the examination of various possible relationships in the above soil database, the results of two interesting trends became apparent (Figure 50). In Figure 50a, the measured Vs appeared related to the sleeve friction for uncemented soils. Figure 50b showed that the proposed relationship by Tanaka & Tanaka (1999) could be modified for soil type according to:

$$G0 \approx 50\, \sigma_{atm} \cdot [(q_t - \sigma_{vo})/\sigma_{atm}]^{m*} \tag{36}$$

where m* = 0.6 for clean quartz sands, 0.8 for silts, and 1.0 for intact clays of low to medium sensitivity. Note the remarkable resemblance to the aforementioned (30).

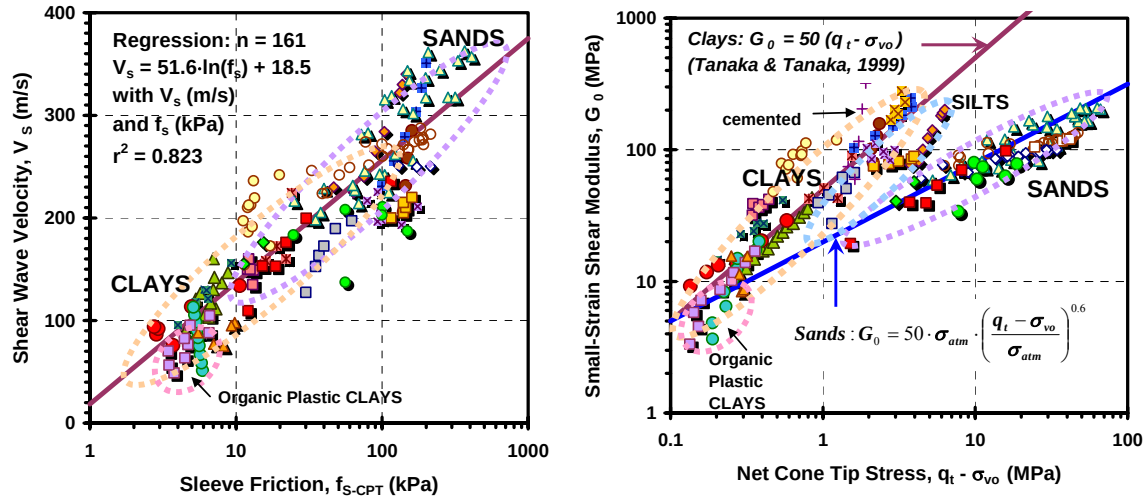

Figure 50. Observed SCPTU trends for soils: (a) shear wave vs. sleeve friction; and (b) small-strain stiffness and net cone tip resistance.

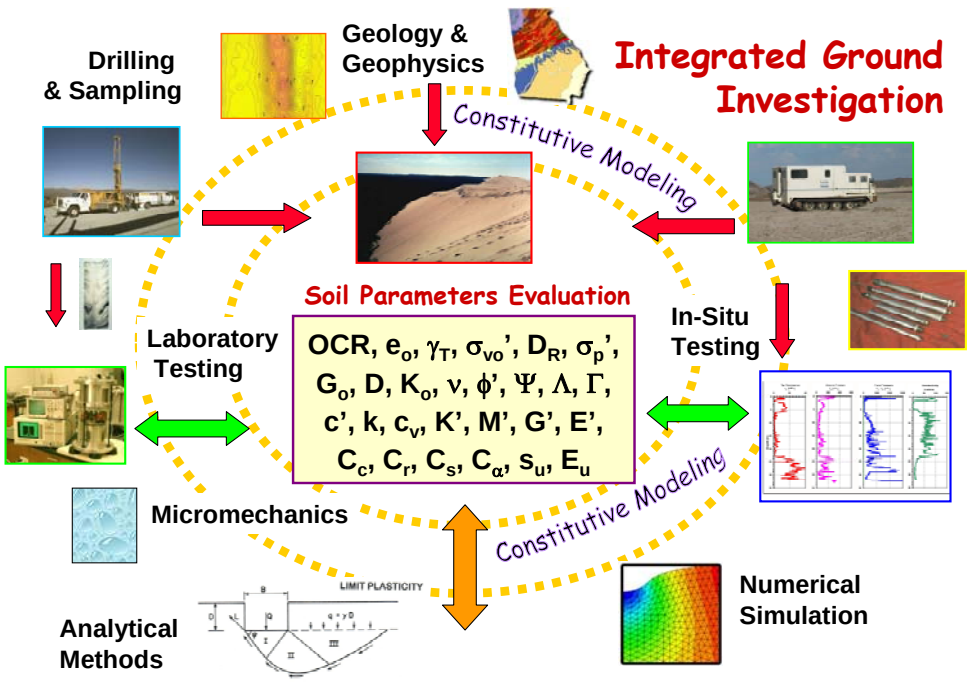

Figure 51. Concept for an integrated geotechnical approach to ground investigations.

5.0 CONCLUSIONS

The interpretation of in-situ tests in soils is currently a mix & match of theoretical, analytical, and empirical relationships that have developed separately and independently based on single-focused needs and research studies. Yet now, a sufficiently high number of well-documented clay and sand sites currently exists to allow a comprehensive calibration of a full suite of in-situ tests within a consistent framework. The results can be validated using high-quality laboratory test data and/or parameters backfigured from full-scale load tests. What is needed is a unified framework based on numerical modeling of all major test types using a rigorous constitutive soil model (likely within the context of critical state soil mechanics). This should be an integrated approach using geophysics, drilling & sampling, laboratory and in-situ testing (Fig. 51).

In the interim, this paper shows that stress history (i.e., OCR and OCD) can play a significant role in unifying the approach to in-situ test interpretations in soils. As a suggested first step, the utilization of a simplified cavity expansion - CSSM approach to fitting CPT, CPTù, and DMT data to clay sites is presented for six sites that range from soft NC to stiff OC states. For clean sands, an empirical approach using SPT, CPT, and DHT V_s data is applied to several well-documented sands and a special undisturbed (frozen) sand database is presented to cross-check relationships developed from large scale calibration chamber test series. Procedures for nontext-book geomaterials are also in dire need of a common methodology that can address clays and sands, as well as intermediate soil types and unusual to difficult soils. Additional global relationships for "well-behaved" and "normal" soils are sought in order to identify problematic and "ill-behaved" geomaterials. In-situ tests which obtain multiple-measurements (i.e., SCPTù and SDMTà) offer the most promise as intra-comparative cross-checks amonst the readings can be used to help discern anomalous soil behavior, as well as provide a suite of engineering parameters for "normal" soils, including stress-strain-strength-flow characteristics. Consequently, it is quite evident that considerable work remains in the development of a rational and validated approach to geotechnical site characterization by in-situ tests.

6.0 ACKNOWLEDGMENTS

The author appreciates the financial support provided currently by the Georgia Dept. of Transportation (GDOT), as well as prior support given by the National Science Foundation (NSF) and Fugro Engineers BV. Any conclusions or findings reported herein do not necessarily reflect the procedures or guidelines of these groups.

REFERENCES

Almeida, M.S.S. and Marques, M.E.S. 2003. The behavior of Sarapuí soft clay. Characterisation & Engineering Properties of Natural Soils, Vol. 1 (Singapore), Swets & Zeitlinger, Lisse: 477-504.

Andrus, R.D. and Stokoe, K.H. 2000. Liquefaction resistance of soils from shear wave velocity. ASCE Journal of Geotechnical & Geoenvironmental Engineering 126 (11): 1015-1025.

Andrus, R.D., Piratheepan, P., Ellis, B. Zhang, J. and Juang, C.H. 2004. Comparing liquefaction evaluation methods using penetration-V_s relationships. Soil Dynamics & Earthquake Engrg. 24: 713-721.

Atkinson, J.H. 2000. Nonlinear soil stiffness in routine design. Geotechnique 50 (5), 485-508.

Ballivy, G. (ed) 1995. The Pressuremeter and Its New Avenues (Proc. ISP4, Sherbrooke), Balkema, Rotterdam: 488 pages.

Been, K. and Jefferies, M.G. 1985. A state parameter for sands. Geotechnique 35 (2), 99-112.

Been, K., Crooks, J.H.A., Becker, D.E. and Jefferies, M.G. 1986. The cone penetration test in sands: state parameter. Geotechnique 36 (2): 239-249.

Been, K., Lingnau, B.E., Crooks, J.H.A. and Leach, B. 1987. Cone penetration test calibration for Erksak Beaufort Sea sand. Canadian Geotechnical J. 24 (4): 601-610.

Been, K, Crooks, J.H.A. and Jefferies, M.G. 1988. Interpretation of material state from the CPT in sands and clays. Penetration Testing in the UK, Thomas Telford, London: 215-218.

Blackburn, J.T., Sylvester, K. and Finno, R.J. 2005. Observed bracing responses at the Ford Design Center excavation. Proc. 16_{th} ICSMGE, Vol. 3 (Osaka), Millpress, Rotterdam: 1443-1446.

Bolton, M.D. 1986. The strength and dilatancy of sands. Geotechnique 36 (1), 65-78.

Boulanger, R.W. and Idriss, I.M. 2004. State normalization of penetration resistance and the effect of overburden stress on liquefaction resistance. Proc. 11th Soil Dynamics & Earthquake Engrg. (Proc. 3rd ICEGE), Berkeley, CA: 484-491.

Briaud, J-L. 1992. The Pressuremeter, A.A. Balkema, Rotterdam, 336 p.

Briaud, J-L. and Gibbens, R.M. (ed) 1994. Predicted & Measured Behavior of Five Spread Footings on Sand. GSP No. 41, ASCE, Reston/VA: 256 pages.

Briaud, J-L. 2000. The NGES at Texas A&M University: clay and sand. National Geotechnical Experimentation Sites, GSP 93, ASCE, Reston/VA: 26-51.

Bruzzi, D., Ghionna, V., Jamiolkowski, M., Lancellotta, R. and Manfredini, G. 1986. Self-boring pressuremeter in Po River Sand. Pressuremeter and Its Marine Applications, STP 950, ASTM, West Conshohocken/PA, 57-74.

Budhu, M. 2000. Soil Mechanics & Foundations, Wiley & Sons, New York, 586 pages.

Burland, J.B. 1989. Small is beautiful: the stiffness of soils at small strains. Canadian Geotechnical J. 26 (4), 499-516.

Burns, S.E. and Mayne, P.W. 1998. Monotonic and dilatory pore pressure decay during piezocone tests. Canadian Geotechnical Journal 35 (6), 1063-1073.

Burns, S.E. and Mayne, P.W. 2002. Analytical cavity expansion-critical state model for piezocone dissipation in fine-grained soils. Soils & Foundations 42 (2), 131-137.

Camp, W.M., Mayne, P.W. and Brown, D.A. 2002. Drilled shaft axial design values in calcareous clay. Deep Foundations 2002, Vol. 2, GSP 116, ASCE, Reston, 1518-1532.

Campanella, R.G. 1994. Field methods for dynamic geotechnical testing. Dynamic Geotechnical Testing II (STP 1213), ASTM, West Conshohocken/PA, 3-23.

Campanella, R.G., Robertson, P.K., and Gillespie, D. 1986. Seismic cone penetration test. Use of In-Situ Tests in Geotechnical Engineering (GSP 6), ASCE, Reston/VA: 116-130.

Carter, J.P., Booker, J.R. and Yeung, S.K. 1986. Cavity expansion in cohesive frictional soils. Geotechnique 36 (3): 349-358.

Chandler, R.J. 1988. The in-situ measurement of the undrained shear strength of clays using the field vane. Vane Shear Strength Testing in Soils. STP 1014, ASTM, West Conshohocken/PA, 13-44.

Chen, B.S-Y. and Mayne, P.W. 1994. Profiling the overconsolidation ratio of clays by piezocone tests. Report GIT-CEEGEO-94-1 to National Science Foundation by CEE/Georgia Tech, 280 pages. Download available from: http://www.ce.gatech.edu/~geosys/Faculty/Mayne/papers/index.html

Chen, B.S-Y. and Mayne, P.W. 1996. Statistical relationships between piezocone measurements and stress history of clays. Canadian Geotechnical J. 33 (3), 488-498.

Cho, G.C. and Santamarina, J.C. 2001. Unsaturated particulate materials: particle-level studies. Journal of Geotechnical & Geoenvironmental Engrg. 127 (1), 84-96.

Cho, G-C., Dodds, J. and Santamarina, J.C. 2006. Particle shape effects on packing density, stiffness, and strength: natural & crushed sands. J. of Geotechnical & Geoenvironmental Engrg. 132 (5): 591-602.

Chung, S.F. 2005. Characterisation of soft soils for deep water developments. *PhD dissertation*, School of Civil & Resource Engrg, Univ. Western Australia, Perth.

Clark, B.G. and Gambin, M. P. 1998. Pressuremeter testing in onshore ground investigations: A report by the ISSMGE Committee TC 16. Geotechnical Site Characterization, Vol. 2 (Proc. ISC-1, Atlanta), Balkema, Rotterdam: 1429-1468.

Clark, B.G. and Wroth, C.P. 1988. Comparison between results from flat dilatometer and self-boring pressuremeter tests. Penetration Testing in the UK, Thomas Telford, London: 295-298.

Danzinger, F.A.B., Almeida, M.S.S., and Sills, G.C. 1997. The significance of strain path analysis in interpretation of piezocone dissipation data. Geotechnique 47 (5): 901-914.

Dahlberg, R. 1974. Penetration, pressuremeter, and screw-plate tests in a preloaded natural sand deposit. Proc. European Symposium on Penetration Testing, Vol. 2.2, Stockholm: 68-87.

DeGroot, D. and Lutenegger, A.J. 1994. A comparison between field & lab measurements of hydraulic conductivity in a varved clay. Hydraulic Conductivity and Waste Contaminant Transport in Soil, ASTM STP 1142, American Society for Testing & Materials, West Conshohocken, PA: 300-317.

DeJong, J.T., Yafrate, N.J., DeGroot, D.J. and Jakubowski, J. 2004. Evaluation of the undrained shear strength profile in soft layered clay using full-flow probes. Geotechnical & Geophysical Site Characterization, Vol. 1 (Proc. ISC-2, Porto), Millpress, Rotterdam: 679-686.

Demers, D., and Leroueil, S. 2002. Evaluation of preconsolidation pressure and the overconsolidation ratio from piezocone tests of clay deposits in Quebec. Canadian Geotechnical Journal 39 (1): 174-192.

Diaz-Rodriguez, A., Leroueil, S. and Aleman, J. 1992. Yielding of Mexico City clay and other natural clays. Journal of Geotechnical Engineering 118 (7): 981-995.

Duncan, J.M. 1994. The role of advanced constitutive relations in practical applications. Proc. 13th Intl. Conf. Soil Mechanics & Foundation Engrg. (5), New Delhi, Balkema, Rotterdam: 31-48.

Elhakim, A.F. and Mayne, P.W. 2003. Derived stress-strain-strength of clays from seismic cone tests. Deformation Characteristics of Geomaterials, Vol. 1 (Lyon), Swets & Zeitlinger, Lisse: 81-87.

Elhakim, A.F. and Mayne, P.W. 2006. Evaluating footing response from seismic piezocone tests. Site & Geomaterial Characterization (GSP No. 149; GeoShanghai), ASCE, Reston/VA: 155-260.

Elsworth, D. 1993. Analysis of piezocone data using dislocation based methods. Journal of Geotechnical Engineering 119 (10): 1601-1623.

Fahey, M. (1998). Deformation and in-situ stress measurement. Geotechnical Site Characterization, Vol. 1 (Proc. ISC-1, Atlanta), Balkema, Rotterdam: 49-68.

Fahey, M. and Carter, J.P. 1993. A finite element study of the pressuremeter in sand using a nonlinear elastic plastic model. Canadian Geotechnical J. 30 (2): 348-362.

Fahey, M. and Goh, A-L. 1995. A comparison of pressuremeter and piezocone methods of determining the coefficient of consolidation. The Pressuremeter & Its New Avenues, Bakema, Rotterdam: 153-160.

Finno, R.J. (ed) 1989. Predicted & Observed Axial Behavior of Piles. (Proc. Foundation Engrg. Congress), GSP No. 23, ASCE, Reston, 388.

Finno, R.J., Gassman, S.L. and Cavello, M. 2000. The NGES at Northwestern University, National Geotechnical Experimentation Sites, GSP 93, ASCE, Reston/Virginia, 130-159.

Foti, S., Lancellotta, R., Marchetti, D., Monaco, P. and Totani, G. 2006. Interpretation of SDMT tests in a transversely isotropic medium. Proc. 2nd Intl. Conf. on the Flat Dilatometer, Wash. DC: 275-280.

Gambin, M., Magnan, J.P., and Mestat, P. (ed). 2005. International symposium: 50 years of pressuremeters (Proc. ISP5 - Pression, Marne-la-Vallée), Lab Central des Ponts et Chaussée, Paris: 740 pages.

Ghionna, V.N. and Jamiolkowski, M. 1991. A critical appraisal of calibration chamber testing of sands. Calibration Chamber Testing (Proc. ISOCCT-1, Potsdam), Elsevier, New York: 13-40.

Ghionna, V.N. and Porcino, D. 2003. Undrained monotonic & cyclic behavior of a coarse sand from undisturbed & reconstituted samples. Deformation Characteristics of Geomaterials, Vol. 1 (Proc. Lyon), Balkema, Rotterdam: 527-534.

Ghionna, V.N. and Porcino, D. 2006. Liquefaction resistance of undisturbed and reconstituted samples of a natural coarse sand from undrained cyclic triaxial tests. Journal of Geotechnical & Geoenvironmental Engineering 132 (2): 194-202.

Ghionna, V.N., Jamiolkowski, M., Pedroni, S. and Piccoli, S. 1995. Cone pressuremeter tests in Po River sand. The Pressuremeter and Its New Avenues, Balkema, 471-480.

Gregersen, O.S., Aas, G., and DiBiagio, E. 1973. Load tests on friction piles in sand. Proc. 8th Intl. Conf. Soil Mechanics & Foundation Engineering, Vol. 2, Moscow: 109-118.

Grozic, J.L.H., Lunne, T. and Pande, S. 2003. An oedometer test study on the preconsolidation stress of glaciomarine clays. Canadian Geotechnical J. 40 (5): 857-872.

Hardin, B.O. 1978. The nature of stress-strain behavior of soils. Earthquake Engineering & Soil Dynamics, Vol. 1 (Proc. Geotech Engrg. Conf., Pasadena), ASCE, Reston/VA: 3-90.

Hatanaka, M. and Uchida, A. 1996. Empirical correlation between penetration resistance and effective friction angle of sandy soil. Soils & Foundations 36 (4): 1 – 9.

Hight, D. and Leroueil, S. 2003. Engineering Characterization and Engineering Properties of Natural Soils (1). Swets and Zeitlinger, Lisse, 255-360.

Hight, D.W., Paul, M.A., Barras, B.F., Powell, J.J.M., Nash, D.F.T., Smith, P.R., Jardine, R.J. and Edwards, D.H. 2003. The characterisation of the Bothkennar clay. Characterisation & Engineering Properties of Natural Soils, Vol. 1 (Singapore), Swets & Zeitlinger, Lisse: 543-597.

Hoeg, K, Dyvik, R., and Sandbækken, G. 2000. Strength of undisturbed versus reconstituted silt and silty sand specimens. Journal of Geotechnical & Geoenvironmental Engineering 126 (7): 606-617.

Hoffman, B.A., Sego, D.C., Robertson, P.K., and Fourie, A.B. 1996. Thawing protocol of undisturbed samples of loose sand obtained by in-situ ground freezing. Proceedings, 49th Canadian Geotechnical Conf. (Frontiers of Geotechnology), Vol. 1, St. Johns, Newfoundland, Canada: 71-80.

Houlsby, G.T. and Teh, C.I. 1988. Analysis of the piezocone in clay. Penetration Testing 1988, Vol. 2, Balkema, Rotterdam: 777-783.

Houlsby, G.T. and Withers, N.J. 1988. Analysis of the cone pressuremeter in clay. Geotechnique 38 (4): 575-587.

Huang, A-B., Bunting, R.D., and Carney, T.C. 1991. Piezoblade testing in a clay calibration chamber. Calibration Chamber Testing (Proc. ISOCCT, Potsdam), Elsevier, New York: 161-173.

Hvorslev, M.J. 1960. Physical components of the shear strength of saturated clays. Proceedings, Research Conference on Shear Strength of Cohesive Soils (Boulder CO), ASCE, New York: 169-273.

Jacobs, P.A. and Coutts, J.S. 1992. A comparison of electric piezocone tips at the Bothkennar test site. Geotechnique 42 (2): 369-375.

Jamiolkowski, M. 2001. Where are we going. Pre-Failure Deformation Characteristics of Geomaterials, Vol. 2 (Proc. Torino'99), Swets & Zeitlinger, Lisse: 1251-1262.

Jamiolkowski, M. and Pepe, M.C. 2001. Vertical yield stress of Pisa clay from piezocone tests. Journal of Geotechnical & Geoenvironmental Engineering 127 (10): 893-897.

Jamiolkowski, M. and Robertson, P.K. 1988. Future trends for penetration testing. Penetration Testing in the UK, Thomas Telford, London: 321-342.

Jamiolkowski, M., Ladd, C.C., Germaine, J. and Lancellotta, R. 1985. New developments in field and lab testing of soils. Proceedings, 11th Intl. Conf. on Soil Mechanics & Foundation Engineering, Vol. 1, San Francisco: 57-154.

Jamiolkowski, M., LoPresti, D.C.F. and Manassero, M. 2001. Evaluation of relative density and shear strength of sands from cone penetration test and flat dilatometer test. Soil Behavior and Soft Ground Construction (GSP 119), ASCE, Reston/VA: 201-238.

Jardine, R.J. 1995. One perspective of the prefailure deformation characteristics of some geomaterials. Pre-Failure Deformation of Geomaterials, Vol. 2 (Proc. Sapporo), Balkema, Rotterdam: 855-885.

Jardine, R.J., Lehane, B.M., Smith, P.R. and Gildea, P.A. 1995. Vertical loading experiments on rigid pad foundations at Bothkennar. Geotechnique 45 (4): 573-598.

Jardine, R.J., Potts, D.M., Fourie, A.B., and Burland, J.B. 1986. Studies of the influence of non-linear stress-strain characteristics in soil-structure interaction. Geotechnique 36 (3): 377-396.

Jardine, R.J., Standing, J.R. and Kovacevic, N. 2005. Lessons learned from full scale observations and the practical application of advanced testing & modeling. Deformation Characteristics of Geomaterials (2), Taylor & Francis Group, London: 201-245.

Jefferies, M.G. 1993. Norsand: a simple critical state model for sand. Geotechnique 43 (1): 91-102.

Jefferies, M.G. and Shuttle, D.A. 2005. Norsand: features, calibration, and use. Soil Constitutive Models: Evaluation, Selection, and Calibration (GSP No. 128), ASCE, Reston/VA: 204-235.

Keaveny, J.M. and Mitchell, J.K. 1986. Strength of fine-grained soils using the piezocone. Use of In-Situ Tests in Geotechnical Engineering (GSP 6), ASCE, Reston/VA: 668-699.

Konrad, J-M. and Law, K.T. 1987. Undrained shear strength from piezocone tests. Canadian Geotechnical Journal 24 (3): 392-405.

Kulhawy, F.H. and Mayne, P.W. 1990. Manual on estimating soil properties for foundation design. Report EPRI EL-6800, Electric Power Research Institute, Palo Alto, 306 p.

Lacasse, S. and Lunne, T. 1982. Penetration tests in two Norwegian clays. Penetration Testing, Vol. 2 (ESOPT-2, Amsterdam), Balkema, Rotterdam: 661-669.

Lacasse, S., Berre, T., and Lefebvre, G. 1985. Block sampling of sensitive clays. Proceedings, 11th International Conference on Soil Mechanics and Foundations Engineering (2), San Francisco: 887-892.

Ladd, C.C. 1991. Stability evaluation during staged construction. Terzaghi Lecture, ASCE Journal of Geotechnical Engineering 117 (4): 540-615.

Lade, P.V. 2005. Overview of constitutive models for soils. Calibration of Constitutive Models, GSP 139 (Proc. GeoFrontiers, Austin), ASCE, Reston/VA: 1-34.

Lancellotta, R. 1995. Geotechnical Engineering, Balkema, Rotterdam, 436 pages.

Lee, J., Salgado, R., and Carraro, J.A.H. 2004. Stiffness degradation and shear strength of silty sands. Canadian Geotechnical J. 41 (5): 831-843.

Lee, K.M., Shen, C.K., Leung, D.H.K. and Mitchell, J.K. 1999. Effects of placement method on geotechnical behavior of hydraulic fill sands. Journal of Geotechnical & Geoenvironmental Engineering 125 (10): 832-846.

Lehane, B. and Cosgrove, E. 2000. Applying triaxial compression stiffness data to settlement prediction of shallow foundations. Geotechnical Engineering 142, Inst. Civil Engrs (Oct.): 191-200.

Lehane, B. and Fahey, M. 2002. A simplified nonlinear settlement prediction model for foundations on sand. Canadian Geotechnical Journal 39 (2): 293-303.

Leroueil, S. and Jamiolkowski, M. 1991. Exploration of soft soil and determination of design parameters. Proceedings, GeoCoast'91, Yokohama, Vol. 2, Port & Harbour Research Institute: 969-998.

Leroueil, S. and Hight, D.W. 2003. Behavior and properties of natural soils and soft rocks. Characterization and Engineering Properties of Natural Soils (1). Swets and Zeitlinger, Lisse, 29-254.

Locat, J., Tanaka, H., Tan, T.S., Dasari, G.R. and Lee, H. 2003. Natural soils: geotechnical behavior and geological knowledge. Characterisation & Engineering Properties of Natural Soils, Vol. 1 (Proc. Singapore Workshop), Swets & Zeitlinger, Lisse: 3-28.

Long, M. and Gudjonsson, G.T. 2004. T-bar testing in Irish soils. Geotechnical & Geophysical Site Characterization, Vol. 1 (Proc. ISC-2, Porto), Millpress, Rotterdam: 719-726.

LoPresti, D.C.F., Pallara, O., Fioravante, V. and Jamiolkowski, M. 1998. Assessment of quasi-linear models for sands. Pre-Failure Deformation Behavior of Geomaterials, Thomas Telford, UK: 363-372.

Lunne, T., Eidsmoen, T., Gillespie, D. And Howland, J.D. 1986. Laboratory & field evaluation of cone penetrometers. Use of In-Situ Tests in Geotechnical Engrg. (GSP 6), ASCE, Reston/VA: 714-729.

Lunne, T., Lacasse, S. and Rad, N.S. (1994). General report: SPT, CPT, PMT, and recent developments in in-situ testing. Proc. 12th Intl. Conf. Soil Mechanics & Foundation Engrg. (4), Rio: 2339-2403.

Lunne, T., Powell, J.J.M. and Robertson, P.K. 1996. Use of piezocone tests in non-textbook materials. Advances in Site Investigation Practice (Proc. ICE, London), Thomas Telford Ltd, London: 438-451.

Lunne, T., Robertson, P.K., Powell, J.J.M. 1997. Cone Penetration Testing in Geotechnical Practice. Blackie Academic EF Spon/Routledge Publishers, New York, 312 p.

Lunne, T., Long, M. and Forsberg, C.F. 2003a. Characterization and engineering properties of Holmen, Drammen sand. Characterisation and Engineering Properties of Natural Soils, Vol. 2 (Proc. Singapore), Swets & Zeitlinger, Lisse: 1121-1148.

Lunne, T., Long, M., and Forsberg, C.F. 2003b. Characterisation and engineering properties of Onsøy clay. Characterisation & Engineering Properties of Natural Soils, Vol. 1 (Singapore), Swets & Zeitlinger, Lisse: 395- 427.

Lunne, T., Randolph, M.F., Chung, S.F., Andersen, K.H., and Sjursen, M. 2005. Comparison of cone and T-bar factors in two onshore and one offshore clay sediments. Frontiers in Offshore Geotechnics (Proc. ISFOG, Perth), Taylor & Francis Group, London: 981-989.

Marchetti, S., Monaco, P., Totani, G. and Calabrese, M. 2001. The flat dilatometer test in soil investigations. Proc. Intl. Conf. on In-Situ Measurement of Soil Properties & Case Histories, Bali: 95-131.

Mayne, P.W. 1991. Determination of OCR in clays by piezocone tests using cavity expansion and critical state concepts. Soils and Foundations 31 (1): 65-76.

Mayne, P.W. 1992. In-situ characterization of Piedmont residuum in eastern US. Proc. NSF US-Brazil Geo-Workshop: Application of Classical Soil Mechanics to Structured Soils, Belo Horizonte: 89-93.

Mayne, P.W. 1993. In-situ determination of clay stress history by piezocone model. Predictive Soil Mechanics, Thomas Telford, London: 483-495.

Mayne, P.W. 1994. CPT-based prediction of footing response. Measured & Predicted Behavior of Five Spread Footings on Sand (GSP 41), ASCE, Reston/VA: 214-218.

Mayne, P.W. 2001. Stress-strain-strength-flow parameters from enhanced in-situ tests. Proceedings, the Intl. Conference on In-Situ Measurement of Soil Properties and Case Histories, Bali, Indonesia: 27-48.

Mayne, P.W. 2003. Class "A" footing response prediction from seismic cone tests. Deformation Characteristics of Geomaterials, Vol. 1 (Proc. IS-Lyon), Swets & Zeitlinger, Lisse: 883-888.

Mayne, P.W. 2005. Integrated ground behavior: in-situ & lab tests. Deformation Characteristics of Geomaterials, Vol. 2 (Lyon), Taylor & Francis, London: 155-177.

Mayne, P.W. 2006a. Interrelationships of DMT and CPT readings in soft clays. Flat Dilatometer Testing (Proc. 2nd Intl. Conf. on DMT, Washington D.C.): 231-236.

Mayne, P.W. 2006b. The 2nd James K. Mitchell Lecture: Undisturbed sand strength from seismic cone tests. Presented at GeoShanghai, 6-8 June 2006. Intl. J. Geomechanics & Geoengineering, Taylor & Francis Group, London, in press.

Mayne, P.W. and Bachus, R.C. 1989. Penetration pore pressures in clay by CPTu, DMT, and SBP. Proceedings, 12th ICSMFE, Vol. 1, Rio de Janeiro, 291-294.

Mayne, P.W. and Brown, D.A. 2003. Site characterization of Piedmont residuum of North America. Characterization & Engrg. Properties of Natural Soils, Vol. 2, Swets & Zeitlinger, Lisse, 1323-1339.

Mayne, P.W. and Campanella, R.G. 2005. Versatile site characterization by seismic piezocone. Proc. 16th Intl. Conf. Soil Mechanics & Geotechnical Engrg, Vol. 2 (Osaka), Millpress, Rotterdam: 721-724.

Mayne, P.W., Christopher, B.R. and DeJong, J. 2002. Subsurface Investigations: geotechnical site characterization. Pub. No. FHWA NHI-01-031, National Highway Institute, Arlington, VA: 300 pages. Download available from: http://www.ce.gatech.edu/~geosys/Faculty/Mayne/papers/index.html

Mayne, P.W. and Kulhawy, F.H. 1990. Direct and indiret determinations of K_0 in clays. Transportation Research Record 1278: Lateral Stresses, National Research Council, Washington, DC: 141-149.

Mayne, P.W. and Mitchell, J.K. 1988. Profiling of OCR in clays by field vane. Canadian Geotechnical Journal 25 (1): 150-157.

Mayne, P.W. and Pearce, R.A. 2005. Site characterization of Bootlegger Cove Clay for Port of Anchorage. Frontiers in Offshore Geotechnics (Proc. Perth), Taylor & Francis Group, London: 951-955.

Mayne, P.W. and Stewart, H.E. 1988. Pore pressure response of K_o-consolidated clays. Journal of Geotechnical Engineering, Vol. 114 (11), 1340-1346.

Mayne, P.W., Burns, S.E., and Chen, B.S-Y. 2002. Discussion: Undrained cavity expansion for piezocone penetration. Geotechnique, Vol. 52 (4), 307-311.

Mayne, P.W., Kulhawy, F.H. and Kay, J.N. 1990. Observations on the development of porewater pressures during piezocone testing in clays. Canadian Geotechnical Journal 27 (4): 418-428.

Mayne, P.W., Mitchell, J.K., Auxt, J.A. and Yilmaz, R. 1995. U.S. national report on CPT. Proc. Intl. Symposium on Cone Penetration Testing, Vol. 1 (CPT'95), Swedish Geot. Society Report 3:95, Linköping: 263-276.

Mayne, P.W., Puzrin, A.M. and Elhakim, A.F. 2003. Field characterization of small- to high-strain behavior of clays. Soil and Rock America 2003, Vol. 1, Proceedings, 12th Pan Am Conference, Verlag Glückauf, Essen: 307-313.

Mayne, P.W., Robertson, P.K. and Lunne, T. 1998. Clay stress history evaluated from seismic piezocone tests. Geotechnical Site Characterization, Vol. 2 (Proc ISC-1), Balkema, Rotterdam: 1113-1118.

Mayne, P.W., Schneider, J.A. and Martin, G.K. 1999. Small- and large-strain soil properties from seismic flat dilatometer tests. Pre-Failure Deformation Characteristics of Geomaterials, Vol. 1 (Proc. Torino), Balkema, Rotterdam: 419-426.

Mesri, G. and Abdel-Ghaffar, M. 1993. Cohesion intercept in effective stress stability analysis. Journal of Geotechnical Engineering 119 (8): 1229-1249.

Mimura, M. 2003. Characteristics of some Japanese natural sands – data from undisturbed frozen samples. Characterisation and Engineering Properties of Natural Soils, Vol. 2 (Proc. Singapore), Swets & Zeitlinger, Lisse: 1149-1168.

Mitchell, J.K. and Keaveny, J.M. 1986. Determining sand strength by cone penetrometer. Use of In-Situ Tests in Geotechnical Engineering (GSP 6, Blacksburg), ASCE, Reston/VA: 823-839.

Mlynarek, Z., Gogolik, S. and Marchetti, D. 2006. Suitability of the SDMT method to assess geotechnical parameters. Proc. 2nd Intl. Conf. on the Flat Dilatometer, Washington, DC: 148-153.

Moss, R.E.S., Seed, R.B. and Olsen, R.S. 2006. Normalizing the CPT for overburden stress. Journal of Geotechnical & Geoenvironmental Engrg. 132 (3): 378-387.

Nash, D.F.T., Powell, J.J.M. and Lloyd, I.M. 1992. Initial investigations of the soft clay test site at Bothkennar. Geotechnique 42 (2): 163-181.

Ohta, H., Nishihara, A., and Morita, Y. 1985. Undrained stability of K_0-consolidated clays. Proc. 11th ICSMFE, Vol. 2, San Francisco, 613-616.

O'Neill, M.W. 2000. The national geotechnical experimentation site: University of Houston. National Geotechnical Experimentation Sites (GSP 93), ASCE, Reston/VA: 72-101.

Pestana, J. and Whittle, A.J. 1999. Formulation of a unified constitutive model for clays and sands. Intl. J. Numerical & Analytical Methods in Geomechanics 23 (12): 1215-1243.

Pestana, J.M., Hunt, and C.E., Bray, J.D. 2002. Soil deformation and excess porewater pressure field around a closed ended pile. Journal of Geotechnical & Geoenvironmental Engrg. 128 (1): 1-12.

Peuchen, J. and Mayne, P.W. 2006. Rate effects in vane testing. Journal of ASTM International Testing, submitted for publication.

Porcino, D. and Ghionna, V.N. 2004. Comparison between in-situ and lab tests on undisturbed frozen samples for a natural coarse sand. Geotechnical & Geophysical Site Characterization, Vol. 2 (Proc. ISC-2, Porto), Millpress, Rotterdam: 1843-1850.

Powell, J.J.M, Quarterman, R.S.T. and Lunne, T. 1988. Interpretation and use of the piezocone test in UK clays. Penetration Testing in the UK (Proc. Birmingham), Thomas Telford, London: 151-156.

Powell, J.J.M. and Shields, C.H. 1995. Field studies of the full displacement pressuremeter in clays. The Pressuremeter & Its New Avenues, (Proc. ISP-5, Sherbrooke), Balkema, Rotterdam: 239-246.

Puzrin, A.M., and Burland, J.B. 1996. A logarithmic stress-strain function for rocks & soils. Geotechnique 46 (1): 157-164.

Randolph, M.F. 2004. Characterization of soft sediments for offshore applications. Geotechnical & Geophysical Site Characterization, Vol. 1 (Proc. ISC-2, Porto), Millpress, Rotterdam: 209-232.

Richart, F.E., Hall, J.R. and Woods, R.D. 1970. Vibrations of Soils & Foundations. Prentice-Hall Inc., Englewood Cliffs, NJ: 414 pages.

Robertson, P.K. 1986. In-situ testing and its application to foundation engineering. Canadian Geotechnical J. 23 (4): 573-594.

Robertson, P.K. 1990. Soil classification using the cone penetration test. Canadian Geotechnical Journal 27 (1): 151-158.

Robertson, P.K. and Campanella, R.G. 1983. Interpretation of cone penetration tests: sands. Canadian Geotechnical Jour-nal 20 (4), 719-733.

Robertson, P.K, Campanella, R.G., Gillespie, D. and Greig, J. 1986. Use of piezometer cone data. Use of In-Situ Tests in Geotechnical Engineering, GSP 6, ASCE, Reston/VA: 1263-1280.

Robertson, P.K., Campanella, R.G., Gillespie, D. and By, T. 1988. Excess pore pressures and the flat dilatometer test. Penetration Testing 1988, Vol. 1 (ISOPT-1, Orlando), Balkema, Rotterdam: 567-576.

Robertson, P.K, Sully, J.P., Woeller, D.Jl, Lunne, T., Powell, J.J.M. and Gillespie, D.G. 1992. Estimating coefficient of consolidation from piezocone tests. Canadian Geotechnical Journal 39 (4): 539-550.

Robertson, P.K., Wride, C.E., et al. 2000a. The Canadian liquefaction experiment: an overview. Canadian Geotechnical Journal 37 (3): 499-504.

Robertson, P.K., Wride, C.E., et al. 2000b. The CANLEX project: summary & conclusions. Canadian Geotechnical Journal 37 (3): 563-591.

Salgado, R., Bandini, P. and Karim, A. 2000. Shear strength and stiffness of silty sand. Journal of Geotechnical & Geoenv. Engrg. 126 (5): 451-462.

Salgado, R., Boulanger, R.W. and Mitchell, J.K. 1997a. Lateral stress effects on CPT liquefaction correlations. Journal of Geotech. & Geoenv. Engrg. 123 (8): 726-735.

Salgado, R., Mitchell, J.K., and Jamiolkowski 1997b. Cavity expansion and penetration resistance in sand. Journal of Geotechnical & Geoenv. Engrg. 123 (4): 344-354.

Salgado, R., Mitchell, J.K., and Jamiolkowski 1998. Calibration chamber size effects on penetration resistance in sand. Journal of Geotech. & Geoenv. Engrg. 124 (9): 878-888.

Salgado, R., Mitchell, J.K., and Jamiolkowski, M. 1997. Cavity expansion and penetration resistance in sand. Journal of Geotechnical & Geoenv. Engrg 123 (4): 344-354.

Sandven, R., Senneset, K. and Janbu, N. 1988. Interpretation of piezocone tests in cohesive soils. Penetration Testing 1988, Vol. 2 (ISOPT), Balkema, Rotterdam: 939-953.

Santos, J.A.D. and Correia, A.G. 2001. Reference threshold shear strain of soil. Proceedings, 15th ICSMGE, Vol. 1, Istanbul: 267-270.

Schmertmann, J.H. 1978. Guidelines for cone penetration test: performance & design. Report FHWA-TS-78-209, Federal Highway Administration, Washington, D.C., 146 pages.

Schnaid, F. 2005. Geocharacterization and engineering properties of natural soils by in-situ tests. Proc. 16th ICSMGE, Vol. 1 (Osaka), Millpress, Rotterdam: 3-45.

Schnaid, F. and Houlsby, G.T. 1992. Measurement of properties of sand in a calibration chamber by the cone pressuremeter test. Geotechnique 42 (4): 587-601.

Schnaid, F., Lehane, B.M. and Fahey, M. 2004. In-situ test characterization of unusual geomaterials. Geotechnical & Geophys. Site Characterization, Vol. 1 (Proc. ISC-2, Porto), Millpress, Rotterdam: 49-74.

Schnaid, F., Gills, G.C., Soares, J.M. and Nyirenda, Z. 1997. Predictions of the coefficient of consolidation from piezocone tests. Canadian Geotechnical J. 34 (2): 315-327.

Schofield, A.N. and Wroth, C.P. 1968. Critical State Soil Mechanics, McGraw-Hill, London, 310 p.

Senneset, K. Sandven, R., Janbu, N. 1989. Evaluation of soil parameters from piezocone tests. Transportation Research Record 1235: 24-37.

Senneset, K., Sandven, R., Lunne, T., By, T. and Amundsen, T. 1988. Piezocone tests in silty soils. Penetration Testing 1988, Vol. 2, Balkema, Rotterdam: 955-974.

Sheahan, T.C., Ladd, C.C. and Germaine, J.T. 1996. Rate-dependent undrained shear behavior of saturated clay. Journal of Geotechnical Engineering, Vol. 122 (2): 99-108.

Shibuya, S., Mitachi, T., Hosomi, A. and Hwang, S.C. 1996. Strain rate effects on stress-strain behavior of clay. Measuring & Modeling Time Dependent Soil Behavior (GSP 61), ASCE, Reston/VA: 214-227.

Shibuya, S., Mitachi, T., Fukuda, F. and Hosomi, A. 1997. Modeling of strain-rate dependent deformation of clay at small strain. Proc. 14th ICSMFE (1), Hamburg: 409-412.

Shuttle, D. and Jefferies, M. 1998. Dimensionless and unbiased CPT interpretation in sand. Intl. J. for Numerical and Analytical Methods in Geomechanics, Vol. 22: 351-391.

Skempton, A.W. 1986. Standard penetration test procedures and the effects in sands of overburden stress, relative density, particle size, ageing, and overconsolidation. Geotechnique 36 (3): 425-447.

Soga, K. and Mitchell, J.K. 1996. Rate-dependent deformation of structured natural clays. Measuring & Modeling Time Dependent Soil Behavior, GSP No. 61, ASCE, Reston/Virginia: 243-257.

Sully, J.P. and Campanella, R.G. 1994. Evaluation of field CPTU dissipation data in overconsolidated fine-grained soils. Proc. 13th Intl. Conf. Soil Mechanics & Fdn Engrg., Vol. 1, New Delhi: 201-204.

Suzuki, Y., Sanematsu, T., and Tokimatsu, K. 1998. Correlation between SPT and seismic CPT. Geotechnical Site Characterization, Vol. 2 (Proc. ISC-1, Atlanta), Balkema, Rotterdam: 1375-1380.

Tan, T.S., Phoon, K.K., Hight, D.W. and Leroueil, S. (ed) 2003. Characterization and Engineering Properties of Natural Soils, Vols. 1 & 2, Swets & Zeitlinger, Lisse: 1532 pages.

Tanaka, H. and Tanaka, M. 1998. Characterization of sandy soils using CPT & DMT. Soils & Foundations 38(3): 55-65.

Tatsuoka, F. and Shibuya, S. 1992. Deformation characteristics of soils and rocks from field and laboratory tests. Report of the Institute of Industrial Science, Vol. 37 (1), Univ. of Tokyo, 136 p.

Tatsuoka, F., Jardine, R.J., LoPresti, D.C.F., DiBenedetto, H. and Kodaka, T. 1997. Theme lecture: Characterizing the pre-failure deformation properties of geomaterials. Proceedings, 14th ICSMGE (4), Hamburg: 2129-2164.

Tatsuoka, F., Masuda, T. Siddiquee, M.S.A. and Koseki, J. 2003. Modeling the stress-strain relations of sand in cyclic PS. Journal Geotechnical & Geoenvironmental Engrg. 129 (6): 450-467.

Teh, C.I. and Houlsby, G.T. 1991. An analytical study of the cone penetration test in clay. Geotechnique 41 (1): 17-34.

Trak, B., LaRochelle, P., Tavenas, F., Leroueil, S. and Roy, M. 1980. A new approach to the stability analysis of embankments on sensitive clays. Canadian Geot. Journal 17 (4): 526-544.

Vaid, Y.P. and Sivathayalan, S. 2000. Fundamental factors affecting liquefaction susceptibility of sands. Canadian Geotechnical Journal, Vol. 37 (3): 592-606.

Vesić, A.S. 1972. Expansion of cavities in infinite soil mass. Journal of the Soil Mechanics & Foundations Division (ASCE), Vol. 98 (SM3): 265-290.

Vesić, A.S. 1977. Design of Pile Foundations. Synthesis of Highway Practice NCHRP 42, Transportation Research Board, Washington, D.C., 68 pages.

Vucetic, M. and Dobry, R. (1991). Effect of soil plasticity on cyclic response. *Jour. of Geotechnical Engng* 117 (1): 89-107.

Watson, P.G., Newson, T.A., and Randolph, M.F. 1998. Strength profiling in soft *offshore* soils. Geotechnical Site Characterization, Vol. 2 (Proc. ISC-1, Atlanta), Balkema, Rotterdam: 1389-1394.

Whittle, A.J. 1993. Evaluation of a constitutive model for overconsolidated clays. Geotechnique 43 (2): 289-313.

Whittle, A.J. and Aubeny, C.P. 1993. The effects of installation disturbance on interpretation of in-situ tests in clay. Predictive Soil Mechanics, Thomas Telford, UK: 742-767.

Whittle, A.J. and Kavvadas, M.J. 1994. Formulation of MIT-E3 constitutive model for overconsolidated clay. Journal of Geotechnical Engineering 120 (1): 173-224.

Whittle, A.J., Sutabutr, T., Germaine, J.T. and Varney, A. 2001. Prediction and interpretation of pore pressure dissipation for piezoprobe. Geotechnique 51 (7): 601-617.

Wood, D.M. 1990. Soil Behaviour & Critical State Soil Mechancis, Cambridge University Press, 462 p.

Woods, R.D. 1978. Measurement of dynamic soil properties. Earthquake Engineering & Soil Dynamics, Vol. I, ASCE Conference, Pasadena: 91-178.

Wride, C.E. and Robertson, P.K. 1999. CANLEX: The Canadian liquefaction experiment: data review report. (Five volumes). BiTech Publishers Ltd, Richmond, BC, Canada: total 1081 pages.

Wride, C.E., Robertson, P.K., Biggar, K.W., Campanella, R.G., Hofmann, B.A., Hughes, J.M.O., Küpper, A. and Woeller, D.J. 2000. Interpretation of in-situ test results from the CANLEX sites. Canadian Geotechnical Journal 37 (3): 505-529.

Wroth, C.P. 1984. The interpretation of in-situ soil tests. Geotechnique 34 (4): 449-489.

Wroth, C.P. 1988. Penetration testing: a more rigorous approach to interpretation. Penetration Testing 1988, Vol. 1, Balkema, Rotterdam: 303-311.

Wroth, C.P. and Houlsby, G.T. 1985. Soil mechanics: property characterization & analysis procedures. Proceedings, 11th ICSMFE, Vol. 1, San Francisco: 1-56.

Yafrate, N.J. and DeJong, J.T. 2005. Considerations in evaluating the remoulded undrained shear strength from full flow penetrometer cycling. Frontiers in Offshore Geotechnics (Proc. ISFOG, Perth), Taylor & Francis Group, London: 991-997.

Yamashita, S., Hori, T., and Suzuki, T. 2003. Effects of fabric anisotropy and stress condition on small-strain stiffness of sands. Deformation Characteristics of Geomaterials, Vol. 1 (Proc. Lyon), Swets & Zeitlinger, Lisse: 187-194.

Yamashita, S., Kohata, Y., Kawaguchi, T. and Shibuya, S. (2001). International round robin test organized by TC-29. Advanced Lab Stress-Strain Testing of Geomaterials, Swets & Zeitlinger, Lisse: 65-110.

Yu, H-S. 2004. James K. Mitchell Lecture: In-situ soil testing: from mechanics to interpretation. Geotechnical & Geophysical Site Characterization, Vol. 1 (Proc. ISC-2, Porto), Millpress, Rotterdam: 3-38.

Yu, H-S. and Mitchell, J.K. 1998. Analysis of cone resistance: review of methods. Journal of Geotechnical & Geoenvironmental Engineering 124 (2): 140-149.